DOI: 10.14750/ME.2022.027

UNIVERSITY OF MISKOLC

Faculty of Earth Science and Engineering

Institute of Geophysics and Geoinformation Science

MŰSZAKI FÖLDTUDOMÁNYI KAR

INTERVAL INVERSION APPROACH FOR INTERPRETATION OF MULTI-WELL LOGGING DATASETS

PhD THESIS

By

Mahmoud Ali Gaballah Abdellatif

Scientific supervisor

Prof. Dr. Norbert Péter Szabó

MIKOVINY SÁMUEL DOCTORAL SCHOOL OF EARTH SCIENCES

Head of the Doctoral School: Prof. Dr. Péter Szűcs

MISKOLC - HUNGARY

2022

DOI: 10.14750/ME.2022.027

CONTENTS

DOI: 10.14750/ME.2022.027

SUPERVISOR'S FOREWORD

for the PhD thesis

„ INTERVAL INVERSION APPROACH FOR INTERPRETATION OF MULTI-WELL LOGGING DATASETS"

by Mahmoud Ali Gaballah Abdellatif

The topic of the Candidate's thesis - joint inversion of borehole geophysical data - is in the focus of international research. The new method developments introduced by the Candidate in the thesis belong to the range of modern data processing tools applied to in situ geophysical data. The suggested 2D inversion methodology is capable to simultaneously process multi-borehole datasets in order to derive both the lateral and vertical variations of petrophysical parameters and layer thicknesses of geological formations in a highly accurate and reliable way. This inversion strategy can be used as a powerful tool in petroleum exploration and several other fields of geosciences, too.

The inversion methodology is a result of a pioneer work, which may open a path to several applications, for instance evaluating 2D/3D structures including groundwater and hydrocarbon formations. In the future, the inversion method can be extended to 3D inversion of multivariate well logging datasets to determine the morphology of rock formations together with the most important reservoir parameters. Due to the high data-to-unknowns ratio of the solved inverse problem, it is possible to estimate new (inversion) unknowns such as physical properties of rock constituents, response function constants and other zone parameters. The extraction of these parameters is not only a scientific innovation, but also it can reduce the financial cost of core sampling operations and lab measurements in practice. Unconventional reservoirs like organic rich shale and tight gas formations are multi-mineral rocks, the matrix volumes, porosity, saturation, kerogen content of which are delicate parameters to be estimated. By the newly developed 2D interval inversion approach, significant quality improvement in their quantitative evaluation is expected. The automated estimation of layer boundaries is a unique achievement of the Department of Geophysics of the University of Miskolc. The Candidate followed this research idea and further developed it in his thesis.

The Candidate's continuous efforts towards scientific research, his creativity, and the results presented in this thesis prove the scientific knowledge and the suitability of

DOI: 10.14750/ME.2022.027

the Candidate for independent research. In my opinion, the Candidate's results, especially those of related to the simultaneous estimation of layer thickness and petrophysical parameters' variations based on global optimization are worth to be published in farther ranked international journals of applied geophysics. The feasibility of the developed inversion method has been proven in international datasets, too. Herewith, I certify that this dissertation contains only valid data, and the presented results are representing the Candidate's own work. In my opinion, the PhD thesis is fully adequate in scope and quality required by the Mikoviny Sámuel Doctoral School of Earth Sciences. Based on all the above, I recommend the public defense to be carried out for completing a successful process of acquiring a PhD title.

25 May 2022, Miskolc

Prof. Dr. Norbert Péter Szabó
supervisor

DOI: 10.14750/ME.2022.027

LIST OF FIGURES PAGE NO.

DOI: 10.14750/ME.2022.027

DOI: 10.14750/ME.2022.027

DOI: 10.14750/ME.2022.027

LIST OF TABLES PAGE NO.

DOI: 10.14750/ME.2022.027

ABBREVIATIONS

Symbol	Description	Unit.
$\emptyset$	Porosity	v/v
S_{x0}	Water saturation in invaded zone	v/v
S_w	Water saturation in uninvaded zone	v/v
V_{sh}	Volume of shale	v/v
V_{sd}	Volume of sand	v/v
B_q	q-th expansion coefficient	-
Ψ_q	q-th basis function	-
B:	Expansion coefficient	-
$\mathbf{G}^{-g}$	Generalized inverse matrix	-
D_d	Data distance	%
Cov	Covariance matrix	-
$Corr$	Correlation matrix	-
S	Mean spread value	-
δ	Kronecker delta symbol	-
$S_{hc,irr}$	Irreducible hydrocarbon saturation	v/v
$S_{hc,mov}$	Movable hydrocarbon saturation	v/v
GR	Gamma-ray intensity	API
K	Potassium concentration	%
Th	Thorium concentration	ppm
U	Uranium concentration	ppm
GR_{sh}	Natural gamma intensity of shale	API
ρ_{sh}	Shale density	g/cm^3
GR_{sd}	Natural gamma intensity of sand	API
ρ_{sd}	Sand density	g/cm^3
k_{mf}	Potassium concentration of mud filtrate	%
ρ_{mf}	Mud filtrate density	g/cm^3
K_{sh}	Potassium concentration in shale	%
K_{sd}	Potassium concentration in sand	%
Th_{sh}	Thorium concentration in shale	ppm
Th_{sd}	Thorium concentration in sand	ppm

DOI: 10.14750/ME.2022.027

U_{sh}	Uranium concentration in shale	ppm
U_{sd}	Uranium concentration in sand	ppm
ρ_b	Bulk density	g/cm^3
$\emptyset_N$	Neutron porosity	v/v
$\emptyset_{N,mf}$	Neutron porosity of mud filtrate	v/v
C_{cor}	Mud filtrate coefficient	-
S_{hf}	Hydrocarbon coefficient	-
ρ_{hc}	Hydrocarbon density	g/cm^3
ρ_{mf}	Mud filtrate density	g/cm^3
Δt	Acoustic propagation time	μs/ft
Δt_{mf}	Acoustic propagation time of mud filtrate	μs/ft
Δt_{ch}	Acoustic propagation time of hydrocarbon	μs/ft
Δt_{sh}	Acoustic propagation time of shale	μs/ft
Δt_{sd}	Acoustic propagation time of sand	μs/ft
R_d	Deep resistivity	ohm-m
R_s	Shallow resistivity	ohm-m
R_w	Water resistivity	ohm-m
P_e	Photoelectric adsorption index	barn/e
$p_{e_{mf}}$	Photoelectric adsorption index of mud filtrate	barn/e
$p_{e_{hc}}$	Photoelectric adsorption index of hydrocarbon	barn/e
p_{e_c}	Photoelectric adsorption index of dolomite	barn/e
V_c	Volume of carbonate	v/v
SA	Simulated Annealing	-
b	Perturbation term	-
E	Energy function	%
α	Random number generated with uniform probability from the interval of 0 and 1	-
ε	Damping factor	-
c_i	Control parameter	-

DOI: 10.14750/ME.2022.027

1. INTRODUCTION

Geophysical studies of the inaccessible Earth's interior by making measurements at or near the ground surface are affected by the internal distribution of physical properties. Detailed analyses of the measured information can assist to reveal not only the vertical variation of these properties, but the lateral variation as well. Applied geophysics involves physical methods such as gravity, magnetic, seismic, direct current, electromagnetic, and nuclear, which can be used to record the various physical responses of the interior of the earth and assist in solving different practical problems in terms of subsurface structures and phenomena (Kearey et al. 2002). The applicability of these geophysical methods since the variation of the physical quantities measured as a function of depth, time or sometimes frequency and energy can be also the reference proportion are the consequence of changes in the different material properties. The variations in these properties are primarily connected to the boundaries of different rock formations or fluids content.As a result, further useful information is provided for the oil and mining industry, hydrological, geotechnical, environmental, and archaeological surveys.

In the last decades, significant success has been shown by Geophysics in oil and mineral ores exploration. Several geophysical techniques have been developed for the detection or/and mapping of hidden deposits and structures related to hydrocarbon accumulation. Of course, borehole geophysics is one of the most widely used of all geophysical tools. It used to obtain further in-depth (in-situ) information that is crucial in better understanding of subsurface conditions via measuring, investigating, and analyzing the physical properties of the surrounding rocks by means of the drilled borehole. The most frequent and useful applied borehole geophysical methods are based on self-potential, electrical resistivity, sonic or acoustic velocity, temperature, natural and induced radioactivity. It is possible to figure out the drilled wells by examining core samples but the gained information via this way would be incomplete even useless to define the nature of the drilled rocks and clarify or distinguish between the types of fluids presented in the rock formations if not complemented by certain new borehole logging techniques which represent a tremendous source of information (Serra 1984). Substantially, the measured data through these techniques are typically effective in characterizing geologic, fluid flow, fracture patterns, and structural properties especially with the continual refinement that have been launched to the equipment and the

DOI: 10.14750/ME.2022.027

automated interpretation systems used for this purpose (Aguilera 1980; Bonter et al. 2019; Akbar 2021).

Well-logging is a relatively new science where the initial work on the field goes back to less than 130 years. In 1896 lord kelvin in Britain measured the temperature with depth through shallow holes. Most of us think that the interior of the earth was as cold as caves, but the coldness does not exceed only a few meters. In general, the subsurface temperature increases at a rate of one or two degrees per 100 feet, and such changes show much of what is present around the drilled well which is not indicated by any other measurements. The idea of well- logging, especially the electric logs is taken from the method of measuring resistance at the surface which was firstly used by Schlumberger brothers in France for prospecting the metal ore mining industry but gradually extended its activities to involve exploration of possible oil-bearing structures. To better understand the surface measurements, the Schlumberger brothers needed to incorporate resistivity information from deeper formations and the first attempt was made in 1927. This first log marked a turning point in the history of hydrocarbon exploration despite being a little more than a simple hand-plotted graph. By 1929 the international demand for this process grew and subsurface logging was conducted in different countries around the world. Consecutively, new tools have been designed to complement electrical logging methods and provide measuring new parameters such as diameter, temperature, and inclination of the borehole. A significant contribution has been made through studying the relationship between resistivity, porosity, and water saturation in oil bearing formations (Archie 1942) and it known as Archie´s law which has become the basis of petrophysical interpretation yet.During the 1950s and 1960s, various electric logs were introduced, including the laterolog tool for measuring formation resistivity beyond the invaded zone using widely spaced electrodes, the microlaterlog tool for measuring the resistivity of the flushed zone with minimal influence from the mudcake or the undisturbed zone, and the microlog tool for detecting permeable zones across which a mudcake has formed. In addition to that sonic measurements are conducted for better depth control and placing equipment's of well completion, the slowing down time technique is used to measure formation hydrogen concentration by detecting energy reduction of source neutrons and finally the first density log enables realization of bulk density measurement using gamma ray attenuation. Furthermore, the latter three logs sonic, neutron and density have been independently used to estimate the apparent

DOI: 10.14750/ME.2022.027

porosity. As a result of growing computer power and engineering development in the 1970s the SARABAND and CORIBAND programs have been introduced as the first computerized reservoir analysis. The SARABAND program was designed to analyze shaly sand rocks via measuring volume of clay minerals and calculating fluid saturations while CORIBAND deals with multimineral lithology (Schlumberger 2017).

The year 1980 marked the beginning of a qualitative leap in the interpretation and processing of wireline logging data collected from deep borehole. Several computer-based inversion methods equipped with quality checking tools have been launched by petroleum companies for evaluating hydrocarbon formations such as Global system by Schlumberger (Mayer and Sibbit 1980), Ultra system by Gearhart (Alberty and Hashmy 1984), and Optima system by Baker Atlas (Ball et al. 1987).These computer-processed log interpretation systems provide more accurate and reliable estimation of petrophysical proprieties such as porosity, water saturation and matrix volumes compared to the conventional (quick look or deterministic) methods. Through the inversion methods, all the available data sets are combined in a joint inversion procedure to accurately derive the petrophysical parameters, while they are derived by using the conventional ones separately from each other by the analysis of a specific (single) well log.

Inversion of well-logging data using the previously mentioned systems is conducted in a local way which means processing data acquired in a particular depth-point and providing an estimate for the petrophysical parameter only to that point in a set of separate inversion runs (Drahos 2005; Mayer and Sibbit 1980). Such local inverse problem can be solved by using linear optimization techniques with obtaining fast and satisfactory results in typical cases. Since the number of probe measurements to some extent exceeds that of the petrophysical parameter unknowns (e.g., porosity, clay content, water saturation in invaded and uninvaded zones) to be determined in each depth-point, the problem represents a marginal overdetermined inverse one along the borehole. It is a known fact that in the case of inversion of a small number of measurement data, (and poor a priori information), the result is strongly affected by the measurement error (noise), thus we not always obtain a satisfactory result in terms of the accuracy and reliability of the local parameter estimation (Dobróka et al. 2016). It is possible to overcome this problem and obtain more accurate results by increasing the measured information from several well-logs, but it also has known technological limitations and additional costs. Given that the precise calculation of hydrocarbon

DOI: 10.14750/ME.2022.027

reserves demands the most reliable estimations of the petrophysical parameters by reducing the harmful effect of data noise, a new method namely interval inversion has been introduced for the analysis of open-hole logging data (Dobróka 1995; Dobróka and Szabó 2001).

By means of the interval inversion method, all data of a longer depth interval are processed in one joint inversion procedure. Through the inversion procedures, the petrophysical properties of the geologic formations (unknowns) are related to the measured data by setting depth - dependent response functions. The series expansion-based approach (Dobróka 1995) is suitable for discretizing the model parameters by expanding them into a series and approximating them not only in one point but also in the entire processed depth-interval. By this formulation, the relative number of measured data compared to the series expansion coefficients which represent the unknowns of the inverse problem can be effectively increased. Hence, a high data to unknown parameters ratio can be achieved which enhances the quality of the interpretation results. The great advantageous property of the interval inversion method is its capability to treat an increasing number of unknowns without significant decrease of overdetermination ratio.

The geophysical inverse problems can be solved by seeking the minimum of the objective function which is expressed as the misfit between the measured data and the calculated one. There are several optimization approaches that can be used to find the extremum of such an objective function. The most considerable ones are depending on the solution of sets of linear equations and termed as linear or gradient-based techniques (Marquardt 1963; Menke 1984; Tarantola 1987). The linear methods are more favorable in practice due to their speed and efficiency, especially when having a proper initial model. Nevertheless, these methods assign the solution to a local optimum of the objective functions and cause truncation errors; hence they are not absolute minimum searching techniques. It is possible to avoid the local optimum solution of linear inversion methods and effectively find the absolute global optimum of the objective function by means of using global optimization methods. These meta-heuristic methods are characterized by high performance and efficiency such as Simulated Annealing (Metropolis et al. 1953), Genetic Algorithm (Holland 1975; Goldberg 1989) and Particle Swarm Optimization (Kennedy and Eberhart 1995). As a result, several studies have been conducted based on these methods in the analysis of borehole geophysical data (Zhou et al. 1992; Dobróka and Szabó 2001, 2012; Goswami et al. 2004; Szabó 2004).

DOI: 10.14750/ME.2022.027

The interval inversion method has been introduced (Dobróka 1995; Dobróka and Szabó 2001) and further developed by the research work of the inversion and tomography research team of the Department of Geophysics, University of Miskolc and still of interest so far. The main objectives of my PhD studies are to further develop the interval inversion method for 1D petrophysical parameter distributions and its extension 2D cases. At first, I develop the Chebyshev polynomials-based interval inversion approach to characterize the reservoir rock in Komombo basin, Upper Egypt. I use a new alternative basis function (Chebyshev polynomials) for discretizing the model parameters. Thereafter, I further improve the 1D interval inversion method to evaluate the 2D petrophysical models. The 2D developments represent new innovative inversion approaches which integrate datasets of several neighboring deep wells to estimate lateral change of layer boundary coordinates together with the lateral and vertical variation of the petrophysical parameters. To accomplish this, I apply Legendre polynomials as an orthogonal set of basis functions instead of (non-orthogonal) power functions used in earlier applications. Thus, 2D petrophysical models can be obtained in a more accurate and reliable manner and geometry of the layer boundary of the geologic structures can be figured if the specified wells are in the same range.

DOI: 10.14750/ME.2022.027

2. CHEBYSHEV POLYNOMIALS-BASED INTERVAL INVERSION METHOD FOR THE ANALYSIS OF WELL LOGGING DATA

The inversion methods local and interval inversion ones play a vital role in the valuable analysis of borehole data. Regarding the local inversion approach, the model parameters are predicted point by point in a marginally overdetermined inverse problem. Although the method succeeded in setting the unknown model parameters (Dobróka et al. 2016), it is rather sensitive to the uncertainty of measured data and limited in estimation accuracy. To overcome this problem and obtain more accurate results by increasing the measured information from several well logs, but it also has known technological limitations and additional costs. Given that the truthful calculation of hydrocarbon reserves demands the most reliable estimations of the petrophysical parameters by reducing the harmful effect of data noise, a new method termed interval inversion has been introduced for the analysis of wire logging data (Dobróka and Szabó 2001). By means of the interval inversion method, all data sets of a longer depth interval are processed in one joint inversion procedure. The petrophysical properties of the geologic formations (unknowns) are related to the measured data by setting depth-dependent response functions. A series expansion approach (Dobróka 1995) allowed discretizing the model parameters and approximating them not only in one point but in the entire processed depth-interval as well. By this formulation, the relative number of measured data compared to the series expansion coefficients which represent the unknowns of the inverse problem is increased. Hence, a high data-to-unknowns (overdetermination) ratio can be achieved which enhances the quality of the interpretation results (Dobróka and Szabó 2002, 2005). The method was further developed, and the so-called zone parameters are computed with the petrophysical parameters as new inversion unknowns (Dobróka et al. 2007; Dobróka and Szabó 2011). Also, complex reservoirs were processed by the method, thus more than 3 matrix components which may be presented in volcanic or metamorphic can be determined (Dobróka et al. 2012). The application of the method also extended to evaluate organic-rich shale (Szabó and Dobróka 2020) and tight gas (Szabó et al. 2022).

In mathematics it is known that the classical orthogonal polynomials include the Hermite, Laguerre and Jacobi polynomials. The latter comprises Genebauer, Chebyshev, and Legendre polynomials (Abramowitz 1983). Up to this time, all the previous studies by using interval inversion method for reservoir characterization are based Legendre

DOI: 10.14750/ME.2022.027

polynomials as a discretization technique with the aim of increasing the vertical resolution in hydrocarbon-bearing formations (Dobróka et al. 2016). In my research, I tried to discriminate the possibilities of applying Chebyshev polynomials as an alternative orthogonal basis function for characterizing the reservoir rock in Komombo basin, Upper Egypt.

2.1 Developed inversion procedures

At first, I formulated the forward modeling for computing the calculated data. In the case of the local inversion the column vector of the model parameters given as

$$\mathbf{m} = [\emptyset,\ S_{x0},\ S_w,\ V_{sh}]^{\mathrm{T}}, \tag{1}$$

where $\emptyset$ is the porosity, S_{x0} *and* S_w are the water saturation in the invaded and uninvaded zones respectively, and the volume of shale given as V_{sh}.

The volume of sand can be calculated by using the following material balance equation

$$V_{sh} + V_{sd} + \emptyset = 1. \tag{2}$$

The *l*-th calculated data ($d_l^{(calc)}$) isobtained by using the following relationship

$$d_l^{(calc)} = g_l(m), \tag{3}$$

where the nonlinear operator g_l represents the *l*-th response function. The response functions of Wyllie et al. (1956), Alberty and Hashmy (1984) and Schlumberger (1989) are used to derive the calculated data.

In case of the interval inversion method (equation 3) is modified to be a depth-independent function for estimating the *f*-th calculated data ($d_f^{(calc)}$)

$$d_f^{(calc)} = d^{(calc)}(z_i) = g_f\big(\emptyset(z_i), S_{x0}(z_i), S_w(z_i), V_{sh}(z_i)\big), \tag{4}$$

where z_i represents the coordinate of the *i*-th depth (i = 1, . . ., N_s) and N_s is the number of the measurement points of the *f*-th well log.

The *i*-th model parameter in equation (4) is discretized by using series expansion approach

$$m_i(z) = \sum_{q=1}^{Q_i} B_q^{(i)} \Psi_q(z), \tag{5}$$

where m_i denotes the *i*-th petrophysical parameter, B_q is the *q*-th expansion coefficient and Ψ_q is the *q*-th basis function (up to Q number of additive terms). The Chebyshev

DOI: 10.14750/ME.2022.027

polynomial is used as an alternative basis function for approximating the variation of model parameters.

There are four kinds of Chebyshev polynomials, and all have the same recurrence relation (equation 11) but with different starting polynomials $p1$, where $p1=z$, $2z$, $2z$-1and $2z+1$ for first, second, third and fourth kinds, respectively. The first and second kinds are more common comparing with the other ones

$$p_0 = 1\,, \quad p_n(z) = 2zp_{n-1}(z) - p_{n-2}(z). \tag{6}$$

In this study, I used the Chebyshev polynomials of the first kind which are orthogonal over the interval [1, -1]

$$\int_{-1}^{1} T_m(z)T_n(z)\, w(z)\, d(z) = 0 \qquad if\ n \neq m, \tag{7}$$

where w (z) represents the weight function (w) which equals to $(1-z^2)^{-1/2}$. In terms of (z), it can be computed by the following recurrence relations

$$T_0\,(z) = 1, \tag{8}$$

$$T_1\,(z) = z, \tag{9}$$

$$T_n(z) = 2zT_{n-1}(z) - T_{n-2}(z) \qquad (n \geq 2). \tag{10}$$

The priority of using the first kind of Chebyshev polynomials is that with a large possible managing coefficient its absolute value over the interval [-1 1] is bounded by one unlike the second kind. This can be confirmed by illustrating the Chebyshev polynomials of the first and second kind for fourth and up to fourth degree in Fig.1. Another advantage of the $T_n(z)$ is that they are orthogonal with respect to the inner product. For more clarification, the polynomials of the first kind are orthogonal to each other which give it a more valuable property. By using the Chebyshev polynomials of the first kind the series expansion (10) becomes

$$m_i(z) = \sum_{q=1}^{Q_i} B_q^{(i)} T_{q-1}(z), \tag{11}$$

where T_q represents the q-th Chebyshev polynomial.

The inverse problem is solved by the damped least squares method (Marquardt 1959) for the expansion coefficients to compute the vertical distribution of the petrophysical parameters

$$\mathbf{B} = \mathbf{G}^{-\mathrm{g}}\mathbf{d}^{(\mathrm{m})}, \tag{12}$$

DOI: 10.14750/ME.2022.027

where $\mathbf{d}^{(\mathrm{m})}$ is the vector of measured data and $\mathbf{G}^{-\mathrm{g}}$ is the generalized inverse of the problem. The relative data distance between the calculated data and the measured one is minimized to obtain the optimal value of the expansion coefficients

$$D_d = \sqrt{\frac{1}{K}\sum_{k=1}^{K}\left(\frac{d_k^{(m)} - d_k^{(c)}}{d_k^{(m)}}\right)^2} = min, \tag{13}$$

where K denotes the number of inverted data, $d_k^{(m)}$and, $d_k^{(c)}$ are the k-th measured and calculated data, respectively.

The interval inversion method allows to derive petrophysical parameters more accurately provided that the observed data are reliable. The source of errors has been studied by Horváth (1973), providing an estimation of the uncertainty of different types of well logging data. Several ways have been proposed to quantify the quality of the inversion results. One of these is given by Menke (1984) where the covariance matrix of the estimated petrophysical parameters from the linear optimization techniques is related to the covariance matrix of the measured data including their variances.

Unlike the local inversion method, the petrophysical parameters are derived by interval inversion from the estimated expansion coefficients (**B**) thus the covariance matrix of series expansions can be expressed as follows

$$cov\mathbf{B} = \mathbf{G}^{-g} cov\mathbf{d}^{(\mathrm{m})}(\mathbf{G}^{-g})^{\mathrm{T}}, \tag{14}$$

where $\mathbf{G}^{-g}$denotes the generalized inverse matrix. Hence, the depth-dependent model covariance matrix of the estimated parameters is (Dobróka et al. 2016)

$$[cov\ \mathbf{m}\ (z)]_{ij} = \sum_{n=1}^{Q^{(i)}}\sum_{m=1}^{Q^{(i)}} T_{n-1}(z)(cov\mathbf{B})_{hh'}T_{m-1}(z), \tag{15}$$

where indices are $h=n+Q_1+Q_2+\ldots+Q_{i-1}$, $h'=m+Q_1+Q_2+\ldots+Q_{j-1}$ (I=1,2,..,P and j=1,2,…,P). The error of the estimated parameters is obtained by the main diagonal of the previous covariance matrix

$$\sigma\big(\mathrm{m}_i(z)\big) = \sqrt{cov\mathbf{m}_{ii}(z)}. \tag{16}$$

On the other hand, the reliability of inversion results can be quantified by Pearson's correlation matrix. Because only uncorrelated (or only weakly correlated) parameters can be resolved uniquely by inversion, the solution is considered reliable when the model parameters correlate marginally. If the absolute value of the correlation

DOI: 10.14750/ME.2022.027

coefficient is close to ±1, there is a strong relationship between the model parameters indicating an untrustworthy solution.Reliable solution requires a model with uncorrelated parameters with correlation coefficients between 0 and ± 0.5. In our inverse problem, the correlation matrix of the expansion coefficients estimated by the Chebyshev polynomial-based interval inversion methods used as follow

$$corr\mathrm{B} = \frac{cov\mathrm{B}}{\sigma(\mathbf{B})_l \sigma(\mathrm{B})}. \tag{17}$$

Else, the scalar S is used to characterize the overall correlation matrixof quantity **B** and it is given as

$$S(\mathbf{m}) = \sqrt{\frac{1}{P(P-1)} \sum_{i=1}^{P} \sum_{j=1}^{P} \left(corr\ \mathbf{m}\right)_{ij} - \delta_{ij})^2}, \tag{18}$$

where δ is the Kronecker delta symbol (which is 1 if i=j, and 0 otherwise).

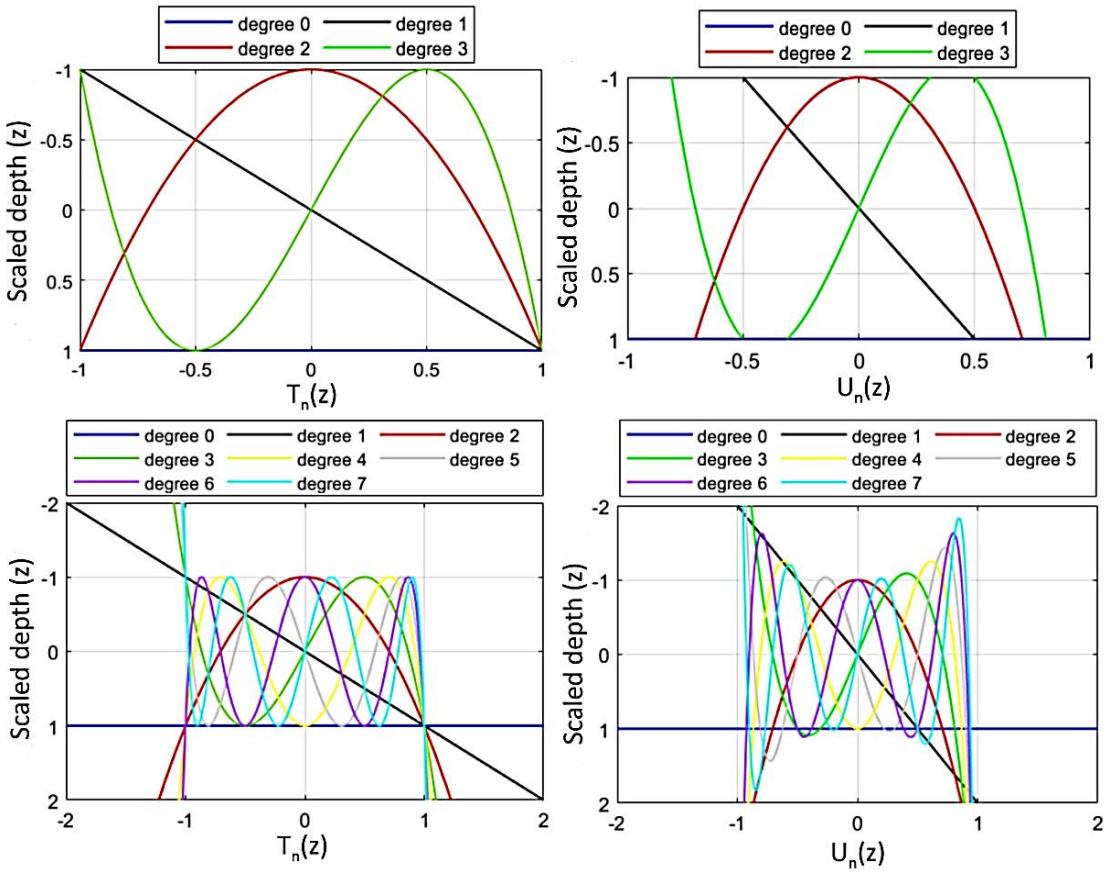

Fig.1 Chebyshev polynomials of the first T_n (z) and the second U_n (z) kinds for n-th degree (n=0, …3) over the interval [-1 1] and n-th degree (n=0, ...,7) over the interval [-2 2]

DOI: 10.14750/ME.2022.027

2.2 Egyptian case study

The proposed method is utilized on the applicable data set of well W. Al Baraka-2, Komombo Basin-Upper Egypt. Komombo Basin lies west of River Nile in the southern Western desert, north of Aswan city bounded by latitudes 24˚10′00″ & 24˚42′00″ N and longitudes 32˚40′00″ & 32˚55′00″ E (Fig. 2a). Komombo area included Al Baraka oilfield which is considered as the first oilfield discovered outside Egypt's conventional producing areas. The concession is situated in the Komombo Basin, located 800 km south of Cairo and is characterized by multiple stacked sand reservoirs. The concession contains the producing Al Baraka oilfield, covering a development area of 50 km^2. The stratigraphic sequence of Southern Western Desert has been deeply investigated by several authors (Klitzsch 1990; Wycisk 1994). This sequence could mainly be described in terms of Late Jurassic, Cretaceous and Paleocene succession (Fig. 2b). The Komombo basin in Upper Egypt is a half-graben system and contains thick non-marine sediments deposited during Early Cretaceous Hauterivian, Neocomian to Barremian followed by marine deposition during Cenomanian/Albian (argillaceous sandstones and shales) and later shales and marine limestones during Late Cretaceous and early Tertiary (Dolson et al. 2001). The main bounding fault of the Komombo Basin is located to the northeast and trending NW–SE, while the subordinate faults are mainly synthetic and of the same trend Fig 2c (Ali et al. 2017).

The available dataset contains five types of well logs. The measured data are natural gamma-ray intensity "*GR* in *API*", shallow resistivity "R_s in *ohm-m*", deep resistivity "R_d in *ohm-m*", bulk density "ρ_b in g/cm^3", and neutron-porosity "$\emptyset_N$ in *v/v*". The environmentally corrected data logs are illustrated in Fig. 3. With a depth matched of the range from 0 to 14 m (relative depth coordinates). Since we have five types of logs with a sampling interval of 0.25, the total number of data is 280 points. The four model parameters ($\emptyset$, S_{x0}, S_w, and V_{sh}) are discretized using orthogonal Chebyshev function with setting the degree of polynomials up to 14. Consequently, the total number of expansion coefficient (unknowns) becomes 60 where, $4(Q^* + 1) = 60$, Q^* is the maximum degree of Chebyshev polynomials thus the data to unknown's ratio is 4.6. The initial values of these are set as 0.01 for porosity, 0.5 for water saturation in invaded and uninvaded zones, and 0.3 for the volume of shale. To obtain more consistent results the uncertainty of the observed data comparably to Horváth (1984) is quantified by studying the effect of data variance on the solution of the inverse problem. The standard

DOI: 10.14750/ME.2022.027

deviations of input data are set as σ_{GR}=0.05, σ_{R_d}=0.04,σ_{R_s}=0.04, σ_{ϕ_N}=0.03, σ_{ρ_b}=0.03. The confidence intervals of measured log types are illustrated in Fig. 3.

The misfit of data distance and the convergence plot of the interval inversion procedures are illustrated in Figs. 4a and 4b. The maximum number of iterations during the inversion process is 50. The relative data distance in the zero-th iteration is D_d= 72.4 %, which reduces to D_d = 3.02 % in the last iteration. Based on these results we can conclude that a steady and rapid convergence to the optimum can be seen despite the data noise which leads to reliable estimation of the petrophysical parameters. The petrophysical parameters are derived from sixty expansion coefficients which are illustrated with their errors in Fig. 5. The standard deviation of water saturation and shale content is smaller than that of the porosity.

The obtained petrophysical parameters with their estimated errors are demonstrated in Fig. 6. The average values of the estimated parameters of the reservoir rock in the investigated area are ranging between 0.14-0.25 v/v for porosity, 0.36-0.81 v/v for clay content, 0.36-1.0 v/v, and 0.28-1.0 v/v for water saturation in the invaded zone and water saturation in the uninvaded zone, respectively. The relative errors of the estimated parameters are 0.02 v/v for porosity, 0.1 v/v for water saturation in invaded and uninvaded zones, and 0.03 v/v for the volume of shale. The correlation between the estimated model parameters is quantified as another check for the quality of our results. The absolute value of the 60-by-60 correlation matrix of inversion unknowns (15 per petrophysical property) can be seen in Fig. 7. The mean value of the correlation coefficients is equal to 0.3 which indicates poorly correlated expansion coefficients and highly reliable inversion results. It is worth mentioning that the most reliable inversion parameters are porosity and shale content. Since water saturations are correlated more strongly inherently, their estimation is riskier, but acceptable in this case (series expansion coefficients with small error ranges).

The reliable estimation of the petrophysical parameters by the modified interval inversion method helped to quantitatively throw light over the hydrocarbon potentiality. The hydrocarbon saturation (S_{hc}) is derived by subtracting the estimated values of water saturation from unity. In more details the irreducible $(S_{hc,irr})$ and movable ($S_{hc,mov}$) hydrocarbon saturations are computed by using equations (19) and (20). Considerable oil saturation is exhibited of the reservoir rock in the study area Fig. 8.

DOI: 10.14750/ME.2022.027

$$S_{hc,irr} = (1 - S_{x0}).100\ \%, \tag{19}$$

$$S_{hc,mov} = (S_{x0} - S_w).100\ \%. \tag{20}$$

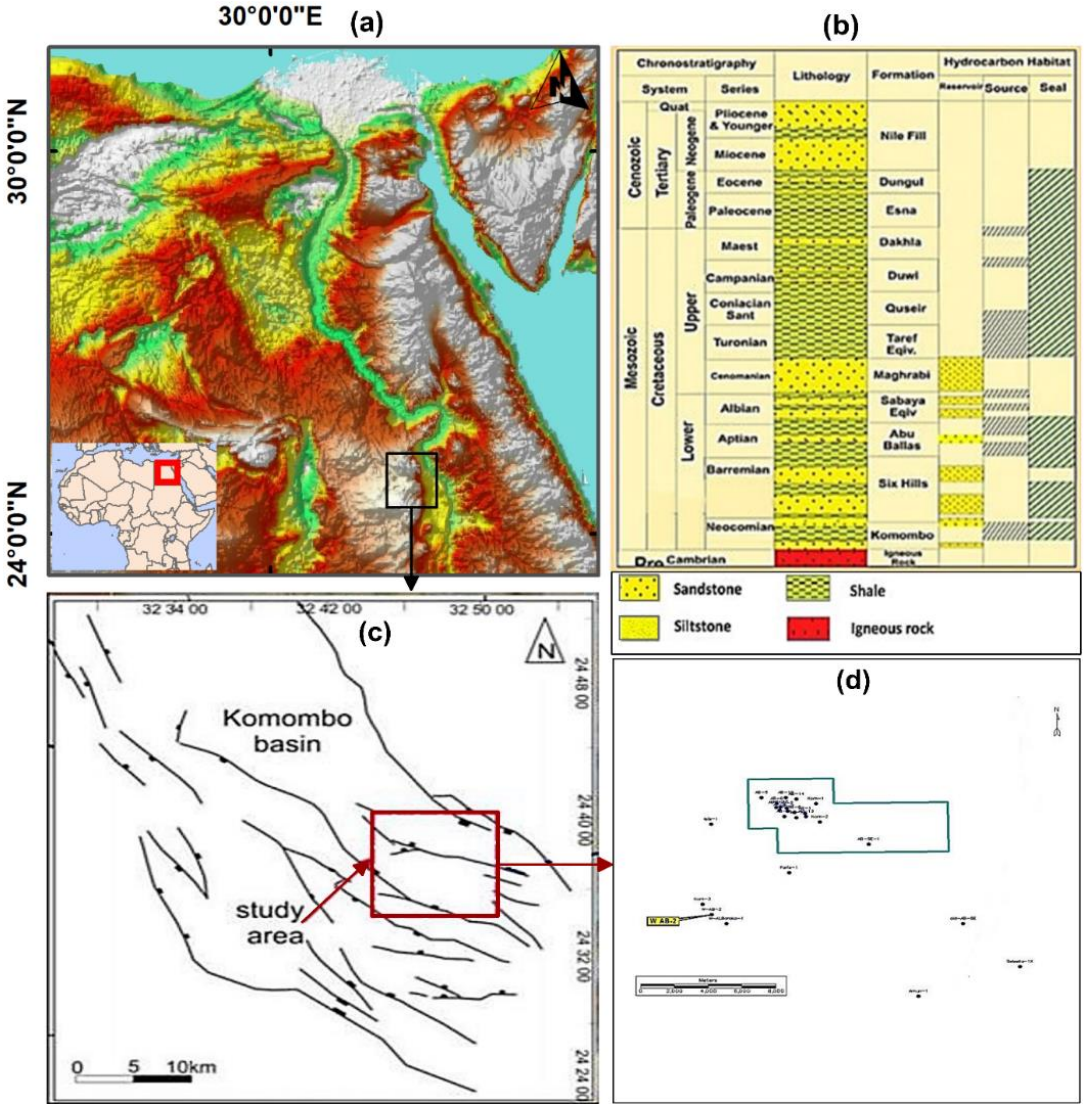

Fig. 2 a) Location of the study area, b) general stratigraphic column of Komombo concession (Repsol1998), c) structural features, d) drilled wells indicating the investigated well in the recent study

DOI: 10.14750/ME.2022.027

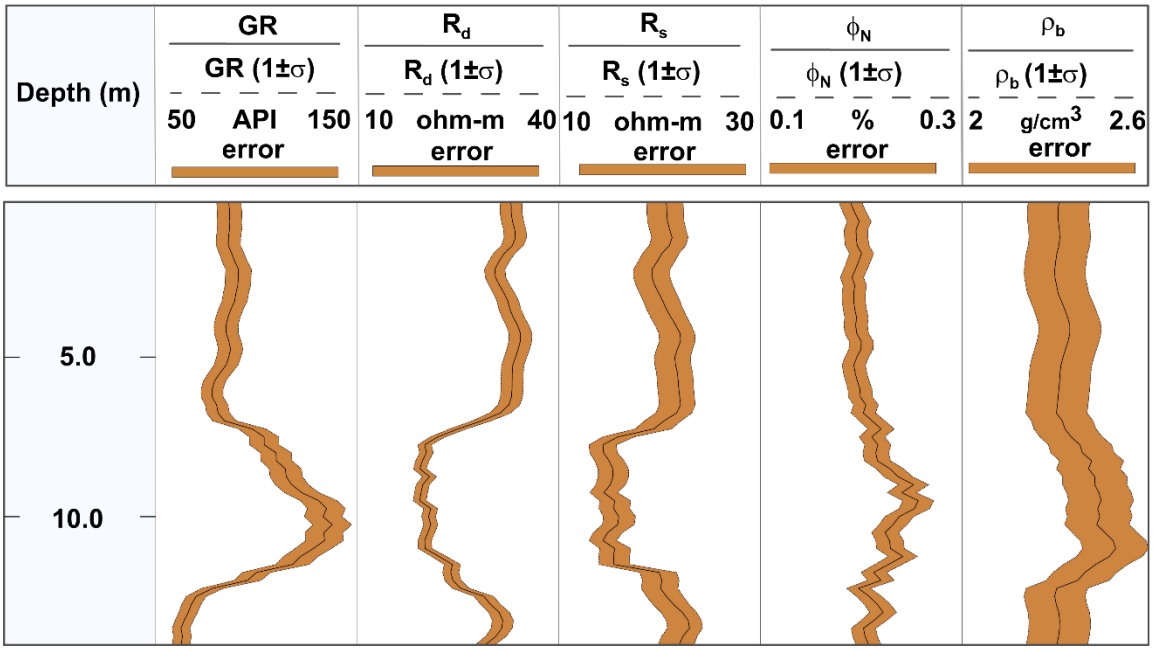

Fig.3 Input well logs measured in W. Al Baraka-2 well and the assumed data uncertainty ranges of log readings for the interval inversion procedures

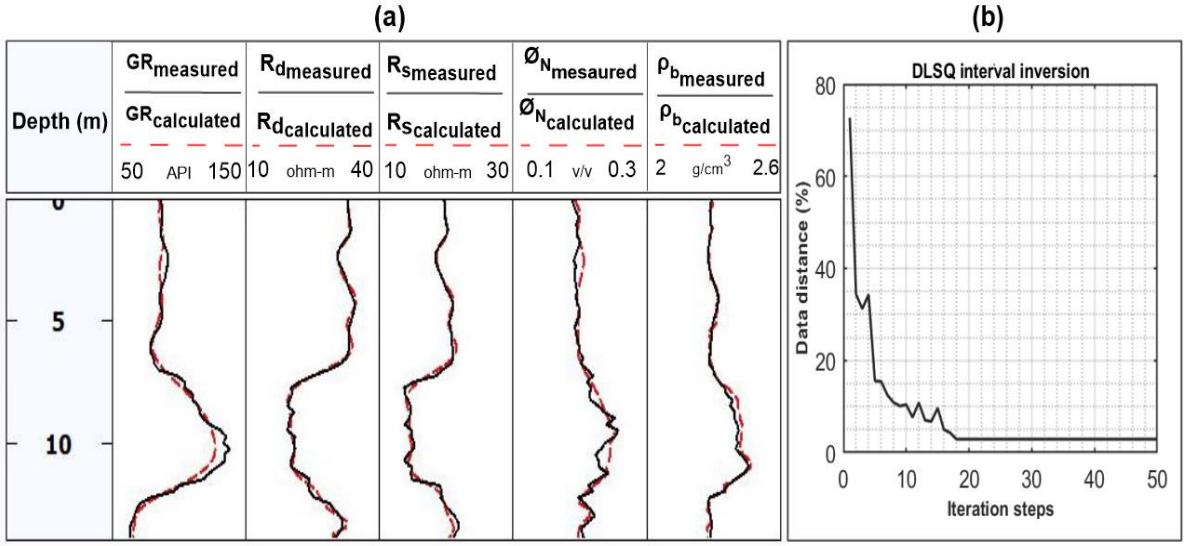

Fig.4 a) Misfit between the measured and calculated data, b) Convergence plot in the subsequent DLSQ inversion procedure

DOI: 10.14750/ME.2022.027

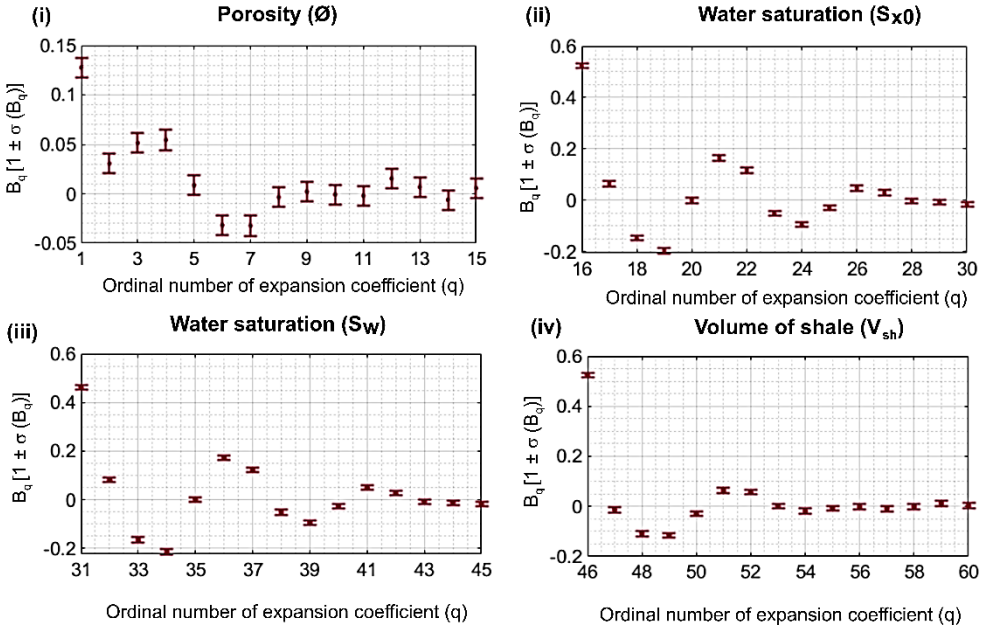

Fig. 5 Results of interval inversion procedure using Chebyshev polynomials of 14 degrees as basis functions in W. Al-baraka well. Estimated values of expansion coefficients for (i) porosity, (ii) water saturation of uninvaded zone, (iii) water saturation of invaded zone, (iv) volume of shale, and their estimation error ranges versus ordinal number of expansion coefficients in the model vector

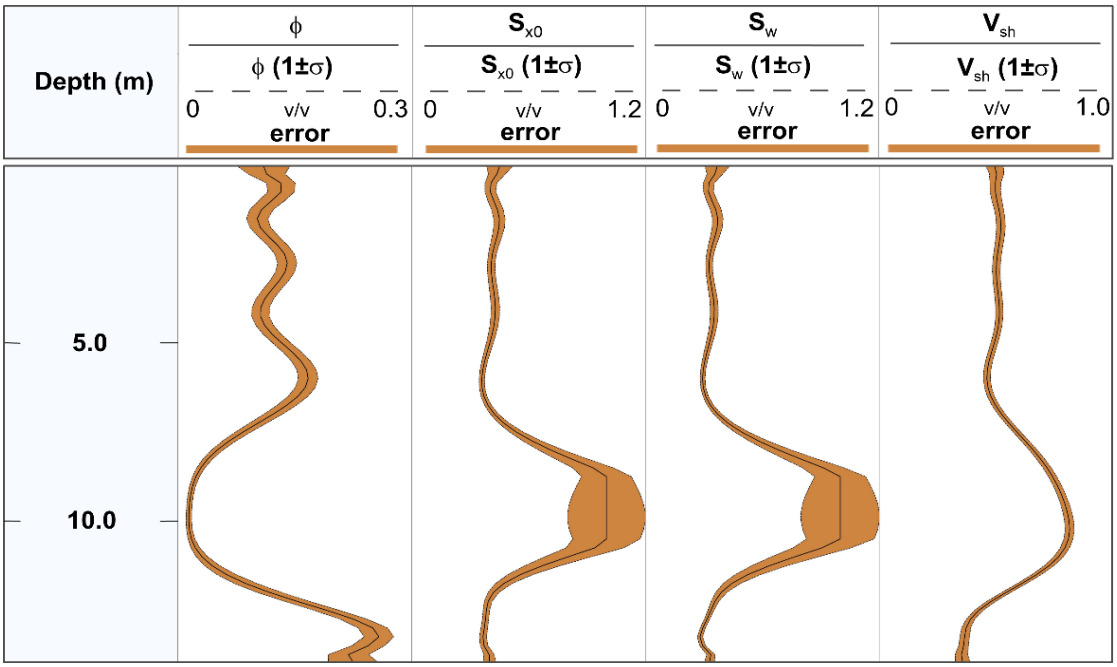

Fig. 6 Well logs of the estimated petrophysical parameters by interval inversion method with their calculated errors

DOI: 10.14750/ME.2022.027

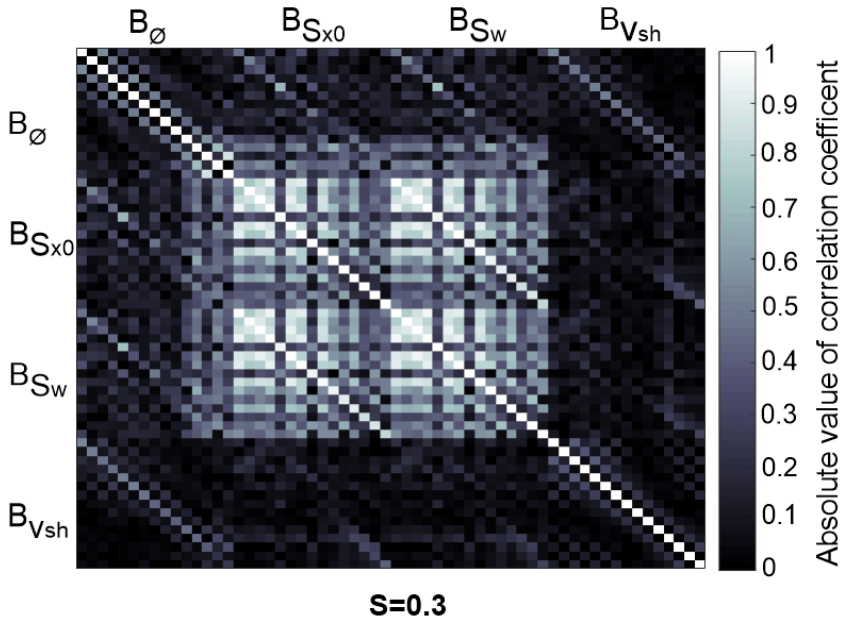

Fig. 7 Pearson's correlation matrix of series expansion coefficients estimated by the interval inversion method

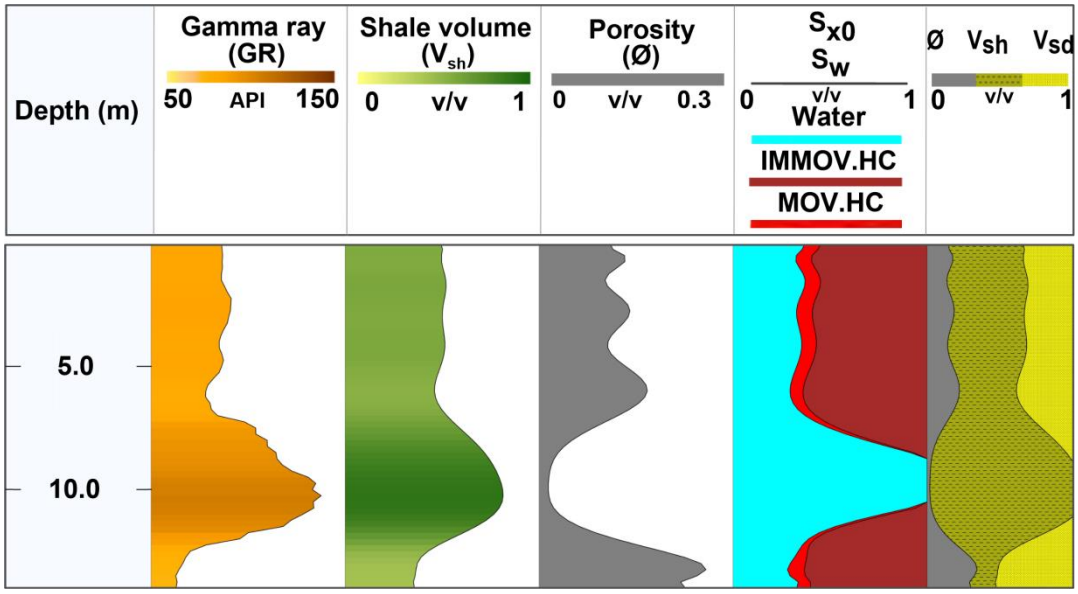

Fig. 8 Interval inversion interpretation plot of the reservoir rock in the investigated area

DOI: 10.14750/ME.2022.027

2.3 Discussion

The newly proposed Chebyshev polynomials-based interval inversion approach has been used to characterize the reservoir rock in Komombo basin, Upper Egypt. As high overdetermination ratio can be achieved, the modified method shows a reliable and consistent estimation of the petrophysical parameters such as porosity, water saturation in invaded and uninvaded zones and volume of shale. A variety of checking quality techniques has been applied in our study. Furthermore, the accuracy of the estimated parameters leads to calculating the hydrocarbon saturation (irreducible and movable) in the investigated area.

Thesis one

I have developed an improved interval inversion method using a new discretization scheme for analyzing well logs measured in hydrocarbon formations. I used Chebyshev polynomials as new alternative basis functions to assure small correlation between the estimated model parameters and great overdetermination ratio. The modified interval inversion algorithm-based using orthogonal Chebyshev basis functions showed a significant success to accurately estimate the model parameters of the Komombo basin, Upper Egypt reservoir rock in steady inversion procedure.

DOI: 10.14750/ME.2022.027

3. LEGENDRE POLYNOMIALS-BASED INTERVAL INVERSION METHOD FOR ESTIMATING LATERAL CHANGES OF LAYER BOUNDARY COORDINATES

In well logging applications, the local inversion method gives an estimate only for the petrophysical parameters at a given depth point and does not contain information about the layer boundaries. In this case, the determination of the rock interfaces is considered using another non-inversion procedure (GR curve analysis, cluster analysis etc.). Taking into consideration, the entire measurement datasets collected from a greater depth interval contains information about the layer boundaries and since the interval inversion method processes the entire dataset in a joint inversion process, it is possible to define the layer boundaries by developing an appropriate algorithm within the inversion (Szabó and Dobróka 2012, 2015). Given the significant advantages of the interval inversion algorithm in determining layer boundaries, I developed a new 2D interval inversion approach that integrates data sets from several neighbouring wells for determining lateral variation of formation boundaries. In my study I introduce the Legendre polynomials as an orthogonal set of basis functions instead of (non-orthogonal) power functions used in the earlier applications (Dobróka et al. 2009).

In the case of the 2D interval inversion method, the petrophysical parameters are defined as a function of *x* and *z* which represents the horizontal and vertical coordinates, respectively. In this regard the straightforward problem (equation 9) for computing the well logging data is modified as

$$d_f^{(calc)} = d_f^{(calc)}(z_i, x_i) = g_f\big(\emptyset(z_i, x_i), S_{x0}(z_i, x_i), S_w(z_i, x_i), V_{sh}(z_i, x_i)\big), \quad (21)$$

where $d^{(calc)}(z_i, x_i)$ indicates the *f*-th calculated data in depth *z* of the borehole situated at *x* coordinate. The series expansion method is used to discretize the model parameters similar to the one used in the 1D interval inversion method

$$m_i(z, x) = \sum_{q=1}^{Q_i} \sum_{l=1}^{L_i} B_{ql}^{(i)} \, \Psi_{q-1}(z) \Psi_{l-1}(x), \quad (22)$$

where m_i denotes the *i*-th petrophysical parameter (*i*=1,..…,*M*), B_{ql} is the *ql*-th expansion coefficient and Ψ_q(z) and Ψ_l(x) are the *q*-th and *l*-th basis function depending on one of the two coordinates, respectively. An orthogonal Legendre- polynomials are

DOI: 10.14750/ME.2022.027

used to approximate the model parameters for obtaining more reliable solutions: $\Psi_{q-1}(x) = p_u(x) = (2^u u!)^{-1} \frac{d^u}{dz^u}(z^2-1)^2$, where u is the degree of polynomial. By applying equation (22) to expand the model parameters in equation (21) into series, the expansion coefficients represent the unknowns of the 2D inverse problem

$$B = [B_1^{(1)}, \dots, B_{Q1}^{(1)}, B_1^{(2)}, \dots, B_{Q2}^{(2)}, B_1^{(M)}, \dots, B_{QM}^{(M)}]^T. \tag{23}$$

Also, the *f-th* function in equation (21) becomes

$$d_f^{(calc)}(z_i, x_i) = g_f\left(B_1^{(1)}(z_i, x_i), \dots\dots\dots\dots, B_{QM}^{(M)}(z_i, x_i)\right). \tag{24}$$

Linear optimization methods like DLSQ (damped least squares procedure) by Marquardt (1959) are used to solve our inverse problem by minimizing the L_2 norm based objective function.

$$E = \frac{1}{FPN}\sum_{f=1}^{F}\sum_{p=1}^{P}\sum_{k=1}^{N}\left(\frac{d_{fpk}^m - d_{fpk}^c}{d_{fpk}^m}\right)^2 \rightarrow min, \tag{25}$$

where F denotes the number of boreholes, P is the number of depth points representing the interval processed and N is the number of applied probes in each well.

Not only the lateral variation of petrophysical properties, but that of the layer boundaries can also be described by the suggested discretization method. Similar to equation (22), the layer thickness functions can also be expanded into series using proper basis functions and the expansion coefficients can be treated as inversion unknowns. I discretize the thickness function of the r-th layer as

$$h_r(x) = \sum_{t=1}^{T_r} C_t^{(r)} \Psi_{t-1}(x), \tag{26}$$

where C_t is the t-th expansion coefficient and $\Psi_t(x)$ is the t-th univariate basis function depending on the lateral coordinate. When using Legendre polynomials, I scale the values of x coordinates to the range of [-1,1], in which the polynomials are orthogonal. Thus, one can reduce the magnitude of the unknown series expansion coefficients and decrease the correlation between them to assure more reliable estimation. The use of bivariate series expansion can be avoided for some practical reasons. The depth of a given layer can be given by expansion coefficient C_1, which equals to the depth

DOI: 10.14750/ME.2022.027

coordinate of the (upper or lower) boundary of the homogenous (plane) layer. A condition that the layers could not intersect each other, and the number of layers is constant during the inversion procedure should be met. This requirement meets when the initial values of C_1 are properly set, and their search domain is preliminary constrained. In 2D inversion, the initial layer boundary coordinates can be assumed as the same constant in each well. Practically, the expansion coefficients corresponding to the higher degree basis functions (t≥2) are slightly changed to describe the thickness variation around the depth level given by C_1. By using a differential genetic algorithm or other global optimization method, it is also possible to fix the search domain of expansion coefficients prior to inversion (Dobróka and Szabó 2012). The vector of inversion unknowns is formed by expanding vector **B** (equation (23)) by coefficients **C**. In case of having a great overdetermination ratio, the 2D interval inversion method solved by minimizing norm (equation 25) may give an automated estimation for both the petrophysical properties and the layer boundary coordinates in a stable and accurate inversion procedure.

3.1 Synthetic modeling experiments

A Legendre polynomials-based 2D interval inversion method is suggested both on noise free and noisy simulated measurements. Two Models A and B of homogenous multilayer structures related to hydrocarbon-bearing reservoirs have been used in the investigation. The first Model A is a three-layered anticline structures made up of shale and hydrocarbon bearing-sand formation (Fig. 9) and the second Model B is a four layered pinchout structure (Fig. 10). The following Gearhart Ultra-response equations (Alberty and Hashmy 1984) are used to generate the simulated well logging data

$$GR = \rho_b^{-1}(V_{sh}\, GR_{sh}\rho_{sh} + V_{sd}GR_{sd}\,\rho_{sd}), \tag{27}$$

$$K = \rho_b^{-1}(\emptyset s_{x0}k_{mf}\rho_{mf} + V_{sh}K_{sh}\rho_{sh} + V_{sd}K_{sd}\rho_{sd}), \tag{28}$$

$$Th = \rho_b^{-1}\left(\emptyset s_{x0}Th_{mf}\rho_{mf} + V_{sh}Th_{sh}\rho_{sh} + V_{sd}Th_{sd}\rho_{sd}\right), \tag{29}$$

$$U = \rho_b^{-1}(\emptyset s_{x0}U_{mf}\rho_{mf} + V_{sh}U_{sh}\rho_{sh} + V_{sd}U_{sd}\rho_{sd}), \tag{30}$$

$$\emptyset_N = \emptyset(\emptyset_{N,mf} - (1 - s_{x0})C_{cor} - 2\emptyset(1 - s_{x0})S_{hf}(1 - 2.2\rho_{hc}).[1 - (1 - s_{x0})(1 - 2.2\rho_{hc})] + V_{sh}\emptyset_{N,sh} + V_{sd}\emptyset_{N,sd}, \tag{31}$$

$$\rho_b = \emptyset\left[\rho_{mf} - 1.07(1 - s_{x0})\left(\alpha_0 - \rho_{mf} - 1.24\rho_{hc}\right)\right] + V_{sh}\rho_{sh} + V_{sd}\rho_{sd}, \tag{32}$$

DOI: 10.14750/ME.2022.027

$$\Delta t = \emptyset[\Delta t_{\mathrm{mf}} s_{x0} + (1 - s_{x0})\Delta t_{ch}] + V_{sh}\,\Delta t_{\mathrm{sh}} + V_{sd}\,\Delta t_{\mathrm{sd}}, \tag{33}$$

$$\frac{1}{R_d} = \frac{\emptyset^2 S_w^2}{aR_w(1-v_{sh})} + \frac{v_{sh}\, s_w}{R_{sh}}, \tag{34}$$

$$\frac{1}{R_s} = \frac{\emptyset^2 S_{x0}^2}{aR_w(1-v_{sh})} + \frac{v_{sh}\, s_{x0}}{R_{sh}}, \tag{35}$$

$$P_e = \emptyset\left[s_{x0} p_{e_{mf}} + (1 - s_{x0}) p_{e_{hc}}\right] + V_{sh} + V_{sd} + V_c p_{e_c}. \tag{36}$$

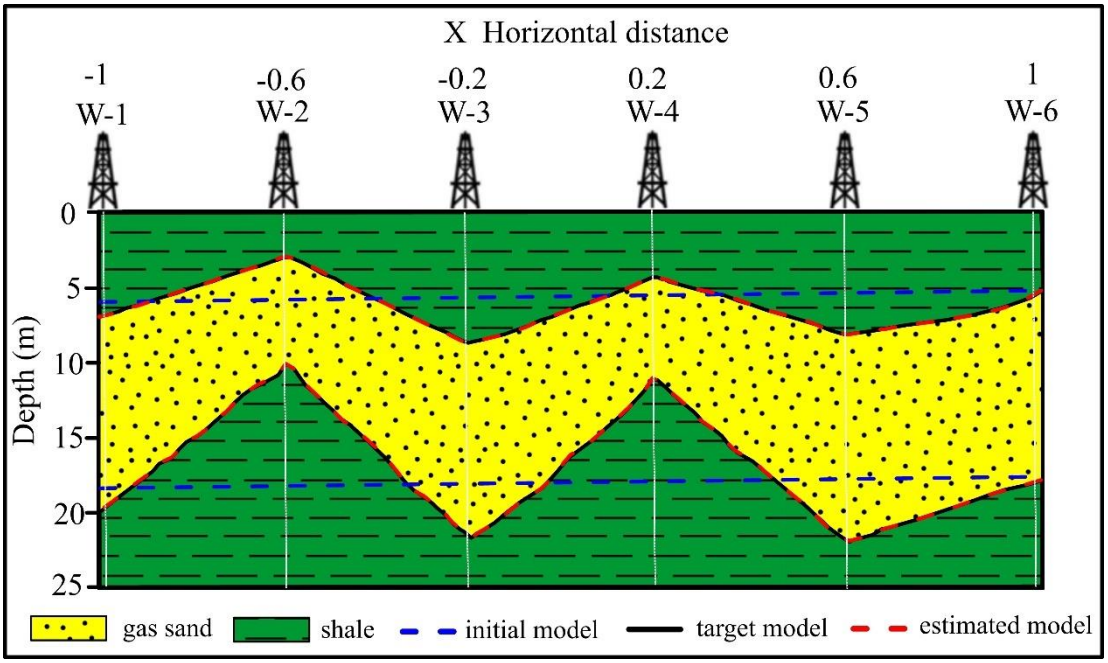

Fig. 9 Layer thickness functions of Model A (blue curve – initial model, green curve – target model, red curve – estimated model by interval inversion method)

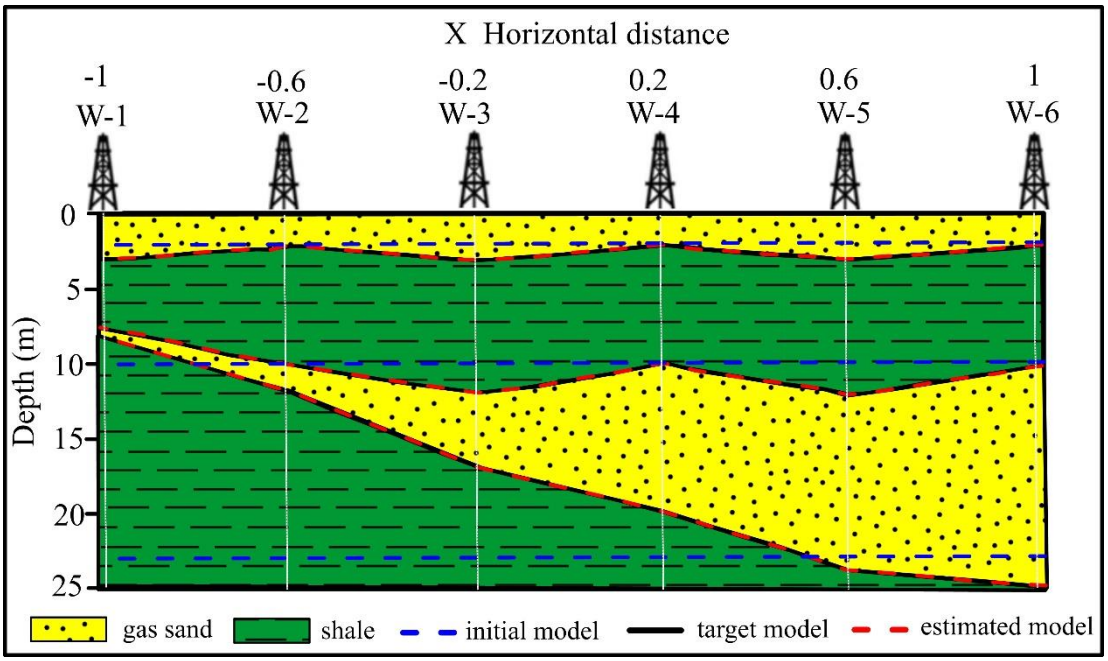

Fig. 10 Layer thickness functions of Model B (blue curve – initial model, black curve – target model, red curve – estimated model by interval inversion method)

DOI: 10.14750/ME.2022.027

The theoretical values of natural gamma ray intensity (*GR*), potassium (*K*), thorium (*Th*), uranium concentration (*U*), neutron porosity ($\emptyset_N$), bulk density (ρ_b), shallow resistivity (R_s), deep resistivity (R_d), and photoelectric absorption index are calculated in six wells (W-1,…, W-6) with *dz* =0.1 m sampling interval. The interval length is about 25 m; thus, I have *N* =15,060 data samples for each model and 5% Gaussian distributed noise is added to compute the noisy simulated measurements.

In case of Model A, the petrophysical parameters and layer thicknesses are shown in Table 1 and the computed types of well logs and their notations are summarized in Table 2. The volumetric fractions are illustrated in Fig. 11, and the calculated log types can be seen in Figs. 12-17.

Table 1 Petrophysical parameters and layer boundary thicknesses of Model A

Layer	Lithology	Petrophysical parameters (v/v)				Layer thickness (m)					
		Ø	S_{x0}	S_w	V_{sh}	W-1	W-2	W-3	W-4	W-5	W-6
1	Shale	0.05	1. 0	1. 0	0.8	7	3	9	4	8	6
2	Gas-sand	0.3	0.8	0.4	0.1	13	7	12	7	14	12
3	Shale	0.1	1. 0	1. 0	0.7	5	15	4	14	3	7

Table 2 Types of open-hole logs applicable to 2D inversion and their notations

Open hole log	Zone parameter	Symbol	Constant	unit
Natural gamma-ray log	Sand Shale	GR_{sd} GR_{sh}	13 160	API API
Potassium concentration log	Sand Shale Mud filtrate	K_{sd} K_{sh} K_{mf}	0.2 3.2 1.6	% % %
Thorium concentration log	Sand Shale Mud filtrate	Th_{sd} Th_{sh} Th_{mf}	2 19 2	ppm ppm ppm
Uranium concentration log	Sand Shale Mud filtrate	U_{sd} U_{sh} U_{mf}	0.5 5 0	ppm ppm ppm

DOI: 10.14750/ME.2022.027

Photoelectric absorption index log	Dolomite Gas Mud filtrate	p_{e_c} $p_{e_{hc}}$ $p_{e_{mf}}$	4.11 0.09 0	barn/e barn/e barn/e
Bulk density log	Sand Shale Mud filtrate Gas Mud filtrate coefficient	ρ_{sd} ρ_{sh} ρ_{mf} ρ_{hc} α	2.65 2.47 1.2 0.153 1.11	g/cm^3 g/cm^3 g/cm^3 g/cm^3 -
Neutron log	Sand Shale Mud filtrate hydrocarbon coefficient Mud filtrate coefficient	$\emptyset_{N,sd}$ $\emptyset_{N,sh}$ $\emptyset_{N,mf}$ Shf Ccor	-0.035 0.3 1 1.17 0.69	v/v v/v v/v - -
Acoustic log	Sand Shale Mud filtrate Gas	Δt_{sd} Δt_{sh} Δt_{mf} Δt_{hc}	56 108 188 211	μs/ft μs/ft μs/ft μs/ft
Resistivity log	Shale Pore-water Cementation exponent Saturation exponent Tortuosity factor	R_{sh} R_w m n a	1 0.4 1.4 1.7 0.9	Ωm Ωm - - -

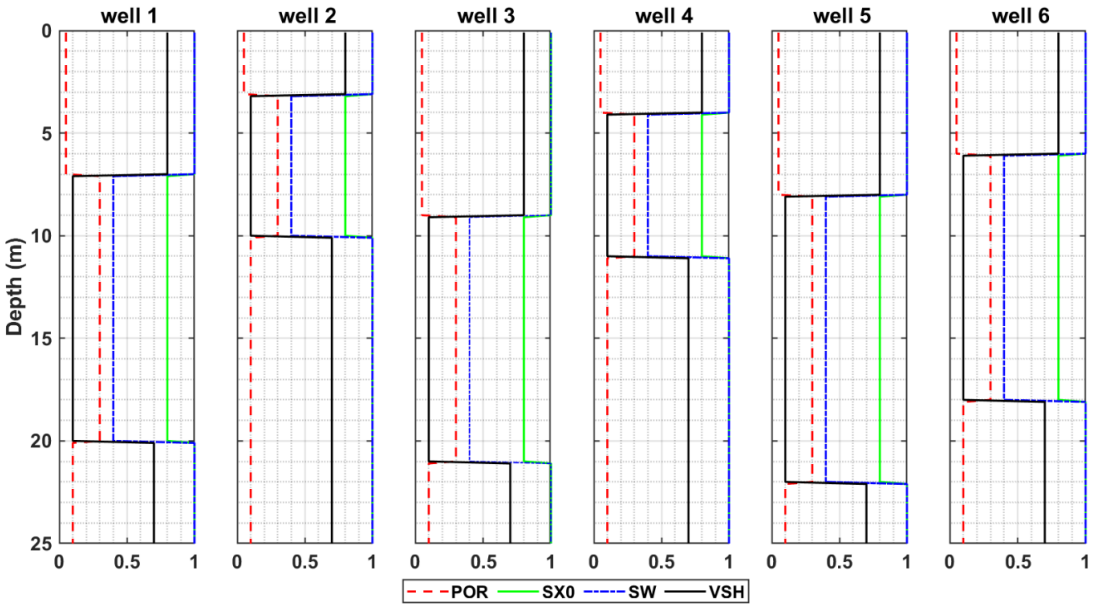

Fig. 11 Volumetric parameters in the 6 well for calculaing the simulated logs of Model A

DOI: 10.14750/ME.2022.027

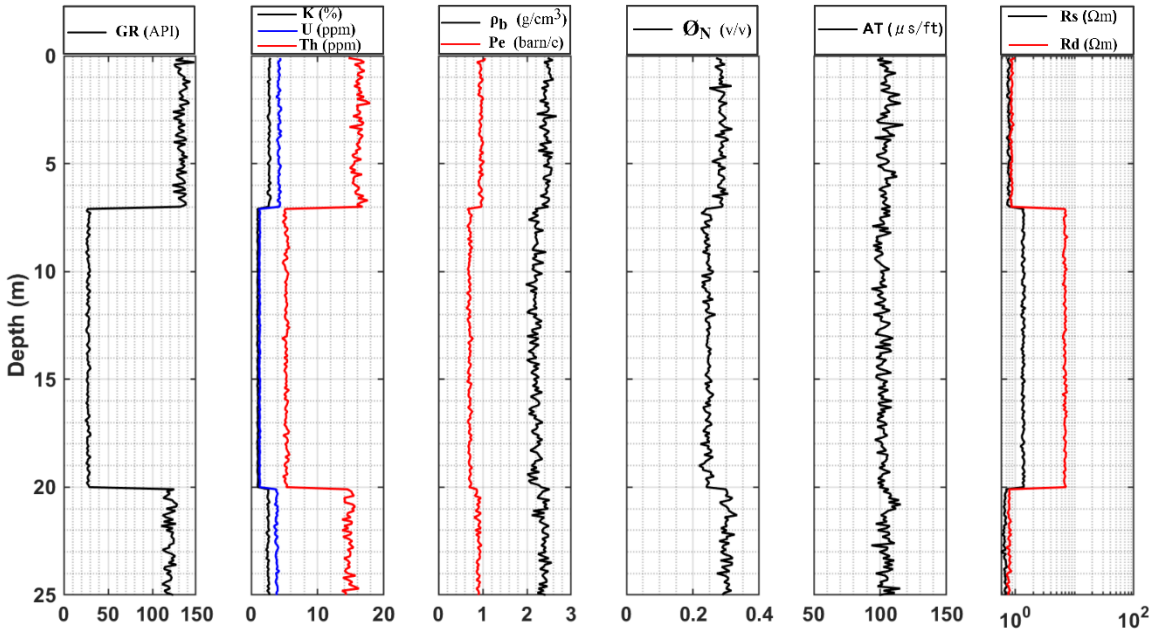

Fig. 12 Simulated logs (5% Gaussian distributed noise) of Model A in well 1

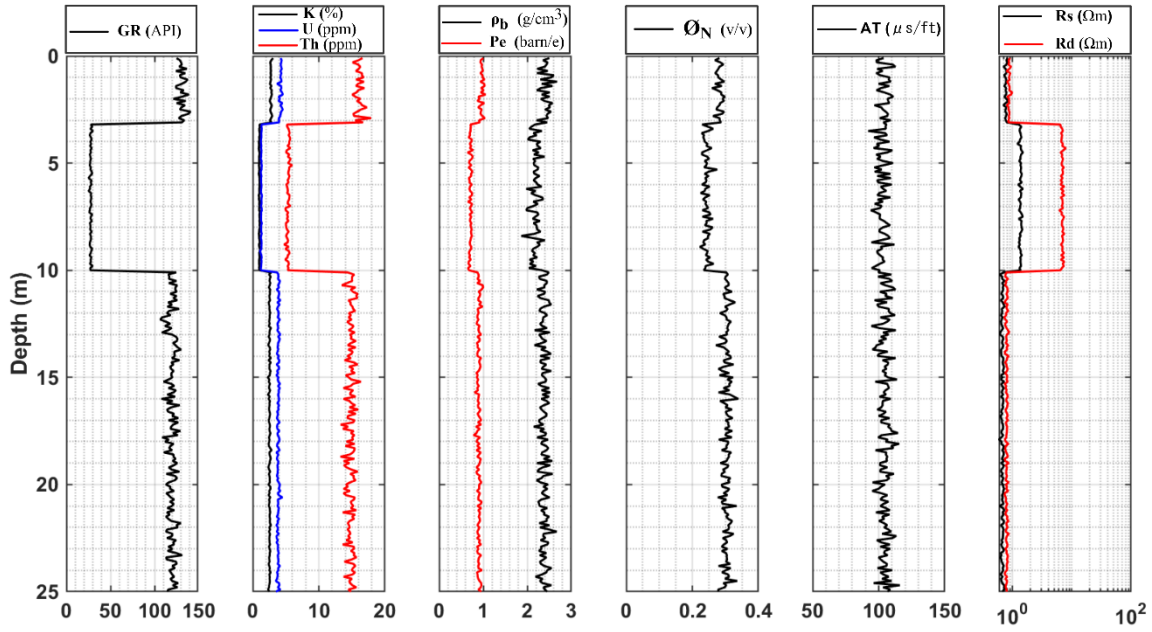

Fig. 13 Simulated logs (5% Gaussian distributed noise) of Model A in well 2

DOI: 10.14750/ME.2022.027

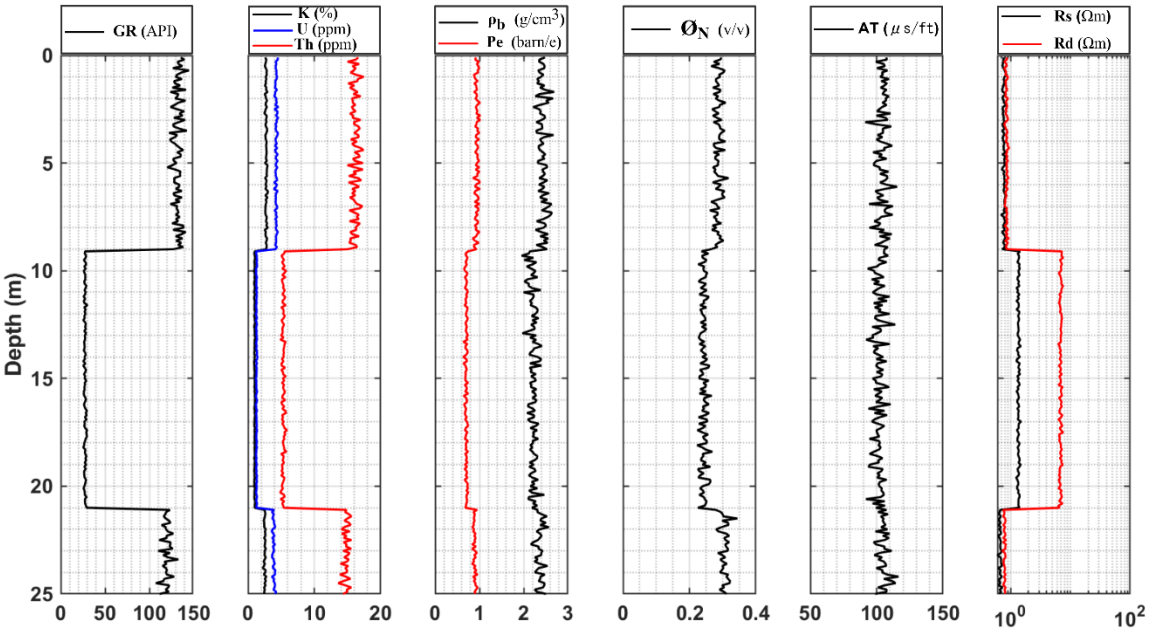

Fig. 14 Simulated logs (5% Gaussian distributed noise) of Model A in well 3

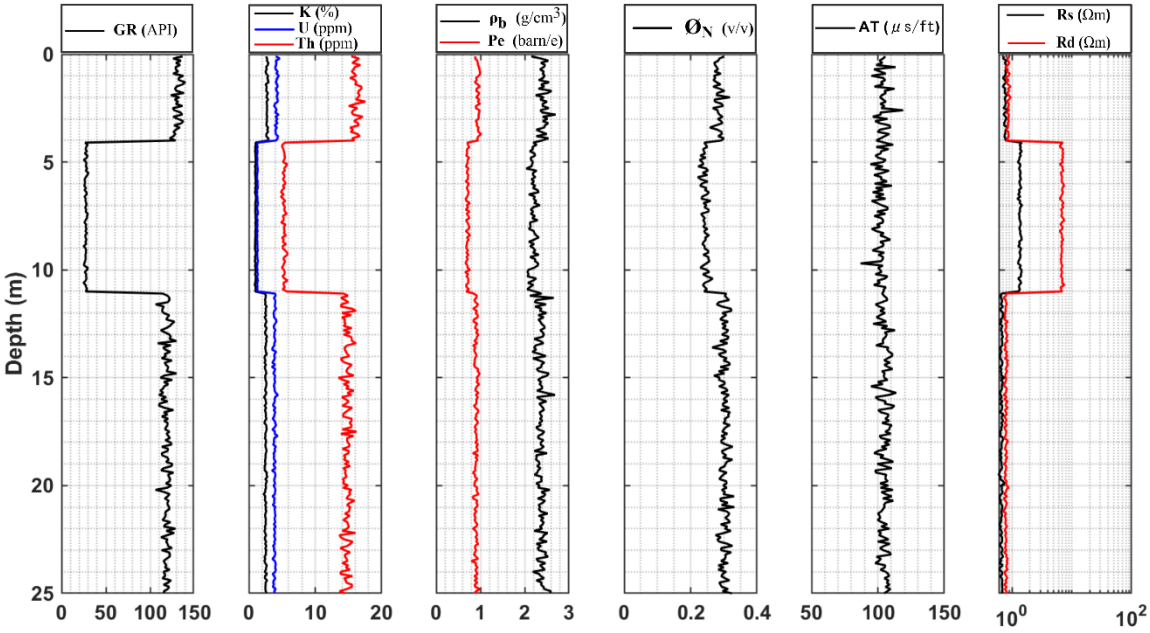

Fig. 15 Simulated logs (5% Gaussian distributed noise) of Model A in well 4

DOI: 10.14750/ME.2022.027

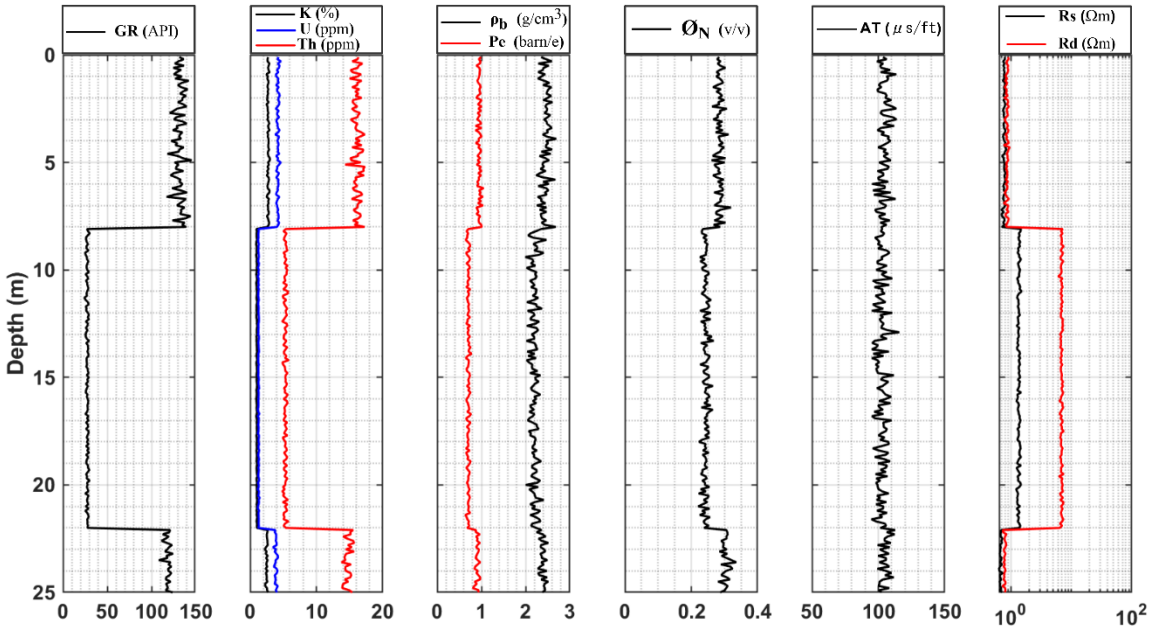

Fig. 16 Simulated logs (5% Gaussian distributed noise) of Model A in well 5

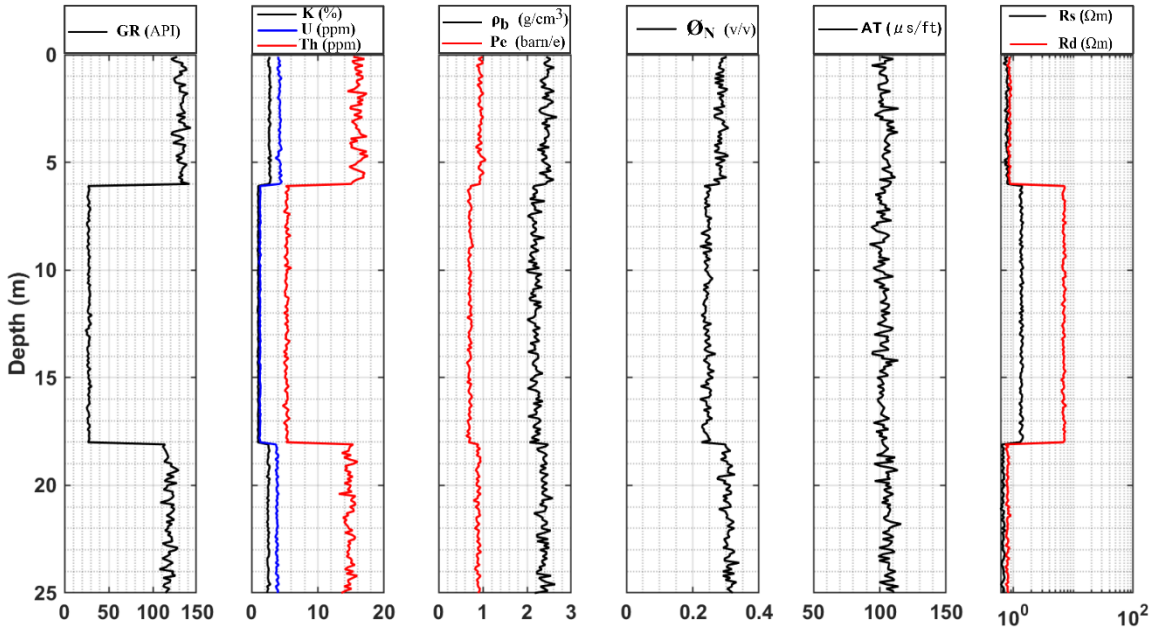

Fig. 17 Simulated logs (5% Gaussian distributed noise) of Model A in well 6

DOI: 10.14750/ME.2022.027

The layer boundary variations between the wells are described as quadratic Legendre polynomials over the $x \subset [-1, 1]$ interval. For our 2D case the polynomial degree is settled as 6 and the initial depth of the upper $H_1(x)$ and the lower boundary $H_2(x)$ of the gas reservoirs are 6 m and 18 m, respectively. The target and the calculated layer boundary coordinates of Model A are presented in Table 3. It was shown that the hydrocarbon zone is well detected.

Table 3 Target and estimated layer boundary coordinates of Model A

Layer thickness function	Wells	Values		
		Target	Estimated (Noise free)	Estimated (Noisy)
$H_1(x)$	W-1	7.0	7.0	7.0
	W-2	3.0	3.0	3.0
	W-3	9.0	9.0	9.0
	W-4	4.0	4.0	4.0
	W-5	8.0	8.0	8.0
	W-6	6.0	6.0	6.0
$H_2(x)$	W-1	20.0	20.0	20.03
	W-2	10.0	10.0	10.0
	W-3	21.0	21.0	21.0
	W-4	11.0	11.0	11.0
	W-5	22.0	22.0	22.0
	W-6	18.0	18.0	18.03

To test the performance of my developed method for estimating more formation boundaries Model B is built with three-layer boundaries to be estimated. The same above-mentioned procedure is followed for calculating the simulated measurements. The volumetric fractions Table 4 are illustrated in Fig. 18 and the calculated log types can be seen in Fig. 19-24. The target and estimated layer boundary coordinates can be seen in Table 5. The newly developed method shows success to estimate extra layer coordinates and detect the upper and lower boundaries of the reservoir rocks in stable inversion procedures. Furthermore, for increasing the number of unknowns, and estimating lateral variation of petrophysical parameters together with layer thickness, it is advisable to combine linear and global inversion algorithms for a more reliable and initial model free estimation.

DOI: 10.14750/ME.2022.027

Table 4 Petrophysical parameters and layer boundary thicknesses of Model B

Layer	Lithology	Petrophysical parameters (v/v)				Layer thickness (m)					
		Ø	S_{x0}	S_w	V_{sh}	W-1	W-2	W-3	W-4	W-5	W-6
1	water-sand	0.25	1	1	0.15	3	2	3	2	3	2
2	shale	0.1	1.0	1.0	0.8	5	8	9	8	9	8
3	gas-sand	0.3	0.8	0.4	0.1	0	2	5	10	12	15
4	shale	0.05	1.0	1.0	0.7	17	13	8	5	1	0

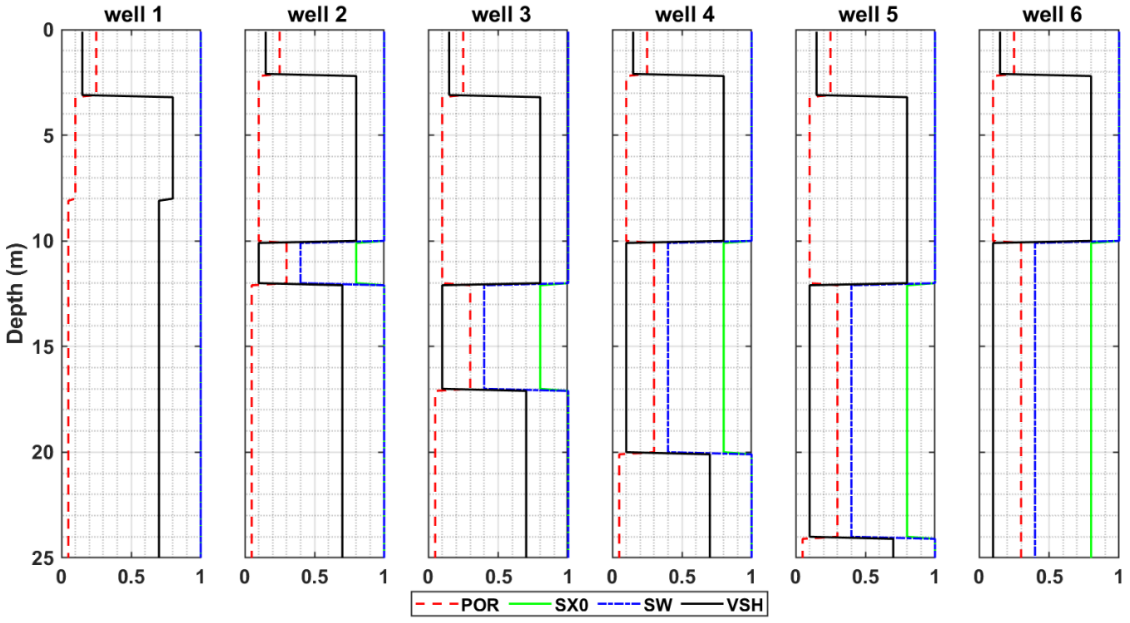

Fig. 18 Volumetric parameters in each well for calculating the simulated logs of Model B

DOI: 10.14750/ME.2022.027

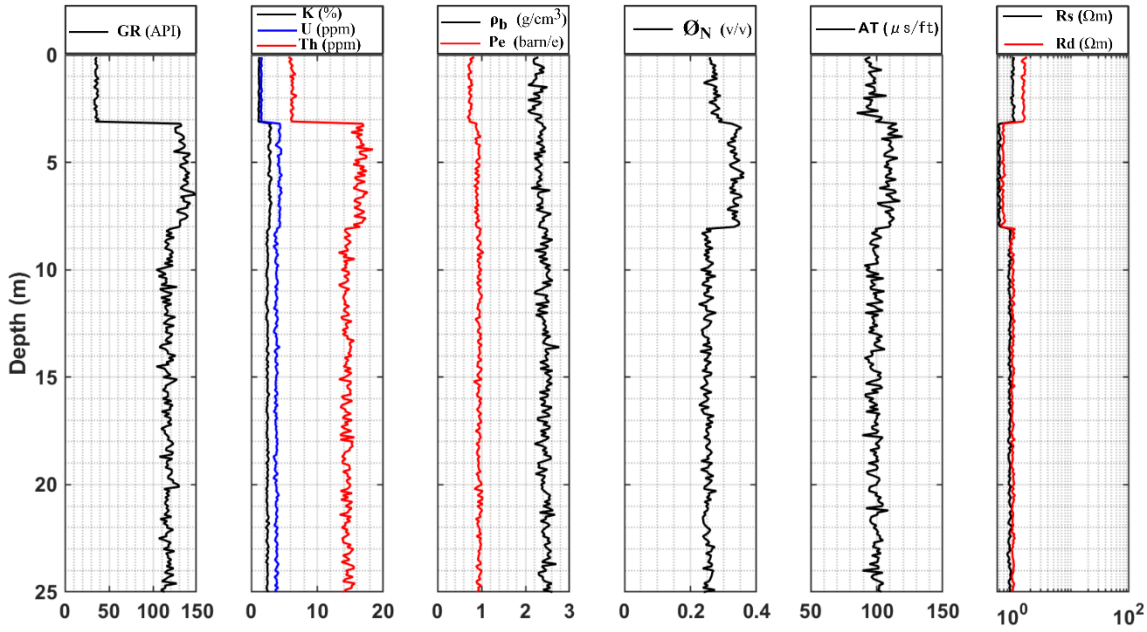

Fig. 19 Simulated logs (5% Gaussian distributed noise) of Model B in well 1

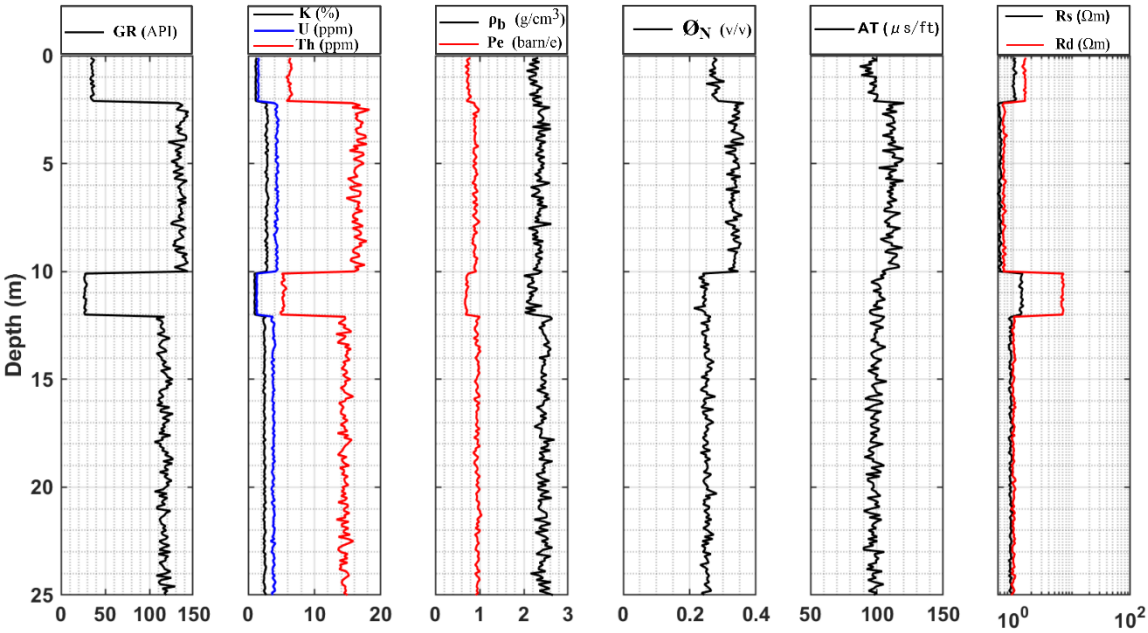

Fig. 20 Simulated logs (5% Gaussian distributed noise) of Model B in well 2

DOI: 10.14750/ME.2022.027

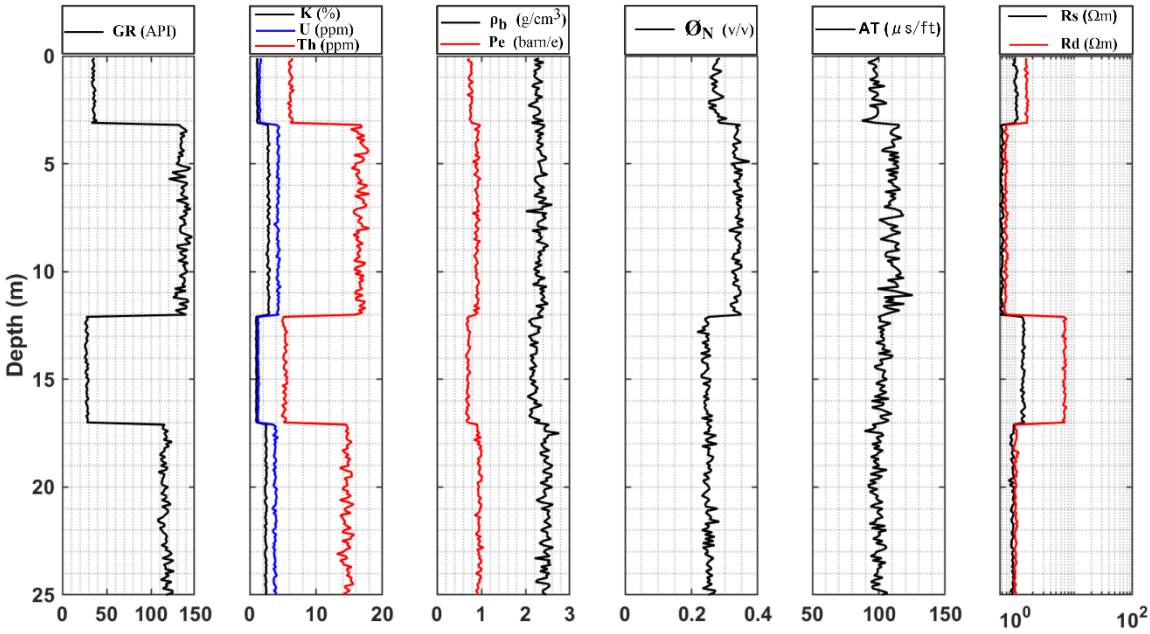

Fig. 21 Simulated logs (5% Gaussian distributed noise) of Model B in well 3

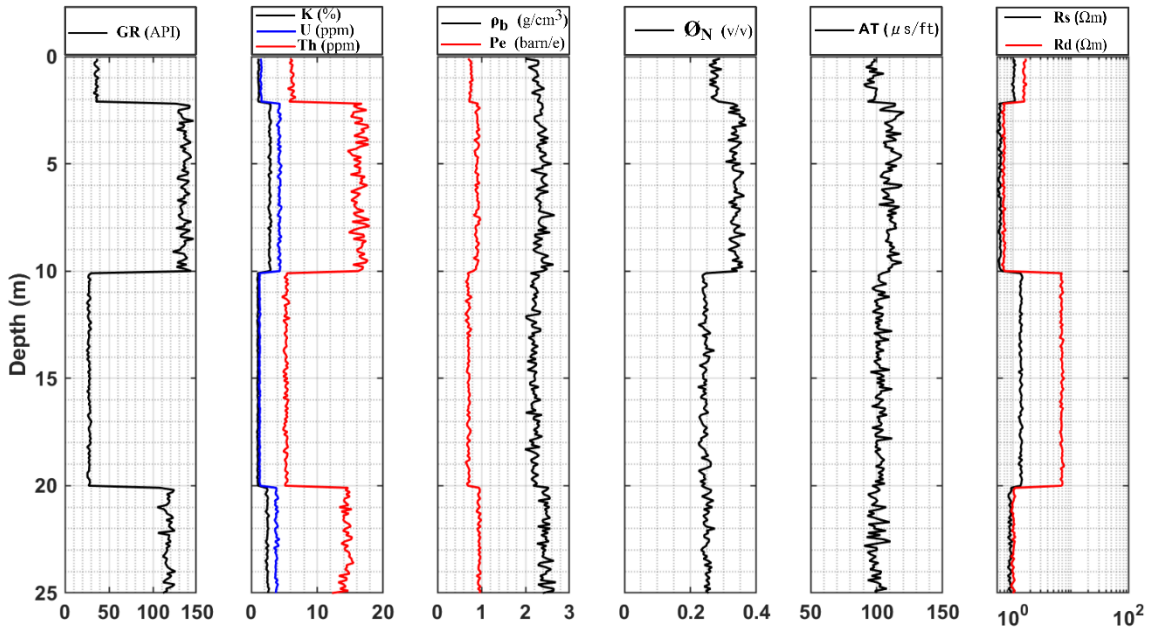

Fig. 22 Simulated logs (5% Gaussian distributed noise) of Model B in well 4

DOI: 10.14750/ME.2022.027

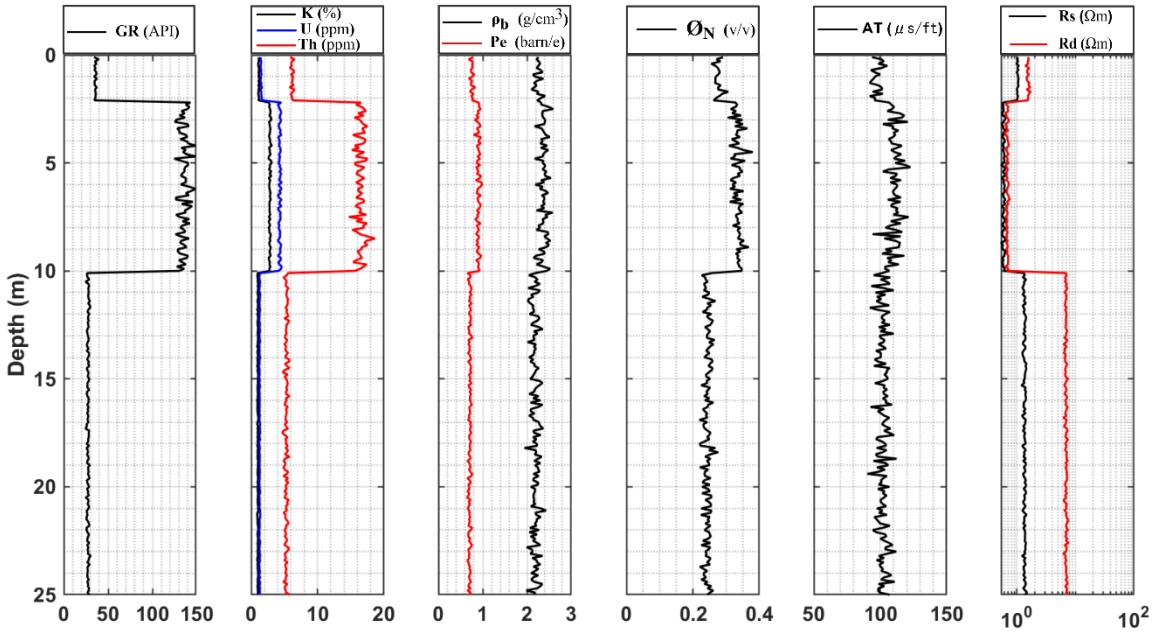

Fig. 23 Simulated logs (5% Gaussian distributed noise) of Model B in well 5

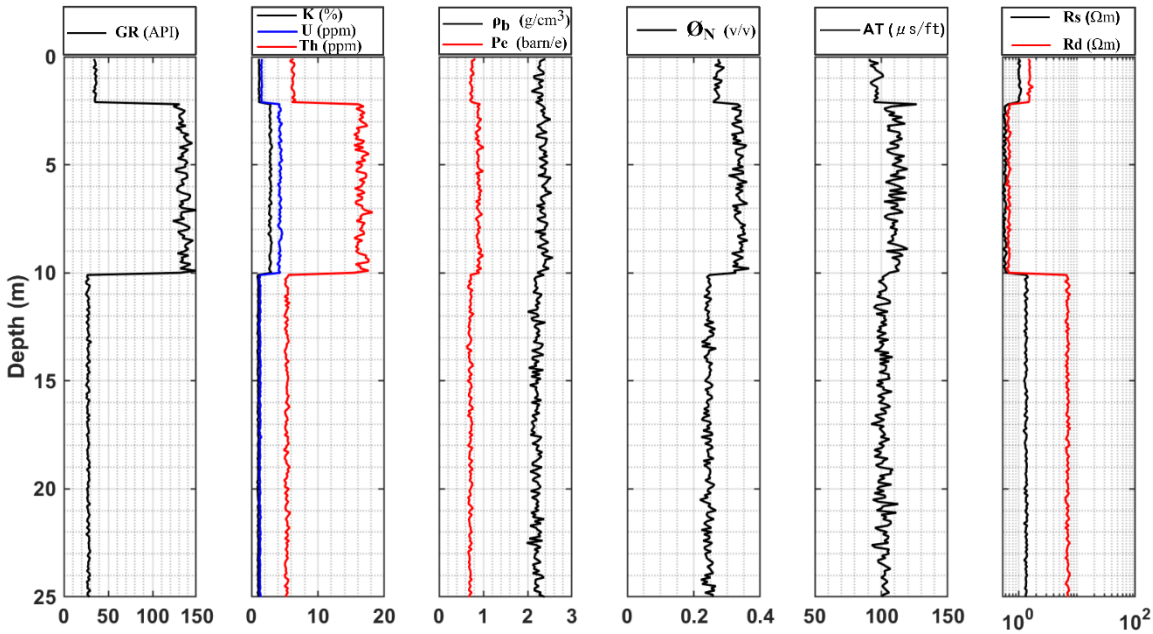

Fig. 24 Simulated logs (5% Gaussian distributed noise) of Model B in well 6

DOI: 10.14750/ME.2022.027

Table 5 Exactly known (target) and estimated layer boundary coordinates of Model B

Layer thickness function	Wells	Values		
		Target	Estimated (Noise free)	Estimated (Noisy)
$H_1(x)$	W-1	3.0	3.0	3.05
	W-2	2.0	2.0	2.0
	W-3	3.0	3.0	3.01
	W-4	2.0	2.0	2.01
	W-5	3.0	3.0	3.0
	W-6	2.0	2.0	2.05
$H_2(x)$	W-1	8.0	8.0	8.09
	W-2	10.0	10.0	10.01
	W-3	12.0	12.0	12.02
	W-4	10.0	10.0	10.02
	W-5	12.0	12.0	12.01
	W-6	10.0	10.0	10.09
$H_3(x)$	W-1	8.0	8.0	8.02
	W-2	12.0	12.0	12.0
	W-3	17.0	17.0	17.0
	W-4	20.0	20.0	20.0
	W-5	24.0	24.0	24.0
	W-6	25.0	25.0	25.02

3.2 Field test

Once the simulated tests were performed, in-situ well logging data acquired in four boreholes side by side located in an Egyptian hydrocarbon field as shown in Fig. 25 were processed by using the developed 2D interval inversion method. Data samples corresponding to given natural gamma-ray intensity (*GR* in *API*), shallow resistivity "R_s in *ohm-m*", deep resistivity "R_d in *ohm-m*", bulk Density "ρ_b in g/cm^3", and neutron-porosity "$\emptyset_N$ in *v/v*". For more reliable delineation of the layer boundary our initial model is set as $H_1(x)$= 4 m and $H_2(x)$=12 m. The polynomial degree is settled as 4 degrees. The number of expansion unknowns which is 10 to 1120 measured data points resulting in a 112 overdetermination ratio. The estimated layer boundary coordinates are shown in Table 6. The illustrated 2D section can be seen in Fig. 26. (The depth coordinates are transformed, not real ones).

DOI: 10.14750/ME.2022.027

Table 6 Estimated layer boundary coordinates of Egyptian field data

Layer thickness function	Wells	Estimated Values
H_1 (x)	W-1 W-2 W-3 W-4	7.03 8.33 7.33 4.03
H_2 (x)	W-1 W-2 W-3 W-4	12.52 10.50 10.50 12.02

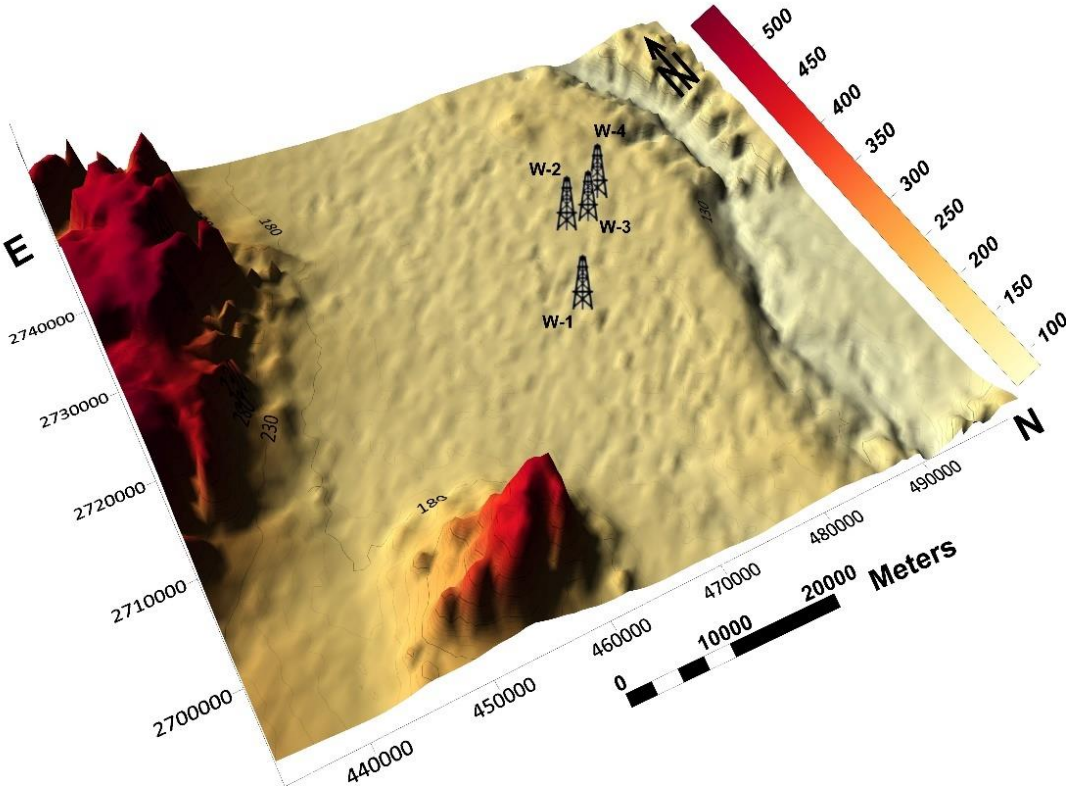

Fig. 25 Location of the wells involved in interval inversion experiments

DOI: 10.14750/ME.2022.027

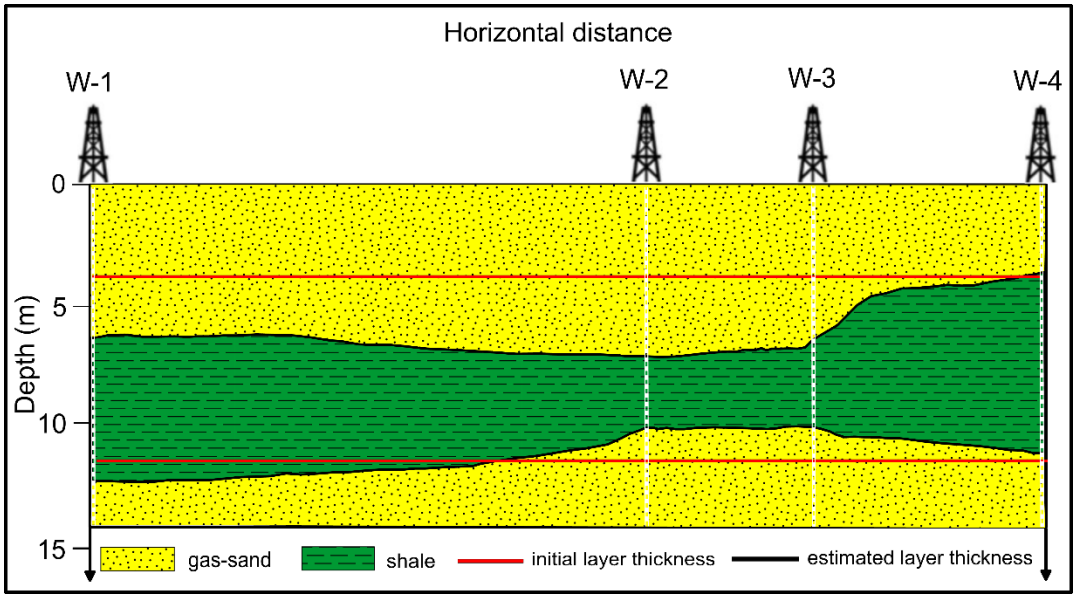

Fig. 26 2D cross section of layer thickness variations obtained by 2D interval inversion procedure

3.3 Discussion

A Legendre polynomials-based interval inversion method has been proposed to estimate the lateral variation of layer boundary. The inverse problem was solved by using the so-called linear optimization techniques DLSQ (damped least squares method). Simulated measurements (noise free and noisy) of multilayer structures related to hydrocarbon bearing formations have been utilized to test the method. In-situ well logging datasets acquired in four wells of Egyptian hydrocarbon field processed by the proposed method and proved its feasibility.

Thesis two

I have developed an orthogonal Legendre polynomials-based 2D interval inversion approach that can determine the lateral changes of layer boundary coordinates. The thicknesses are obtained as cubic functions over the interval [-1, 1]. The inversion method was tested on two Models A and B built-up of homogeneous multilayer structures related to hydrocarbon bearing reservoirs. Linear optimization algorithm has been used to solve the inverse problem. By processing multi-borehole in-situ logging data, I proved the feasibility of the suggested method and successfully estimated the lateral variation of layer boundaries of Egyptian hydrocarbon field.

DOI: 10.14750/ME.2022.027

4. LEGENDRE POLYNOMIALS-BASED INTERVAL INVERSION METHOD FOR ESTIMATING LATERAL VARIATION OF PETROPHYSICAL PARAMETERS

After successfully estimating lateral change of layer boundary coordinates in the previous chapter, the method is equally suitable for the spatial lateral and vertical determination of petrophysical parameters. From a numerical point of view, the advantage of this is that by integrating the borehole measurements, the uncertainty can be further increased, resulting in a qualitative improvement in the accuracy and reliability of the estimated parameters. In this chapter, I introduced a 2D interval inversion method based on a simulated annealing algorithm for determining the vertical and lateral variation of the petrophysical parameters along a 2D cross-section of several neighboring boreholes.

4.1 Global inversion algorithm

Unlike the linear optimization methods which could possibly bring the solution to a local minimum, global optimization seeks the absolute minimum of the objective function. Some of the most used global optimization methods in geophysics are Genetic Algorithm (Holland 1975), Particle Swarm Optimization (Kennedy and Eberhart 1995), and Simulated Annealing (Metropolis et al. 1953). The latter is used in this study to solve the inverse problem.

Simulated annealing (SA) method has been developed by Metropolis et al. (1953) in metallurgy; the removal of work-hardening is realized by a slow cooling manipulation from the temperature of the liquid alloy state. This process decreases progressively the kinetic energy of many atoms with high thermal mobility, which is followed by the starting of crystallization. In theory, the ideal crystal with minimal overall atomic energy can be produced by an infinitely slow cooling schedule. This is analogous with the stabilization of the inversion procedure at the global optimum of the objective function. A fast-cooling process causes grating defects and the solid freezes in an imperfect grid at a relatively higher energy state. It is like the trapping of the inversion procedure in a local minimum. However, the atoms may escape from the high-energy state owing to a special process called annealing to achieve the optimal crystal grating by a slower cooling process. The SA algorithm employs this technology to search the global optimum of the objective (in the terminology energy) function E (equation 25).

DOI: 10.14750/ME.2022.027

The simulated method depends on the modification of the model vector, in this case the *i*-th model parameter in the *n*-th iteration is modified properly as follows

$$m_i^{(n+1)} = m_i^{(n)} \pm b, \tag{37}$$

where b is the amount of changing (perturbation term) which is randomly changing between $0 \leq b \leq b_{max}$, while the parameter b_{max} is renewed according to $b_{max} = b_{max}.\varepsilon$, where $\mathcal{E}$ is a specified number from the interval of 0 and 1. During the random seeking, the energy function E is calculated and compared with the previous one in every iteration step (ΔE). The acceptance probability of the new model relies on the Metropolis criteria

$$p(\Delta E, T) = \begin{cases} 1, & \text{if } \Delta E \leq 0 \\ e^{-\Delta E/T,} & \text{otherwise} \end{cases}, \tag{38}$$

where the model is always accepted when the value of energy function is lower in the new state than that of the previous one. If the energy of the new model increased, there is also some probability of acceptance depending on the values of energy E and control temperature T. If the following criteria

$$\alpha \leq p(\Delta E), \tag{39}$$

fulfills, the new model is accepted, else it is rejected (α is a random number generated with uniform probability from the interval of 0 and 1). These criteria assure the escape from the local minima. It was approved that the global minimum is guaranteed when the schedule cooling of Geman and Geman (1984) is used

$$T(n) = \frac{T_0}{\ln(n)} (n > 1), \tag{40}$$

where T_0 represents the initial temperature. The SA algorithm is very effective, but the logarithmic reduction of temperature in equation (40) is rather time consuming. Various attempts were made to shorten the CPU time. Ingber (1989) proposed a modified SA algorithm called very fast simulated re-annealing (VFSR). Consider different ranges of variation for each model parameter

$$m_i^{min} =\leq m_i^{(n)} \leq m_i^{max}. \tag{41}$$

The perturbation of the *i*-th model parameter at iteration (n + 1) is as follows

$$m_i^{(n+1)} = m_i^n + y_i(m_i^{max} - m_i^{min}), \tag{42}$$

DOI: 10.14750/ME.2022.027

where y_i is a random number between −1 and 1 generated from a specified non-uniform probability distribution function. The global optimum is guaranteed the *i*-th cooling schedule being as the following

$$T_i(n) = T_{0,i} \exp\left(-c_i \sqrt[p]{k}\right), \tag{43}$$

where $T_{0,i}$ is the initial temperature of the *i*-th model parameter, c_i is the *i*-th control parameter, and *P* is the number of model parameters. The acceptance rule of the VFSR algorithm is the same as that used in Metropolis SA method, but the exponential cooling schedule declares much faster convergence to the global optimum than the logarithmic one. A detailed workflow of the SA process can be seen in Fig. 27.

4.2 Synthetic modeling experiments

To test the performance of the developed 2D interval inversion algorithm numerical experiments were made on synthetic models. The inversion of noisy simulated borehole data sets reveals how the procedure returns to a precisely known target model. For the accuracy and reliability of the 2D inversion method numerical test parameters such as data and model distance have been calculated. The approach of the 2D interval inversion is to determine vertical and lateral variation of petrophysical parameters with fixed values of layer boundaries. Two Models A and B are used in the study relating to water and hydrocarbon-bearing reservoirs. In both cases synthetic well-logging data were generated by means of Gearhart Ultra response equations (Alberty and Hashmy 1984).

4.2.1 Inversion over 2D shaly water-bearing sand model

A two-layered anticline structure made up of shale and water-bearing sand Model A was used in the first investigation. To simulate real measurements the synthetic data are calculated in six wells (W-1,…, W-6) with *dz* =0.1 m sampling interval. The interval length is about 20 m, and 5% Gaussian distributed noise are added to *N* =12,060 data samples. The targeted petrophysical parameters are provided in Table 7 while the volumetric fractions and the processed well logs type are illustrated in Figs. 28-34.

DOI: 10.14750/ME.2022.027

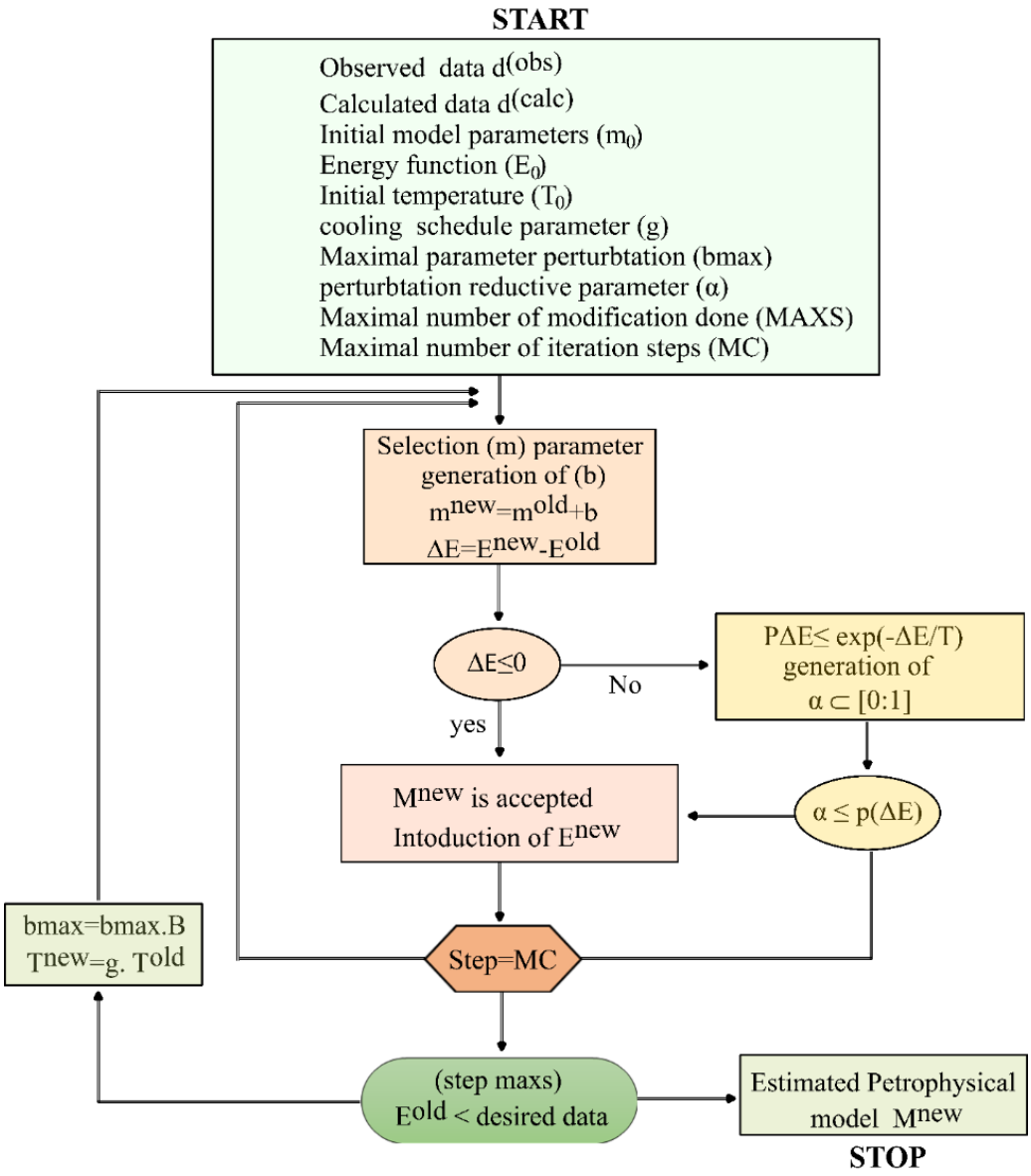

Fig. 27 The process flow diagram of SA algorithm

Table 7 Petrophysical parameters of Model A given in v/v

Layer	Parameter	W-1	W-2	W-3	W-4	W-5	W-6
1 shale	POR	0.10	0.11	0.09	0.10	0.08	0.12
	SX0	1.0	1.0	1.0	1.0	1.0	1.0
	SW	1.0	1.0	1.0	1.0	1.0	1.0
	VSH	0.73	0.71	0.72	0.70	0.72	0.75
2 sand-water	POR	0.22	0.24	0.23	0.25	0.24	0.26
	SX0	1.0	1.0	1.0	1.0	1.0	1.0
	SW	1.0	1.0	1.0	1.0	1.0	1.0
	VSH	0.10	0.12	0.11	0.13	0.12	0.14

DOI: 10.14750/ME.2022.027

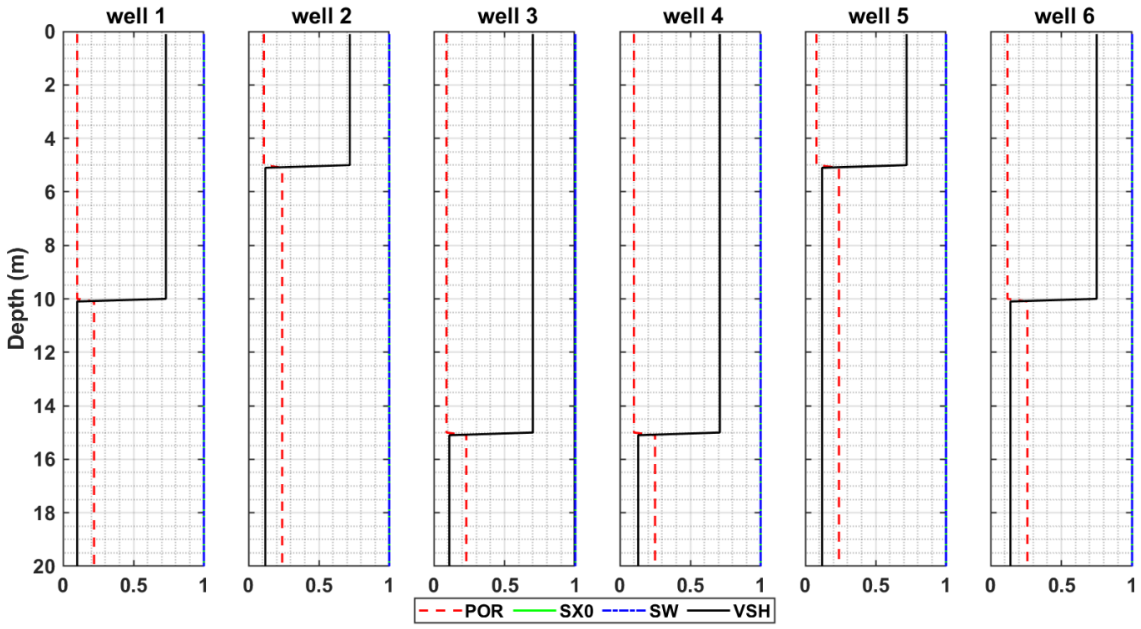

Fig. 28 Volumetric parameters of each well for computing the simulated logs of Model A

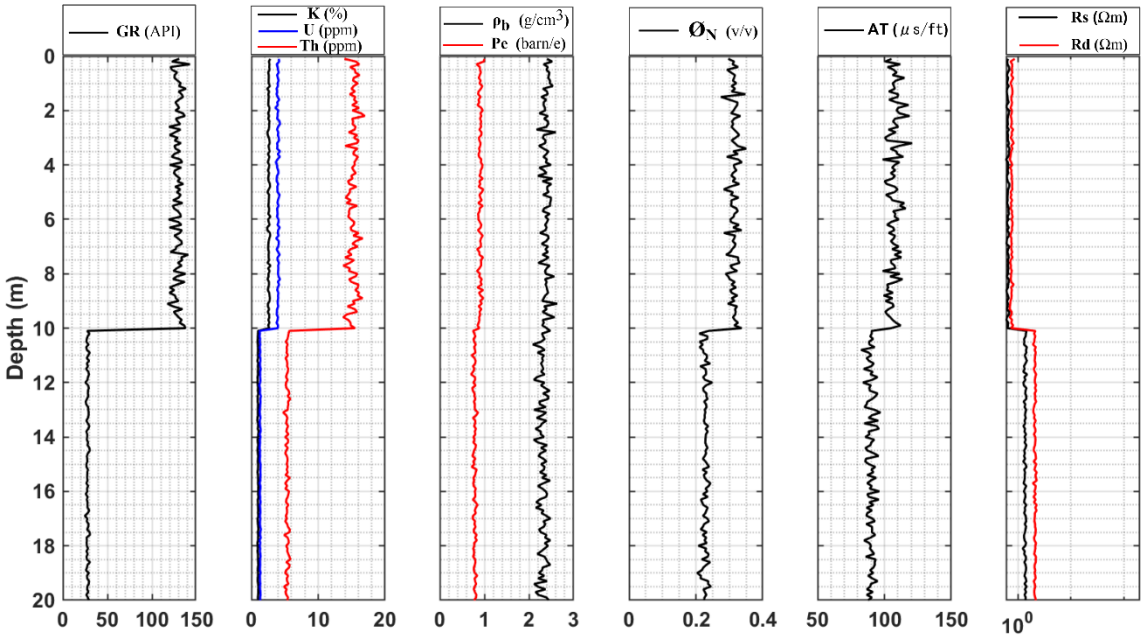

Fig. 29 Simulated logs (5% Gaussian distributed noise) of Model A in well 1

DOI: 10.14750/ME.2022.027

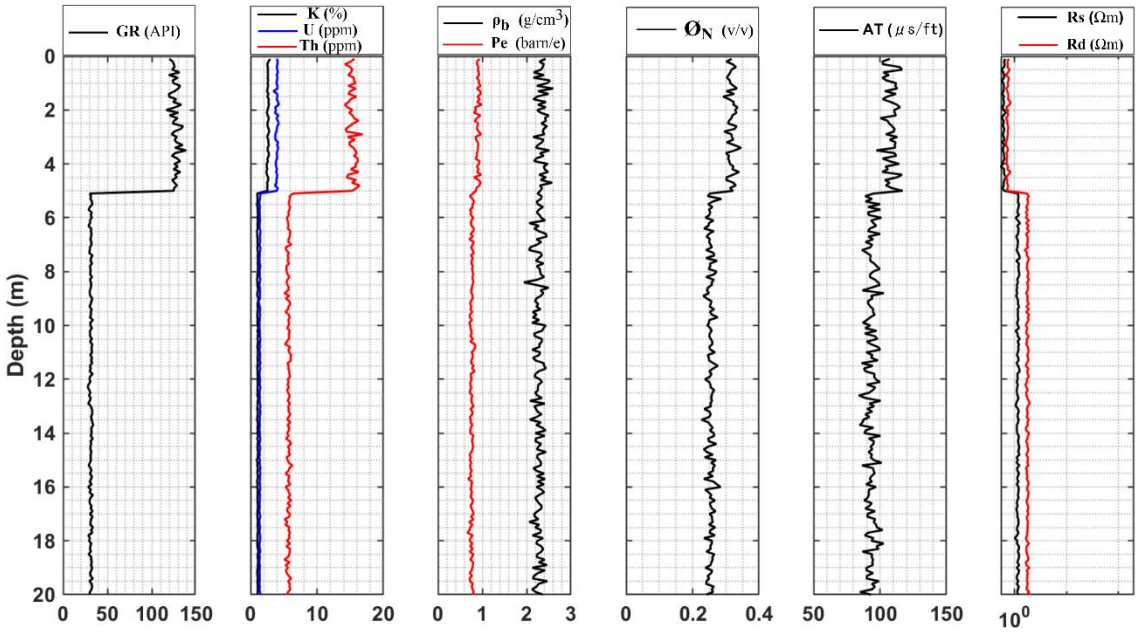

Fig. 30 Simulated logs (5% Gaussian distributed noise) of Model A in well 2

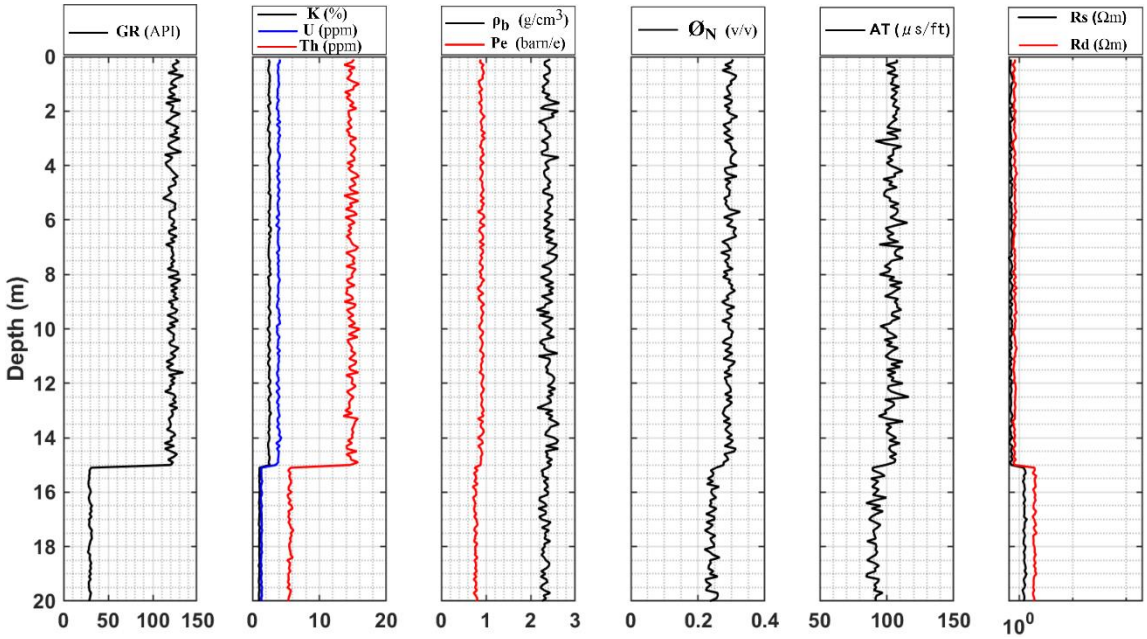

Fig. 31 Simulated logs (5% Gaussian distributed noise) of Model A in well 3

DOI: 10.14750/ME.2022.027

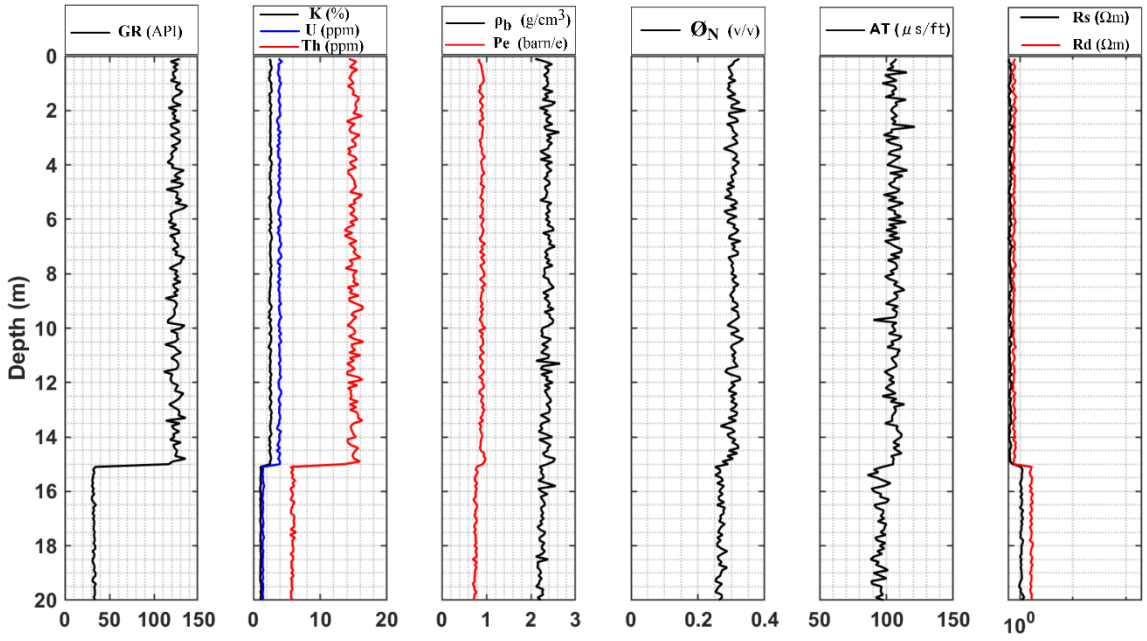

Fig. 32 Simulated logs (5% Gaussian distributed noise) of Model A in well 4

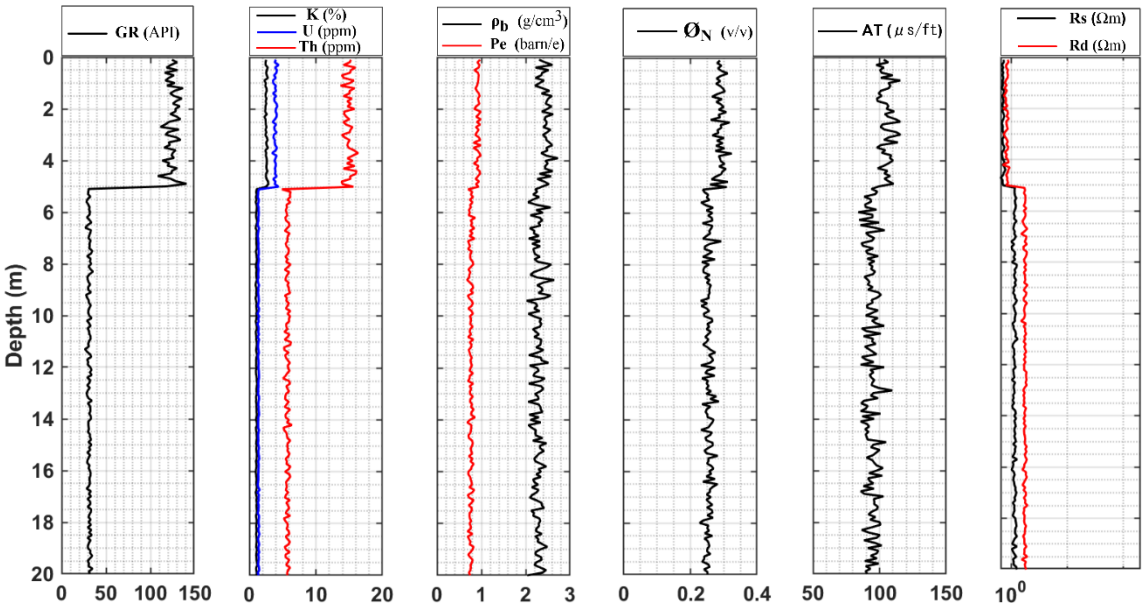

Fig. 33 Simulated logs (5% Gaussian distributed noise) of Model A in well 5

DOI: 10.14750/ME.2022.027

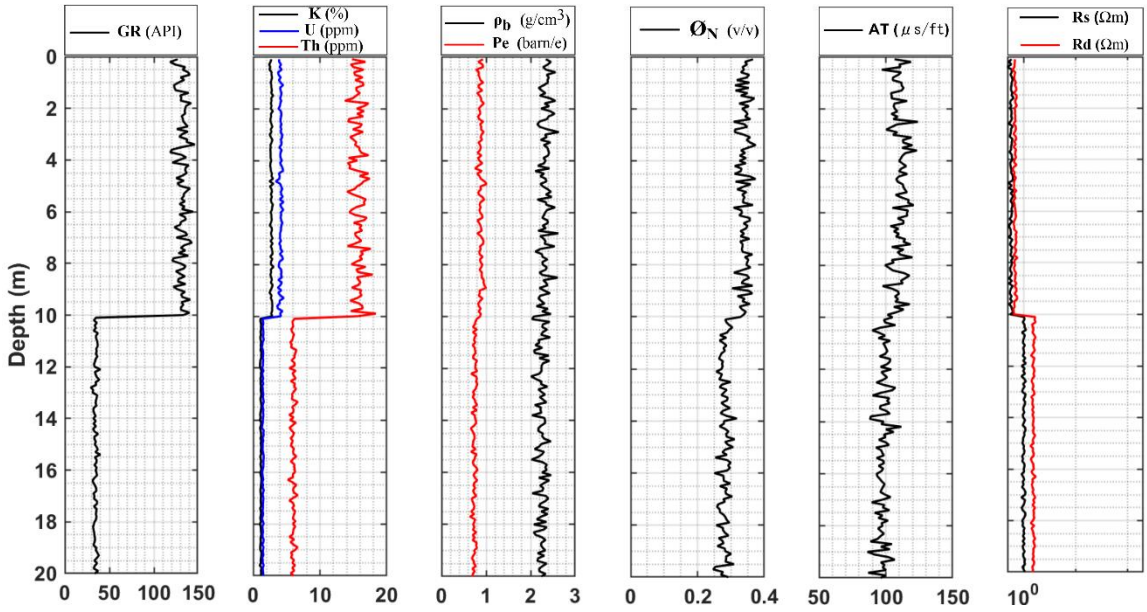

Fig. 34 Simulated logs (5% Gaussian distributed noise) of Model A in well 6

The estimated model vector in equation (1) contained the series expansion coefficients of the petrophysical parameters with fixed values of layer coordinates. Two parameters (porosity and volume of shale) to be estimated along a profile comprised of six wells. For our 2D case the polynomials degree is settled as 5 and the initial values of porosity and volume of shale are chosen as 0.02 and 0.70 for the first layer and 0.2 and 0.1 for the second one respectively. The number of unknowns (expansion coefficients) *M* are 24, resulting in a very high overdetermination ratio 502. The main component of rock matrix was quartz (*VSD*), which could be computed by the material balance equation out of inversion (equation 3). The development of convergence during the inversion procedure is shown in Fig. 35 and the optimum value was found at D_d =4.1 percent data and D_m =1.9 percent model distance. The estimated values are summarized in Table 8 also the targeted values and its estimated one are also illustrated in the form of 2D model Figs. 36-38.

Table 8 Petrophysical parameters of Model A estimated by 2D interval inversion. The dimensional units are v/v

layer	Parameter	W-1	W-2	W-3	W-4	W-5	W-6
1 shale	POR	0.097	0.098	0.091	0.098	0.093	0.123
	VSH	0.734	0.714	0.704	0.703	0.712	0.744
2 sand water	POR	0.221	0.240	0.235	0.246	0.241	0.261
	VSH	0.098	0.120	0.112	0.114	0.121	0.140

DOI: 10.14750/ME.2022.027

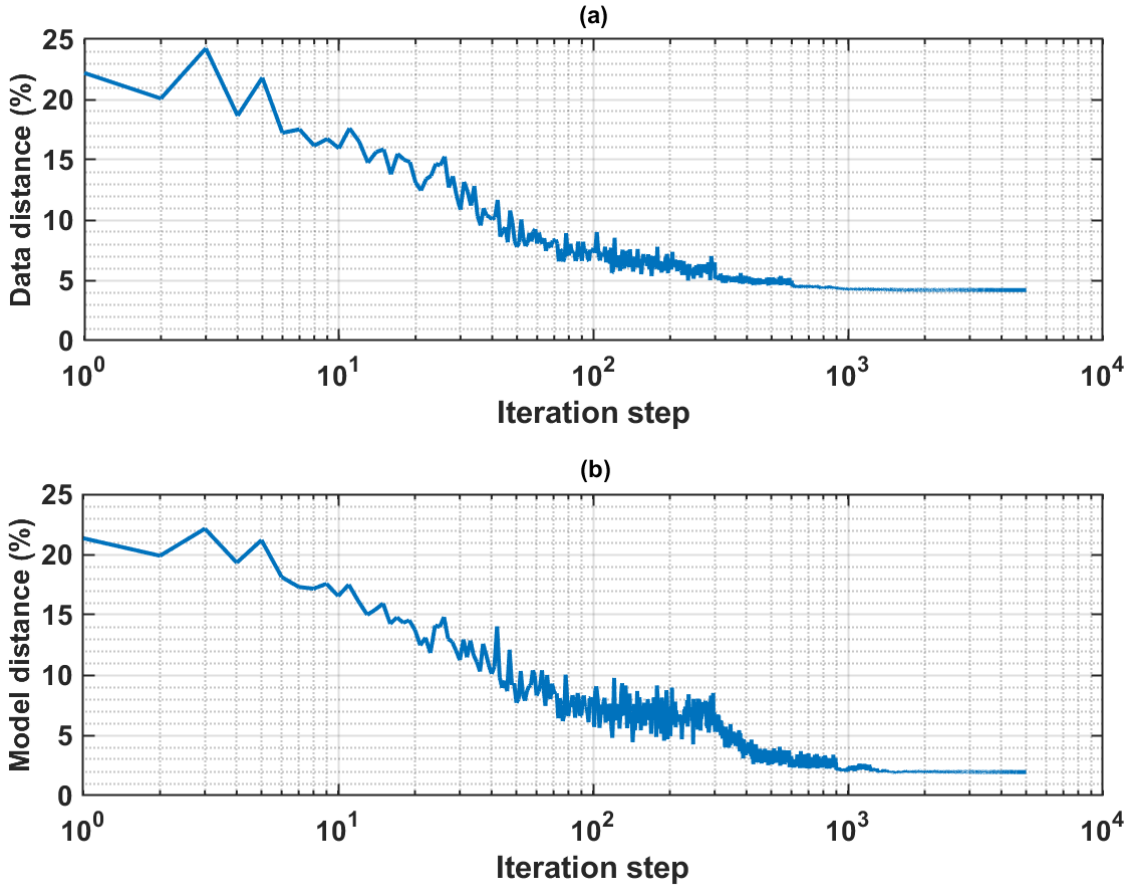

Fig. 35 Development of convergence during the 2D interval inversion procedure. a) Data distance vs. iteration step, b) Model distance vs. iteration step

DOI: 10.14750/ME.2022.027

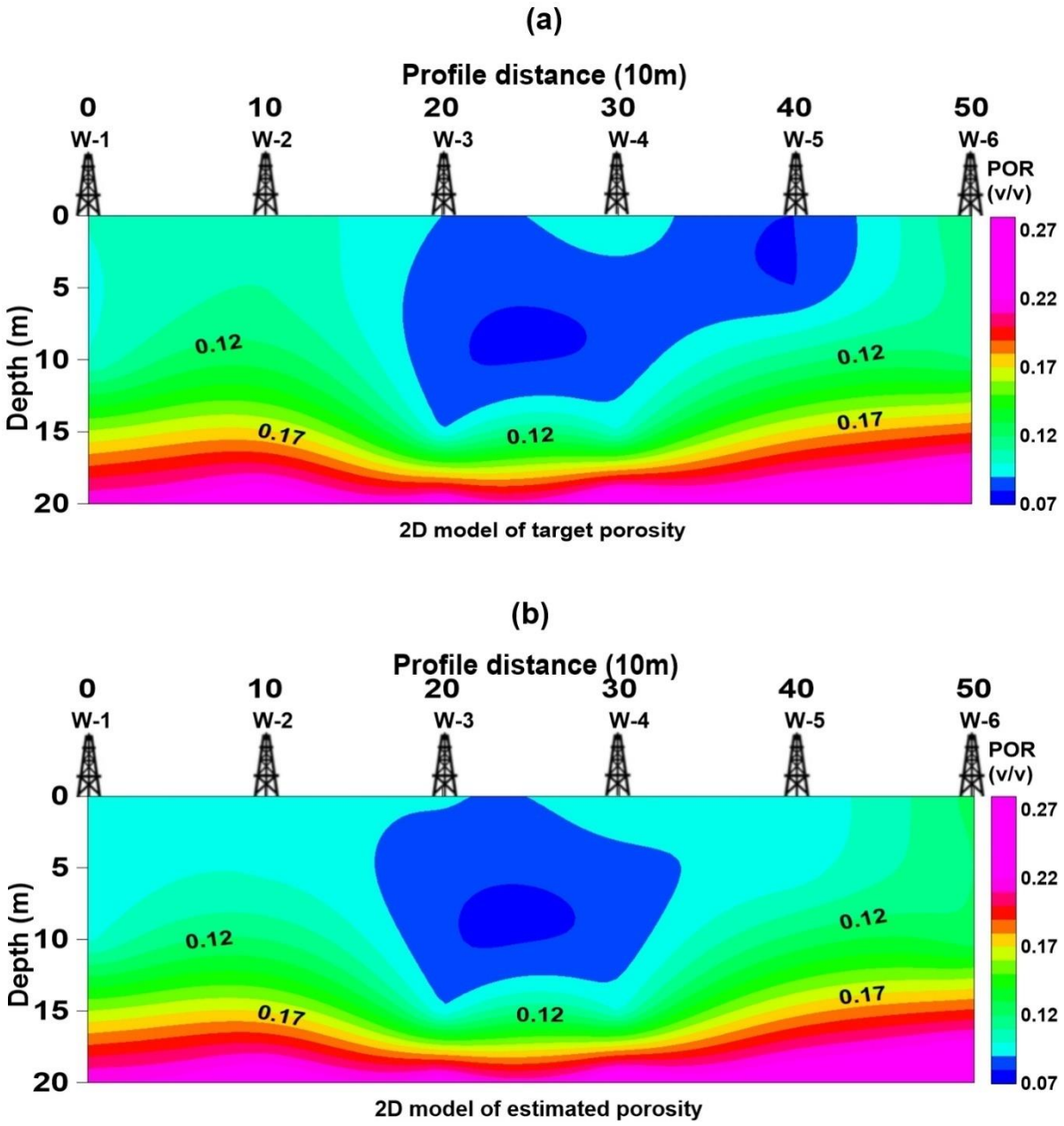

Fig. 36 a) 2D models of target porosity, b) the estimated one by 2D interval inversion

DOI: 10.14750/ME.2022.027

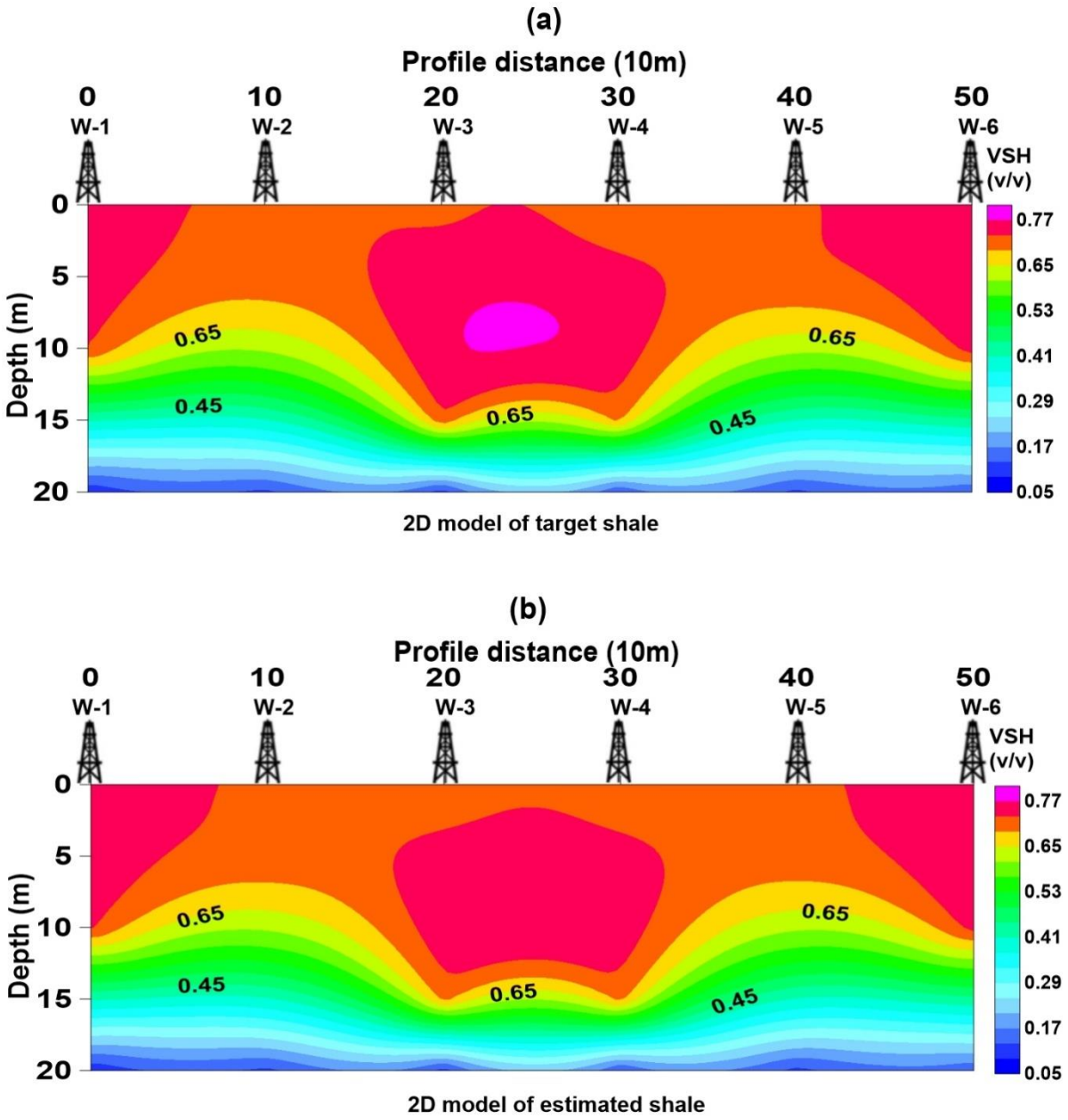

Fig. 37 a) 2D models of target shale content, b) the estimated one by 2D interval inversion

DOI: 10.14750/ME.2022.027

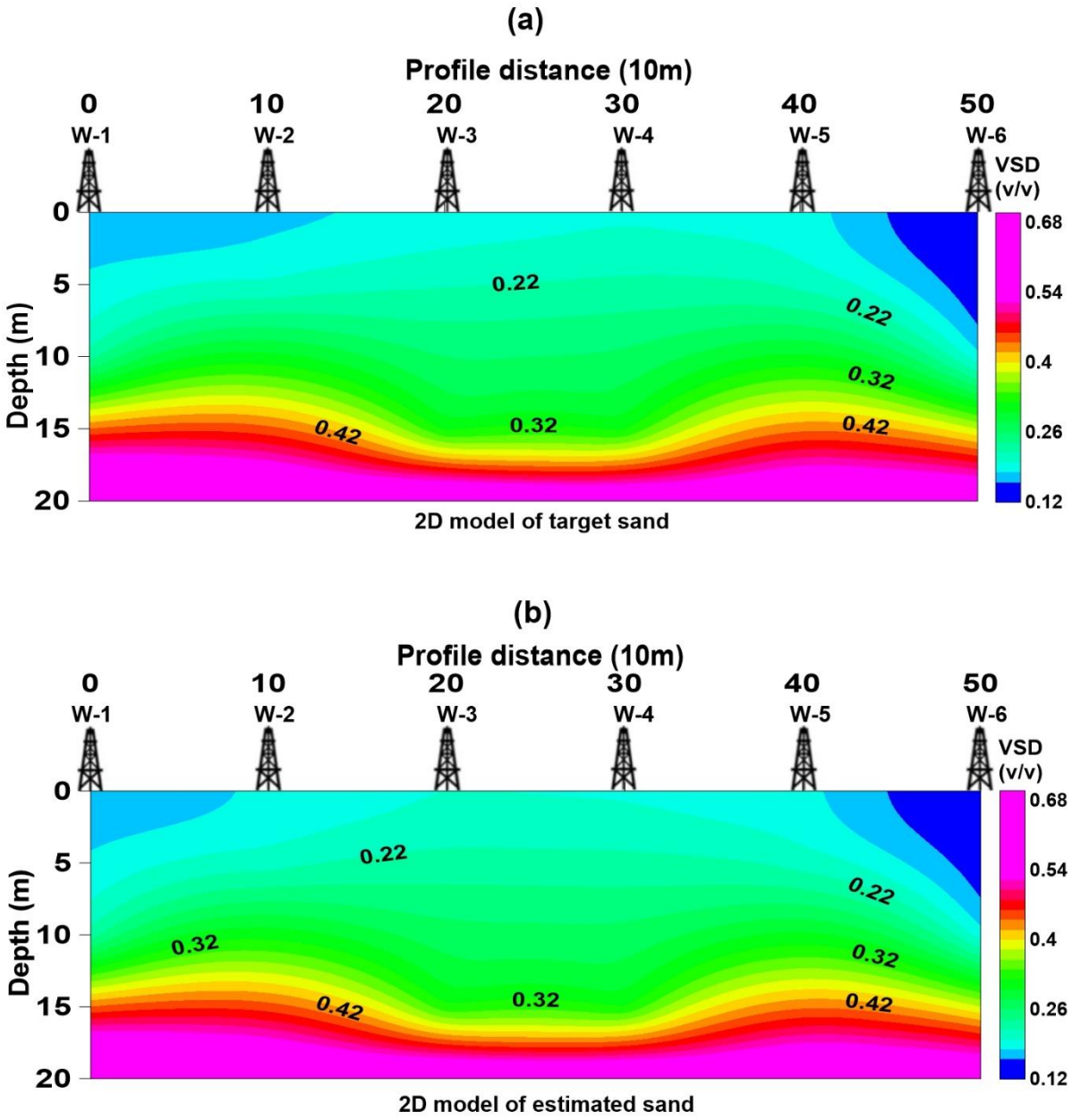

Fig. 38 a) 2D models of target sand content, b) the estimated one directly derived by the inversion results

4.2.2 Inversion over 2D shaly hydrocarbon-bearing sand model

In the second case our Model B was a two-layered structure made of shale and hydrocarbon-bearing sand. I increased the number of petrophysical unknowns of the 2D interval inversion problem which may cause a slight decrease of the overdetermination ratio. The target parameters of the model are shown in Table 9. Same procedures of Model A are followed to simulate the real measurements and the representation of the

DOI: 10.14750/ME.2022.027

volumetric fractions with the computed simulated logs can be seen in Figs. 39-45. Three parameters to be estimated including porosity, water saturation in uninvaded zone and volume of shale. Thus, the number of unknowns *M*=36 and the overdetermination ratio is 335. The volume of quartz (*VSD*) possibly will be also obtained by the material balance equation out of inversion. Another important parameters underlying the calculation of hydrocarbon reserves could be obtained such as irreducible ($S_{hc,irr}$) and movable ($S_{hc,mov}$) hydrocarbon saturations by using equations (19) and (20) also absolute permeability (K) of Timur (1968) is derived by using the following equation (mD)

$$\mathrm{K} = 0.136\ \frac{POR^{4.4}}{S_{w,irr}^{0.2}}, \tag{44}$$

where $S_{w,irr}$ = 0.2 v/v denotes the bound water saturation. Water saturation (S_{x0}) in the disturbed zone was computed by $S_{x0}=S_w^{0.2}$, which is based on huge amount of observations of well log analysts in Miocene gas reservoirs of the Pannonian basin (the exponent of S_w may change between1/2 and 1/5).

Table 9 Target petrophysical parameters of Model B given in v/v

Layer	Parameter	W-1	W-2	W-3	W-4	W-5	W-6
1 shale	POR	0.10	0.09	0.07	0.10	0.08	0. 11
	SX0	1.0	1.0	1.0	1.0	1.0	1.0
	VSH	0.71	0.70	0.72	0.69	0.70	0.74
2 gas-sand	POR	0.23	0.22	0.25	0.24	0.26	0.27
	SX0	0.80	0.82	0.81	0.80	0.83	0.84
	VSH	0.10	0.09	0.11	0.10	0.12	0.13

DOI: 10.14750/ME.2022.027

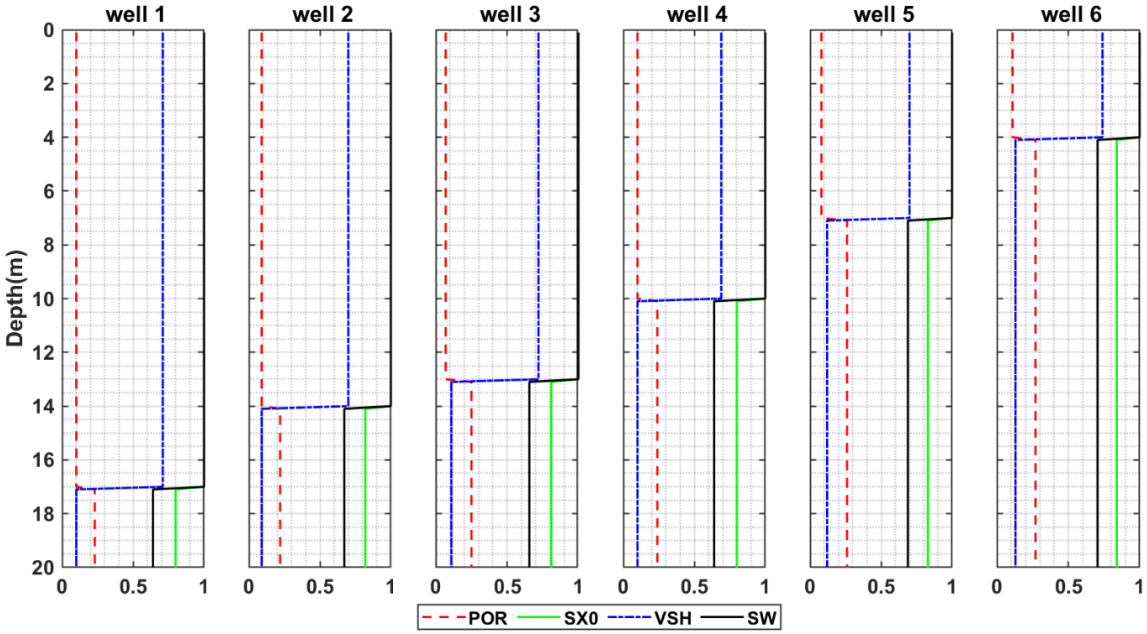

Fig. 39 Volumetric parameters of each well for calculating the simulated logs of Model B

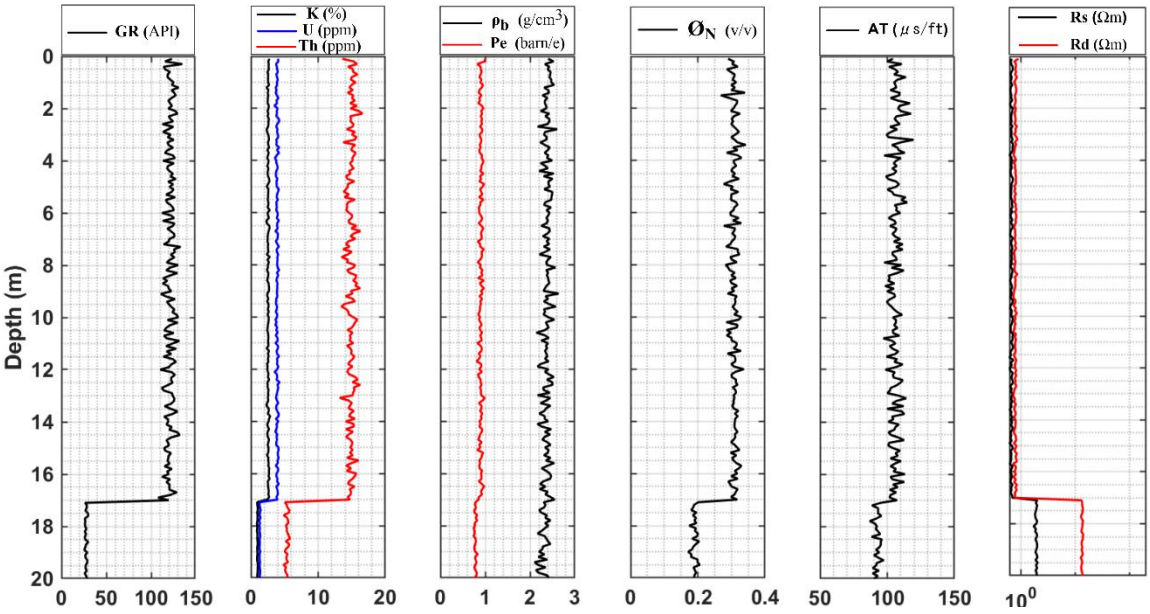

Fig. 40 Simulated logs (5% Gaussian distributed noise) of Model B in well 1

DOI: 10.14750/ME.2022.027

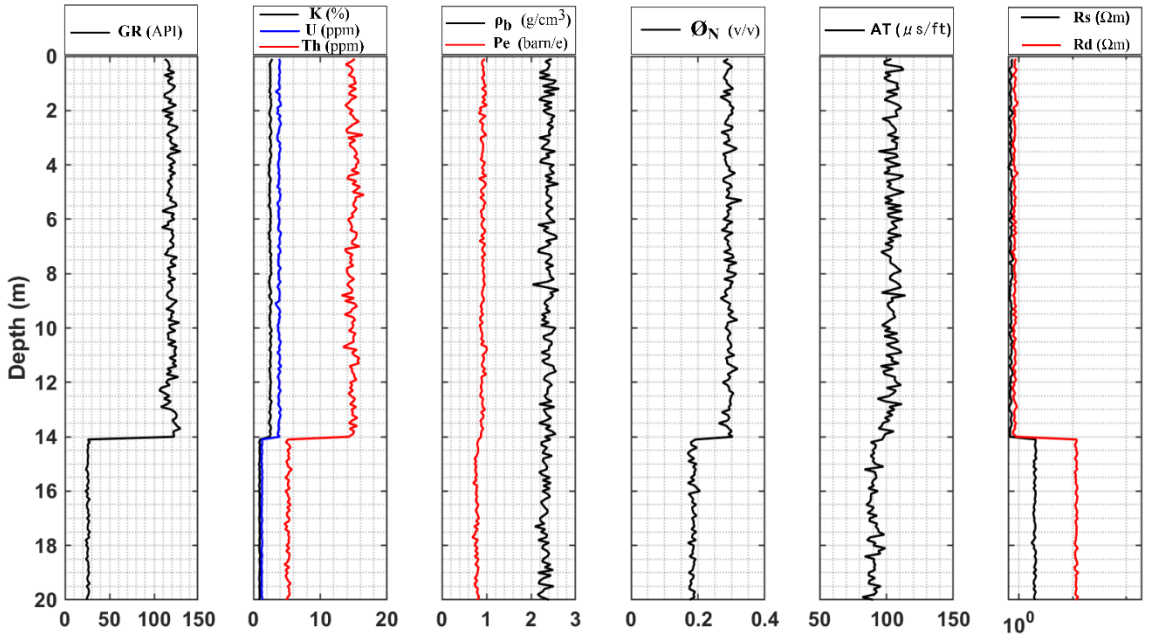

Fig. 41 Simulated logs (5% Gaussian distributed noise) of Model B in well 2

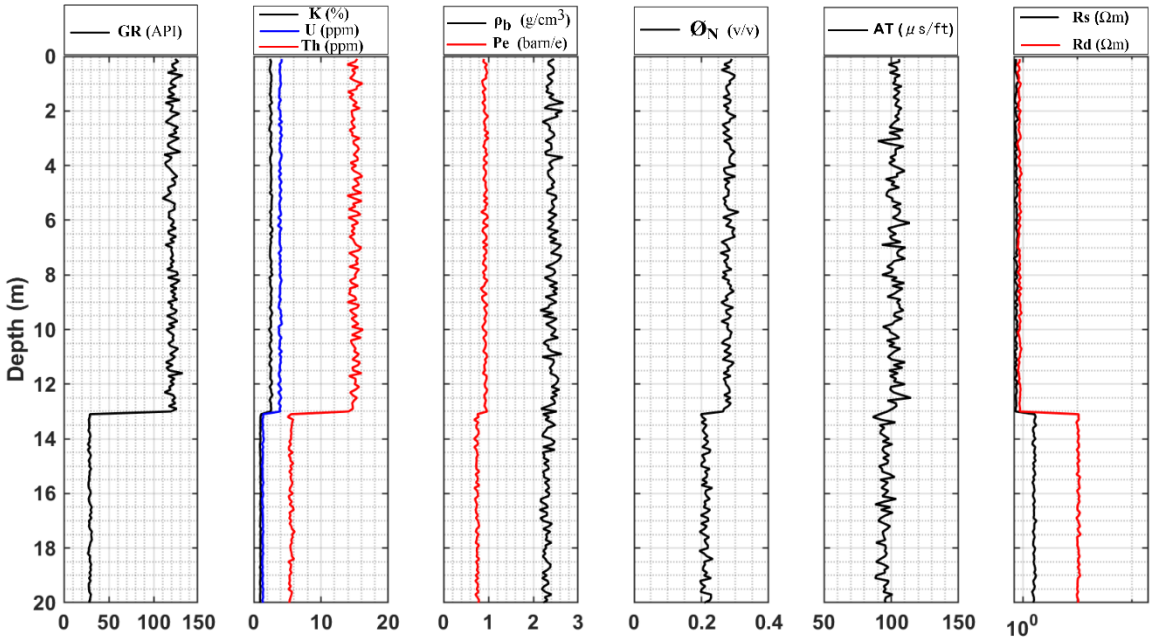

Fig. 42 Simulated logs (5% Gaussian distributed noise) of Model B in well 3

DOI: 10.14750/ME.2022.027

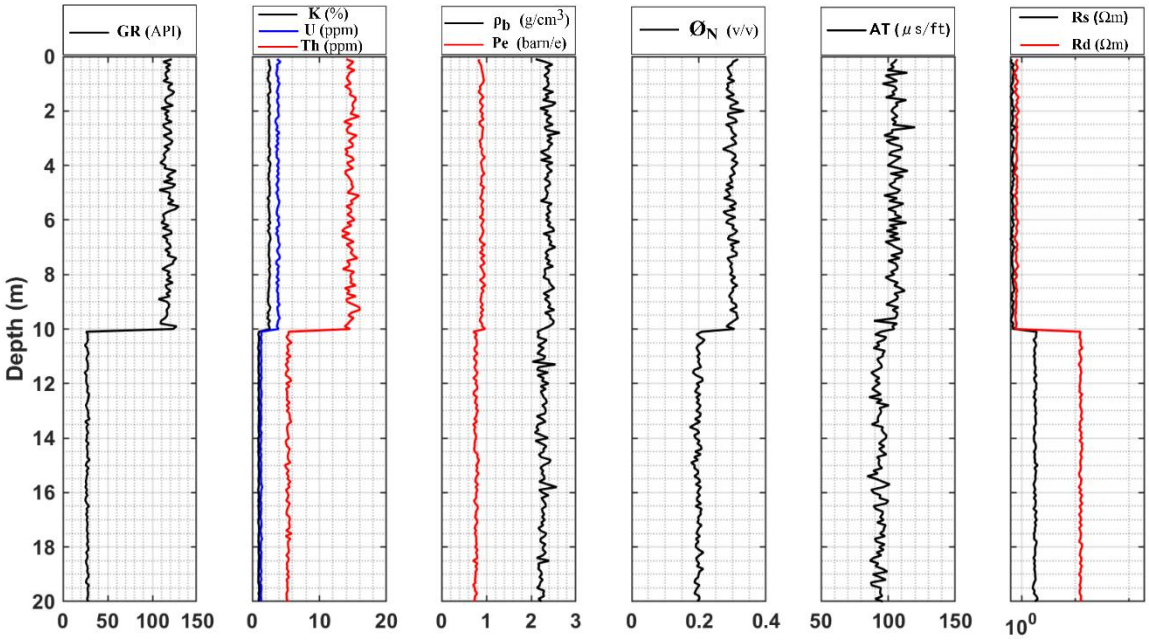

Fig. 43 Simulated logs (5% Gaussian distributed noise) of Model B well 4

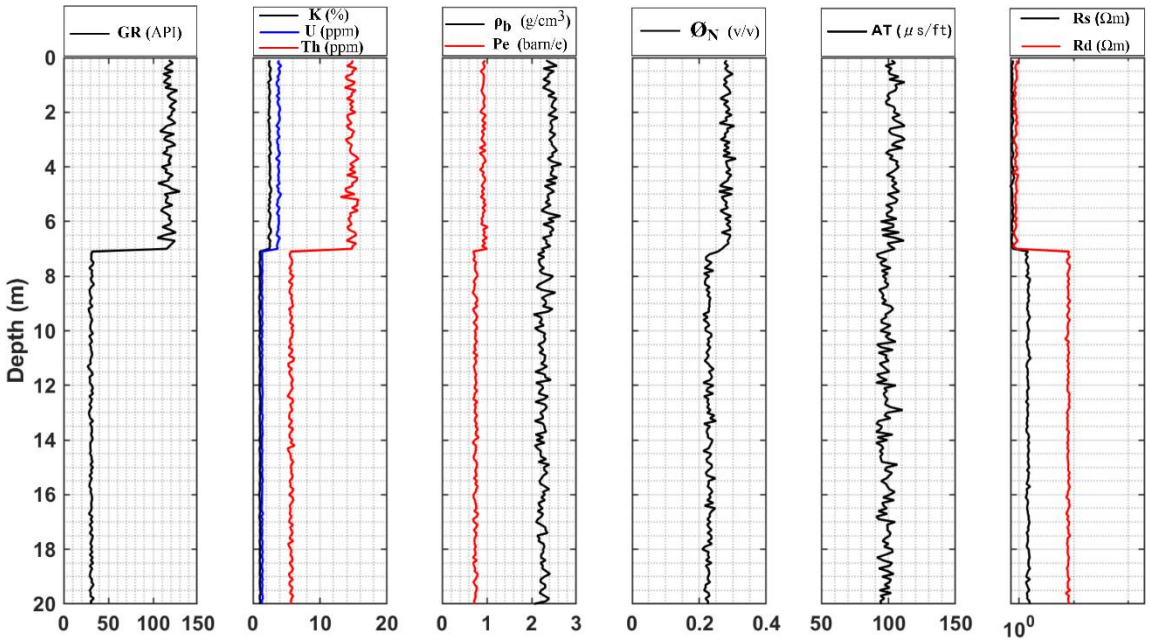

Fig 44 Simulated logs (5% Gaussian distributed noise) of Model B in well 5

DOI: 10.14750/ME.2022.027

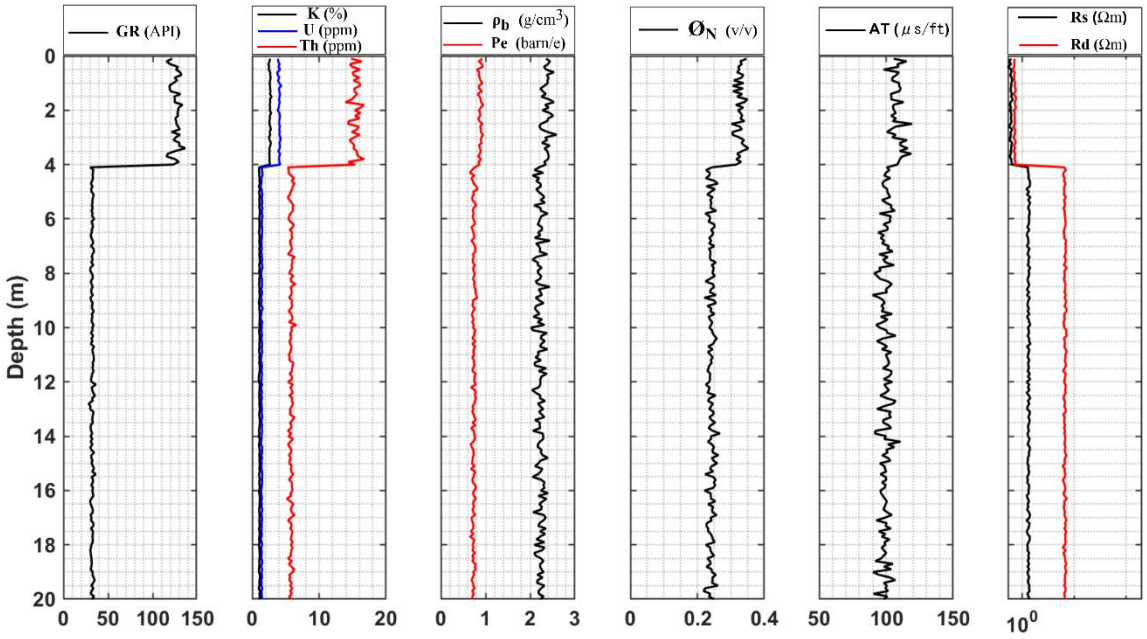

Fig. 45 Simulated logs (5% Gaussian distributed noise) of Model B in well 6

By using 4-degree Legendre polynomials and carefully selected initial values of porosity, water saturation and volume of shale (0.09, 1.0 and 0.80) for the first layer and (0.25, 0.34 and 0.08) for the second layer the 2D interval inversion procedure proved to be stable and convergent. The development of convergence can be seen in Fig. 46, revealing the escaping from several minima during the inversion procedures (for instance, after 100-th iteration). The best solution was obtained at D_d= 5.1 percent data and D_m = 3.7 percent model distance. Table 10 shows good determination of the petrophysical parameters. 2D illustrations of the targeted parameters and the estimated one can be seen in Figs. 46-48.

Table 10 Petrophysical parameters of Model B estimated by 2D interval inversion. The dimensional units are v/v

Layer	Parameter	W-1	W-2	W-3	W-4	W-5	W-6
1 shale	POR	0.100	0.085	0.081	0.91	0.083	0. 111
	SX0	1.001	0.998	1.000	0.999	0.996	1.005
	VSH	0.708	0.698	0.714	0.702	0.703	0.75
2 gas-sand	POR	0.230	0.218	0.239	0.246	0.254	0.269
	SX0	0.811	0.809	0.812	0.809	0.822	0.842
	VSH	0.096	0.096	0.099	0.106	0.118	0.132

DOI: 10.14750/ME.2022.027

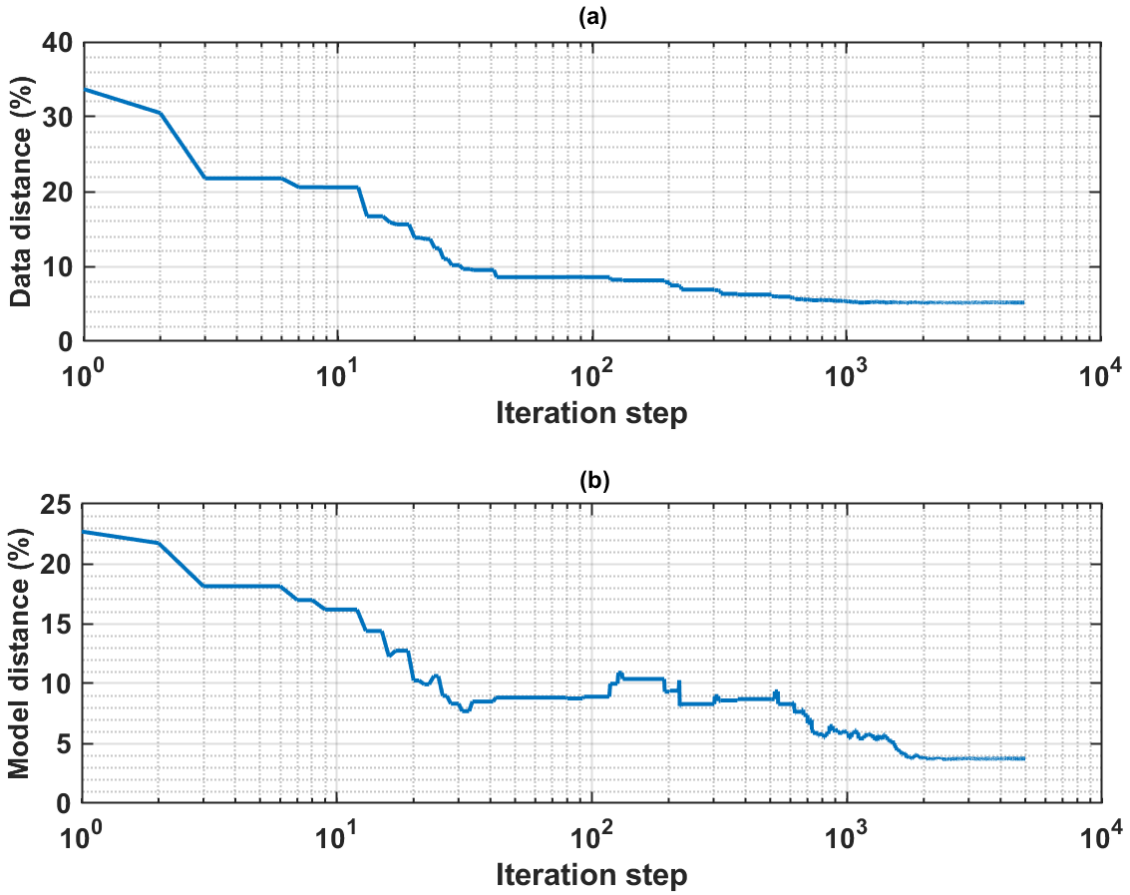

Fig. 46 Development of convergence during 2D interval inversion procedure. a) Data distance vs. iteration step, b) Model distance vs. iteration step

DOI: 10.14750/ME.2022.027

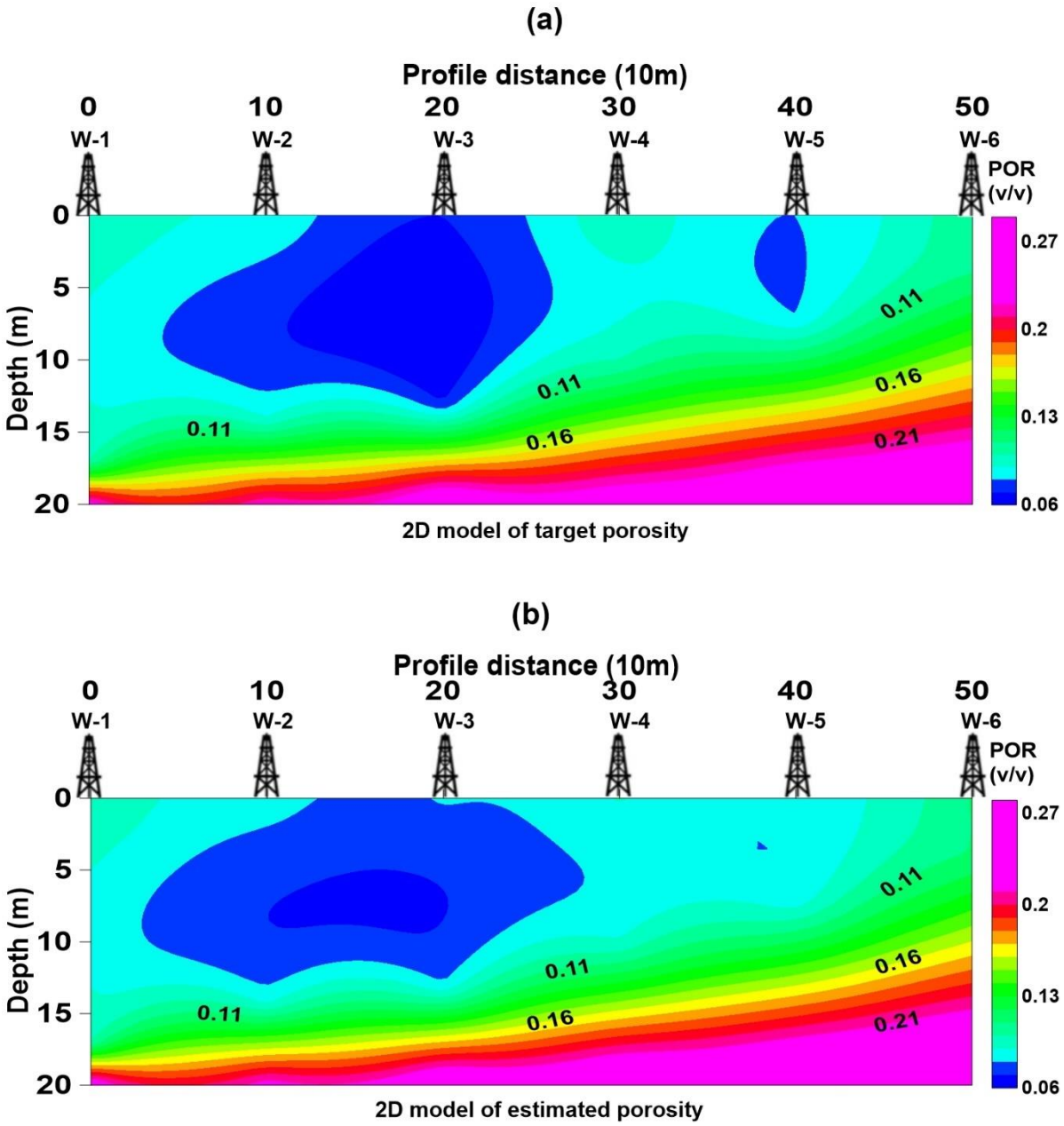

Fig. 47 a) 2D models of target porosity, b) the estimated one by 2D interval inversion

DOI: 10.14750/ME.2022.027

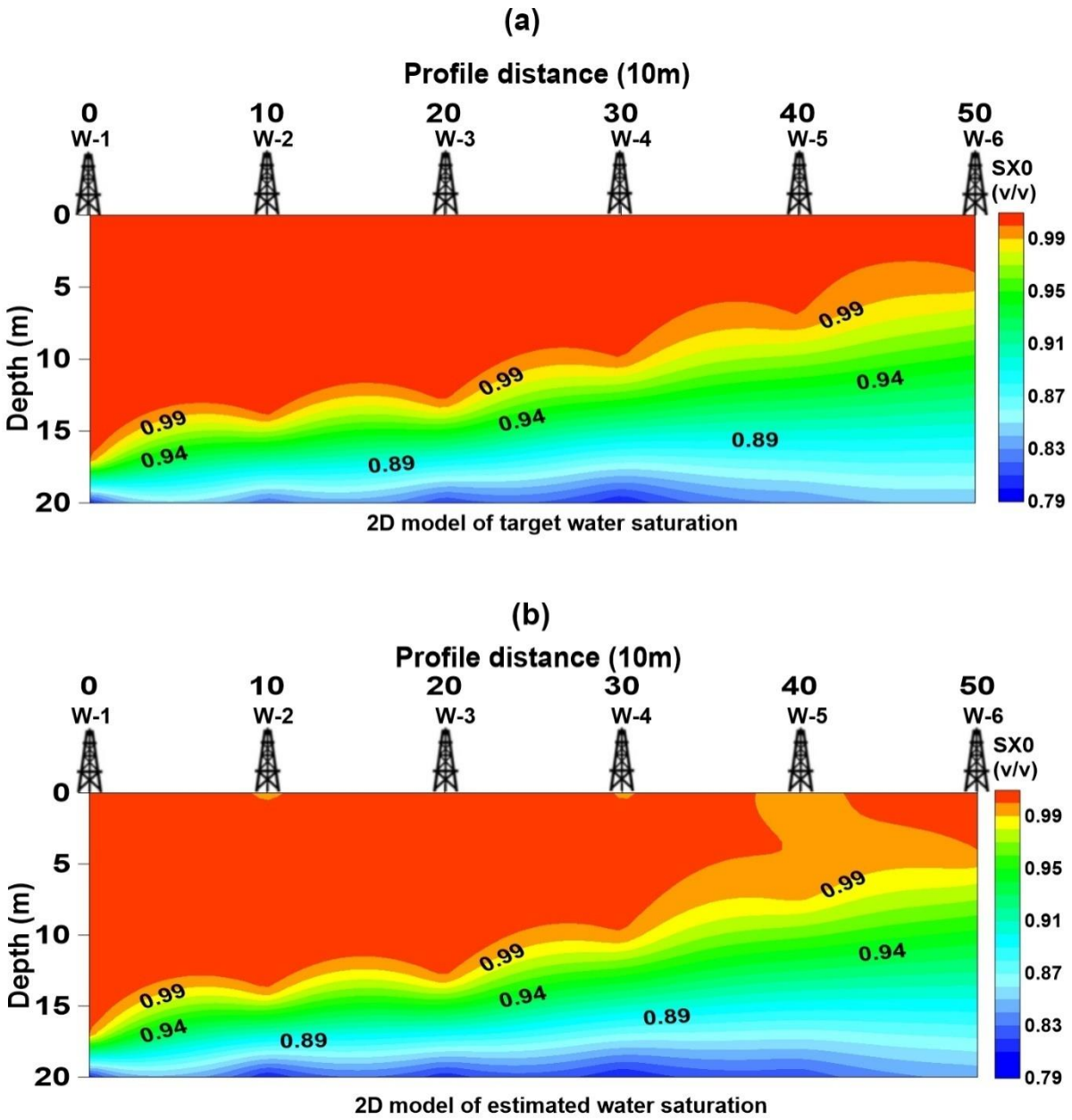

Fig. 48 a) 2D models of target water saturation, b) the estimated one by 2D interval inversion

DOI: 10.14750/ME.2022.027

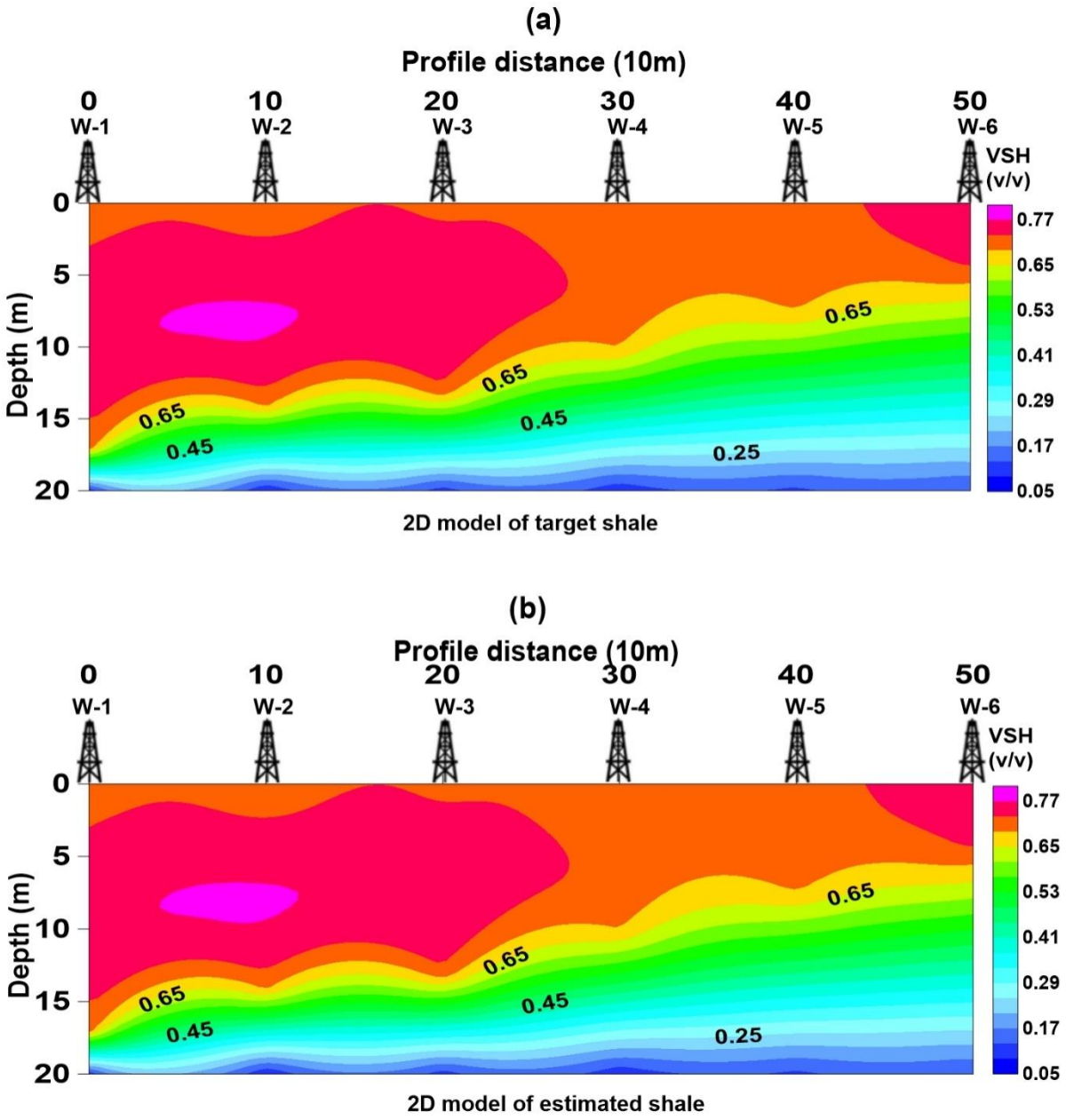

Fig. 49 a) 2D models of target shale content, b) the estimated one by 2D interval inversion

DOI: 10.14750/ME.2022.027

Non-inversion parameters derived from 2D interval inversion results were also accurately estimated. The targeted and estimated parameters can be checked in Tables 11 and 12, respectively.

Table 11 Targeted parameters derived from the interval inversion results

Layer	Parameter	W-1	W-2	W-3	W-4	W-5	W-6
1	VSD	0.19	0.21	0.21	0.21	0.22	0.15
	SW	1.0	1.0	1.0	1.0	1.0	1.0
	$S_{hc,irr}$	0.0	0.0	0.0	0.0	0.0	0.0
	$S_{hc,mv}$	0.0	0.0	0.0	0.0	0.0	0.0
	K	8.0 mD	5.0 mD	2.0 mD	8.0 mD	3.0 mD	13.0 mD
2	VSD	0.67	0.69	0.64	0.66	0.62	0.6
	SW	0.327	0.37	0.348	0.327	0.39	0.418
	$S_{hc,irr}$	0.20	0.18	0.19	0.20	0.17	0.16
	$S_{hc,mv}$	0.473	0.45	0.462	0.45	0.44	0.422
	K	333 mD	274 mD	481 mD	402 mD	571 mD	675 mD

Table 12 Estimated parameters derived from interval inversion results

Layer	Parameter	W-1	W-2	W-3	W-4	W-5	W-6
1	VSD	0.192	0.217	0.205	0.207	0.214	0.139
	SW	1.005	0.99	1.0	0.995	0.98	1.02
	$S_{hc,irr}$	0.0	0.0	0.0	0.0	0.0	0.0
	$S_{hc,mv}$	0.0	0.0	0.0	0.0	0.0	0.0
	K	8.0 mD	4.5 mD	4.0 mD	5.0 mD	4.0 mD	14.0 mD
2	VSD	0.674	0.686	0.662	0.648	0.628	0.599
	SW	0.35	0.346	0.353	0.346	0.375	0.423
	$S_{hc,irr}$	0.189	0.191	0.188	0.191	0.178	0.158
	$S_{hc,mv}$	0.468	0.472	0.465	0.472	0.443	0.419
	K	333 mD	308 mD	417 mD	490 mD	563 mD	695 mD

4.3 Stability test of inversion procedures

To check the stability of 2D interval inversion procedures 10 independent program runs were performed in both Models A and B, respectively. The data distance convergences to the optimal value in all 10 runs are illustrated in Fig. 50, which supports the findings that metaheuristic methods can be effectively used to eliminate the starting model dependence of inverse problems (Pace et al. 2019). Also, escaping from several

DOI: 10.14750/ME.2022.027

local minimums during global optimization can be observed until the optimum solution is reached. The data distance after the 1000-th iteration step is slightly lower for Model A than for Model B, indicating a slight model dependence. The computed average data distances for both Models A and B are 4.13 and 5.18, with average standard deviations of 0.0012 and 0.0014, respectively. This demonstrates the effectiveness of the simulated annealing method for solving the 2D inverse problem in stable procedures.

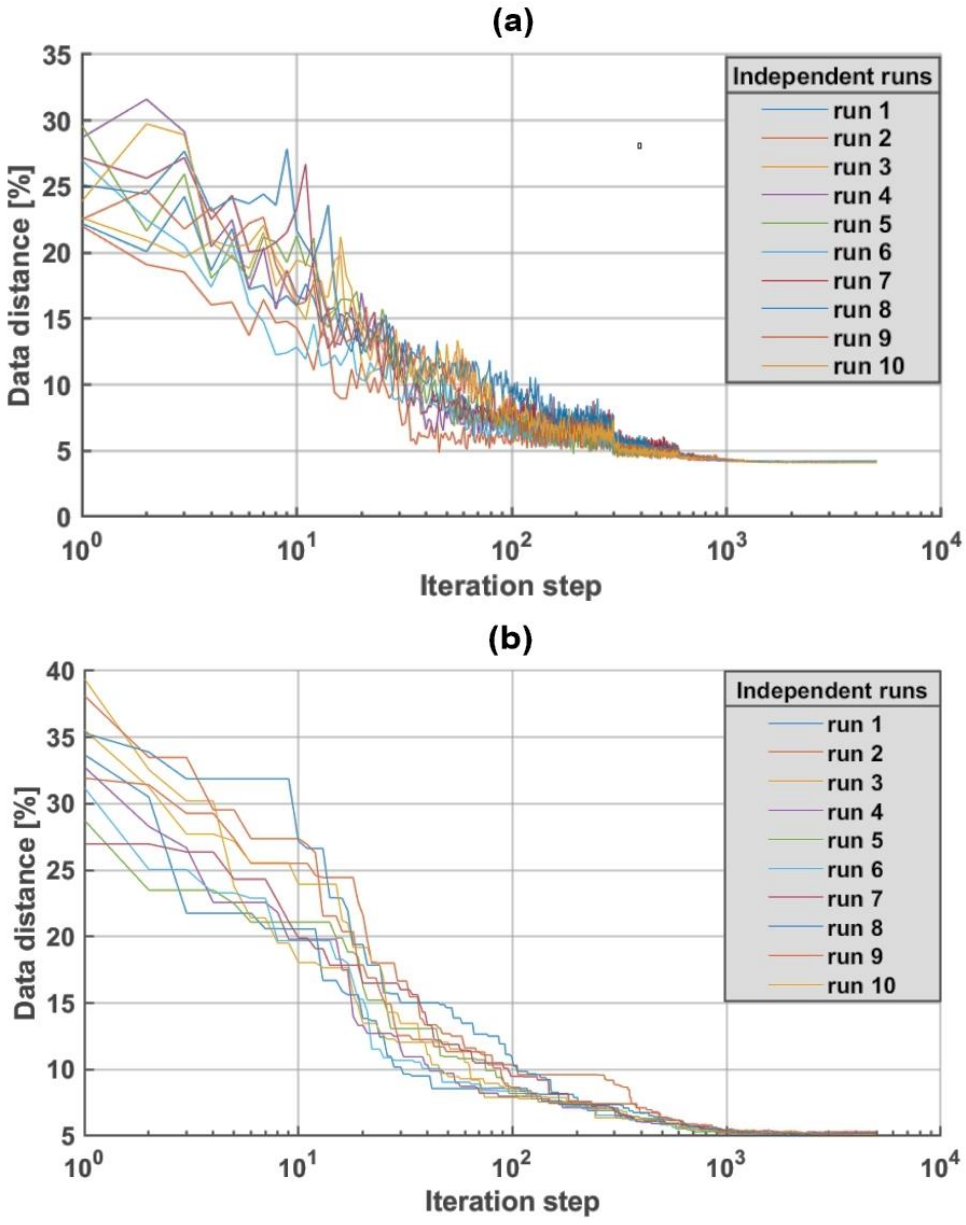

Fig. 50 Convergence plots of the 2D interval inversion procedure for 10 independent runs a) Model A, b) Model B

DOI: 10.14750/ME.2022.027

4.4 In-situ results

It is reasonable to apply the proposed method to field data following assessing it on the simulated examples. As a consequence, the 2D interval inversion approach was used to process in situ-well logging measurements obtained in four boreholes, W-1–W-4, located in an Egyptian hydrocarbon field Fig. 26. The available data samples corresponding to given gamma-ray (*GR*), shallow resistivity "R_s", deep resistivity "R_d", bulk Density "ρ_b ", and neutron-porosity "$\emptyset_N$". The maximum number of iterations for the inversion operation was 5000. In the first layer, the initial values of the expansion coefficients for porosity, water saturation, and shale content are 0.25, 0.40, and 0.09, respectively. In the second, they are 0.16, 0.1, and 0.7, and in the third, they are 0.23, 0.4, and 0.08.The solution was observed at D_d= 6.4 % relative data distance Fig. 51. The estimated petrophysical parameters are summarized in Table 13.

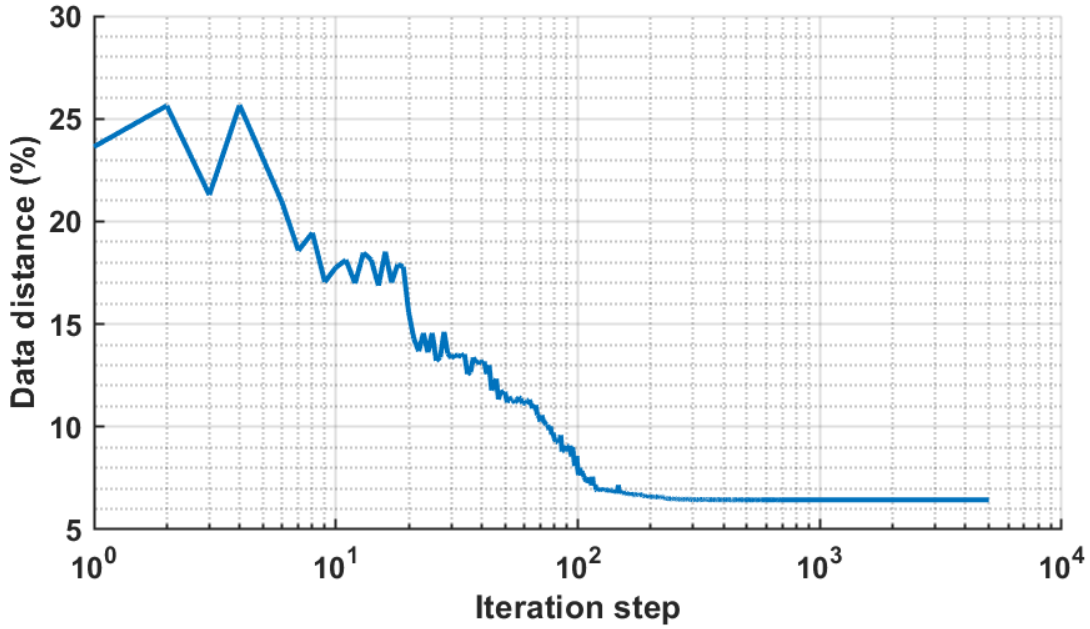

Fig. 51 Convergence plot of the processed Egyptian field data by 2D interval inversion method, the average data distance vs. number of iterations

Table 13 Petrophysical parameters of Egyptian hydrocarbon structure estimated by 2D interval inversion

Layer	Parameter	W-1	W-2	W-3	W-4
1gas-sand	POR	0.228	0.234	0.246	0.262
	SX0	0.840	0.847	0.856	0.860
	VSH	0.115	0.122	0.136	0.144
2 shale	POR	0.024	0.050	0.085	0.111
	SX0	0.995	0.985	0.994	1.0
	VSH	0.621	0.604	0.619	0.669

DOI: 10.14750/ME.2022.027

3 gas-sand	POR	0.246	0.223	0.231	0.258
	SX0	0.815	0.835	0.852	0.876
	VSH	0.123	0.129	0.141	0.165

4.5 Discussion

For determining the lateral variation of petrophysical parameters, a 2D Legendre polynomials-based interval inversion approach is demonstrated. The simulated annealing technique is used to solve the inversion algorithm, which assigns the solution to the global optimum. The petrophysical parameters are derived from the coefficients of series expansion. To evaluate the modified method, simulated measurements contaminated with 5% Gaussian distributed noise of two Models A and B made of groundwater and hydrocarbon bearing zones are generated. The data and model misfits are tested to ensure the inversion procedures' stability and convergence. In the case of the proposed Models, I was able to successfully estimate the lateral variations of the petrophysical parameters. Furthermore, the program's stability was tested by running it ten times independently and calculating the average data distance and standard deviation. The method's feasibility is demonstrated by analyzing in-situ well logging data from four wells in an Egyptian hydrocarbon field.

Thesis three

I developed a 2D Legendre polynomials-based interval inversion approach for determining lateral varying of petrophysical parameters. I assessed the method by using noisy simulated measurements on petrophysical Models made of two-layer structures related to groundwater and hydrocarbon bearing formations. The numerical experiments aided to investigate the stability and convergence of the 2D interval inversion procedure. To ensure the accuracy and reliability of the inversion results, the misfit of data and model distance are tested. A large amount of input data relative to the number of unknown results in a high overdetermination ratio, consequently more reliable estimates are obtained in stable and convergent procedure than in conventional local (1D) inversion schemes. I applied global optimization technique to get the best fit between the measured and calculated data. The feasibility of the 2D interval inversion method is shown by analysing in-situ well logging data acquired in four wells situated in Egyptian hydrocarbon field.

DOI: 10.14750/ME.2022.027

5. INTERVAL INVERSION OF MULTI-WELL LOGGING DATA FOR ESTIMATING SIMULTANEOUSLY LATERALLY VARYING PETROPHYSICAL PARAMETERS AND FORMATION BOUNDARIES

In view of the great benefits of the interval inversion algorithm in separately determining the lateral variation of layer boundary coordinates, the vertical and lateral variations of petrophysical parameters, I improved the algorithm that is capable of determining both in a joint inversion process. Accordingly, the model vector comprised the series expansion coefficients of the petrophysical parameters besides the layer thicknesses. The inverse problem solved by the simulated algorithm. The reliability and accuracy of inversion results is checked by measuring the misfit between measured and calculated data and goodness of model fit as well.

5.1 Numerical results

The improved algorithm is tested on the same two Models A and B which used in the previous chapter. In case of the Model A Fig. 52. The targeted unknowns can be seen in Table 14. The initial model comprised first-guess values of petrophysical parameters and $H_1(x)$ =10 planar layer boundary which are discretized by using Legendre polynomials up of 4 degrees as basis function. The development of convergence during the inversion process is illustrated in Fig. 53. The optimum solution was found at D_d = 4.5 percent data distance and D_m= 3.4 percent model distance. The estimated unknowns of layer boundary coordinates and petrophysical parameters are summarized in Table 15. The upper boundary of the water bearing sand zone is corresponding to the last expansion coefficient reveals detected depth of 10.05 m.

Table 14 Targeted unknowns of Model A

Layer	Parameter	W-1	W-2	W-3	W-4	W-6	W-5
1	POR	0.10	0.11	0.09	0.10	0.08	0.12
	VSH	0.73	0.71	0.72	0.70	0.72	0.75
2	POR	0.22	0.24	0.23	0.25	0.24	0.26
	VSH	0.10	0.12	0.11	0.13	0.12	0.14
Boundary	$H_1(X)$	10.0	5.0	15.0	15.0	5.0	10.0

DOI: 10.14750/ME.2022.027

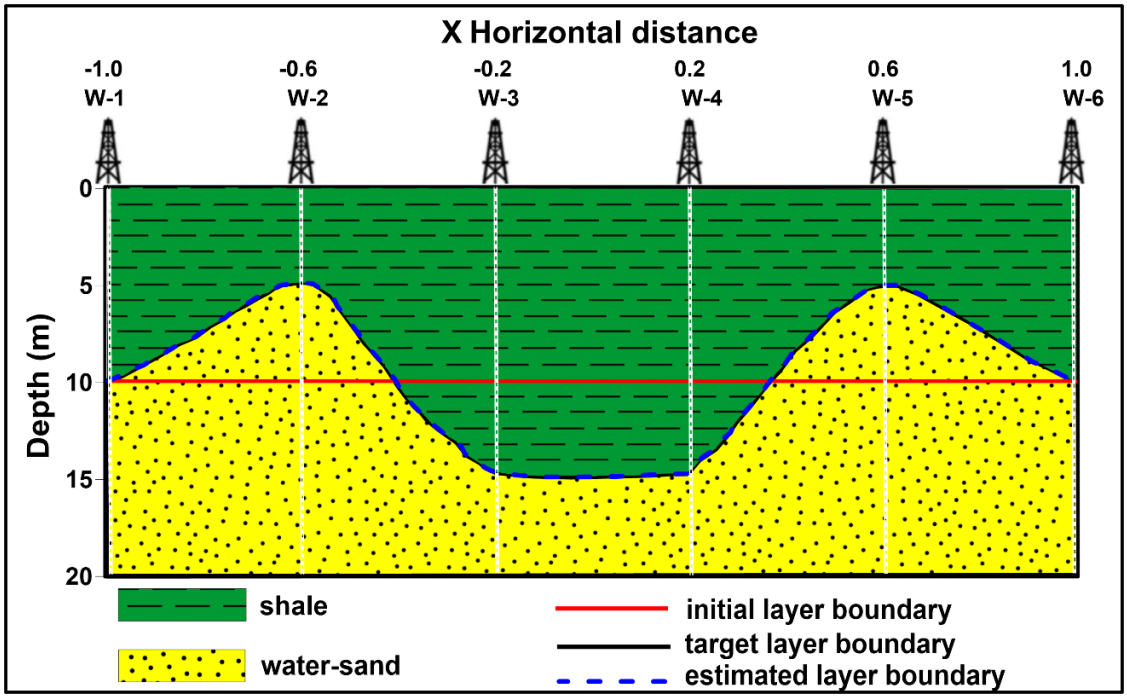

Fig. 52 2D lithological model showing the target, initial, and estimated thickness function

Table 15 Petrophysical parameters and layer-boundary coordinates of Model A estimated by 2D interval inversion

Layer	Parameter	W-1	W-2	W-3	W-4	W-6	W-5
1	POR	0.099	0.099	0.092	0.099	0.093	0.118
	VSH	0.738	0.713	0.699	0.699	0.715	0.755
2	POR	0.222	0.239	0.242	0.239	0.242	0.262
	VSH	0.105	0.116	0.111	0.117	0.118	0.139
Boundary	$H_1(x)$	10.05	5.0	15.01	15.01	5.0	10.05

DOI: 10.14750/ME.2022.027

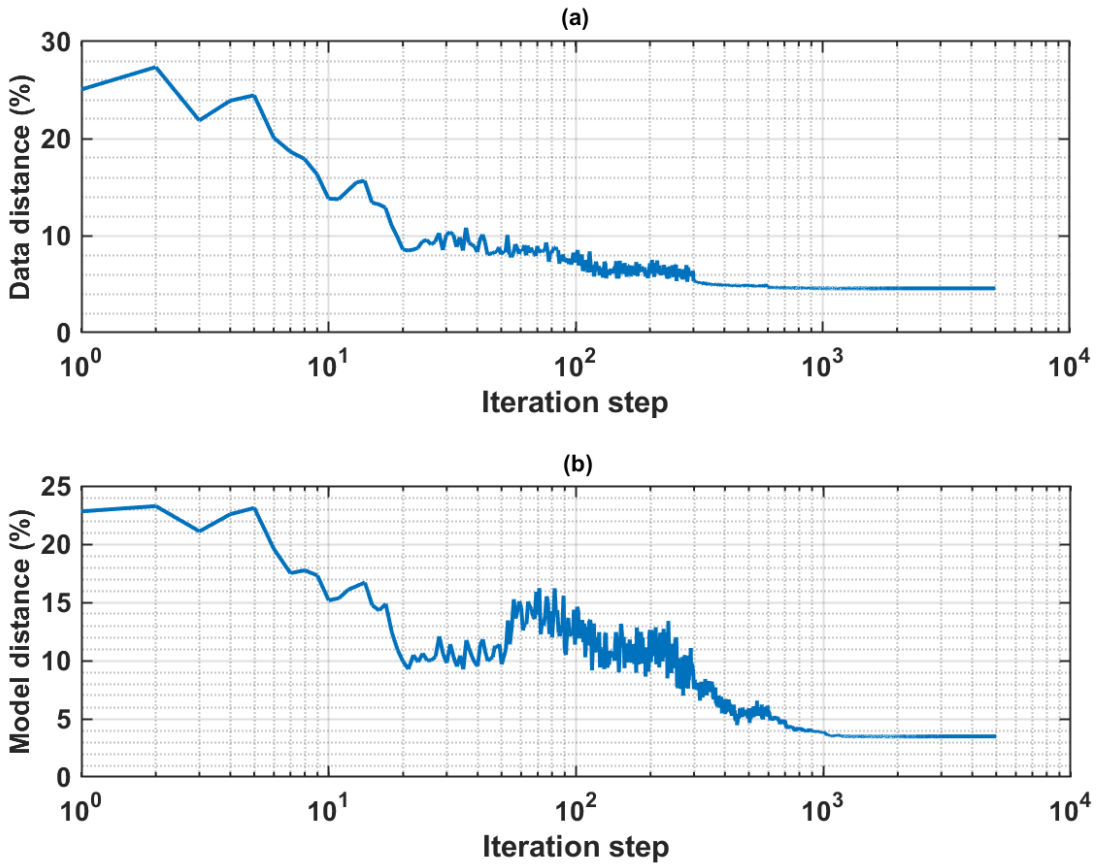

Fig. 53 Development of convergence during 2D interval inversion procedure. a) Data distance vs. iteration step, b) Model distance vs. iteration step

As a next strategy, I applied the improved inversion algorithm for Model B given in Fig. 54. The model parameters ($Ø$, S_{x0} and V_{sh}) with layer boundaries were discretized by using Legendre polynomials of up to 4 degree as basis functions. In this case, the number of unknowns (expansion coefficients) was 35, delivering an overdetermination ratio of 344. Despite the increase of the unknowns, the overdetermination ratio is still high due to the large amount of input datasets, resulting in stable and convergence inversion procedures. The targeted parameters of the model can be checked in Table 16.

The initial model comprised first-guess values of petrophysical parameters and $H_1(x)$ = 4 m planar layer boundary. The development of convergence during the inversion process is illustrated in Fig. 55. The optimum solution was found at D_d = 5.1 percent data distance and D_m = 4.9 percent model distance. The estimated unknowns of layer boundary coordinates and petrophysical parameters are summarized in Table 17. The upper boundary of the hydrocarbon bearing sand zone has detected depth of 4.07 m.

DOI: 10.14750/ME.2022.027

Table 16 Targeted unknowns of Model B

Layer	Parameter	W-1	W-2	W-3	W-4	W-6	W-5
1	POR	0.09	0.10	0.07	0.09	0.08	0.11
	SX0	1.0	1.0	1.0	1.0	1.0	1.0
	VSH	0.79	0.80	0.78	0.79	0.81	0.82
2	POR	0.32	0.30	0.29	0.31	0.30	0.33
	SX0	0.80	0.82	0.81	0.80	0.83	0.84
	VSH	0.10	0.08	0.09	0.07	0.09	0.11
Boundary	$H_1(x)$	17.0	14.0	13.0	10.0	7.0	4.0

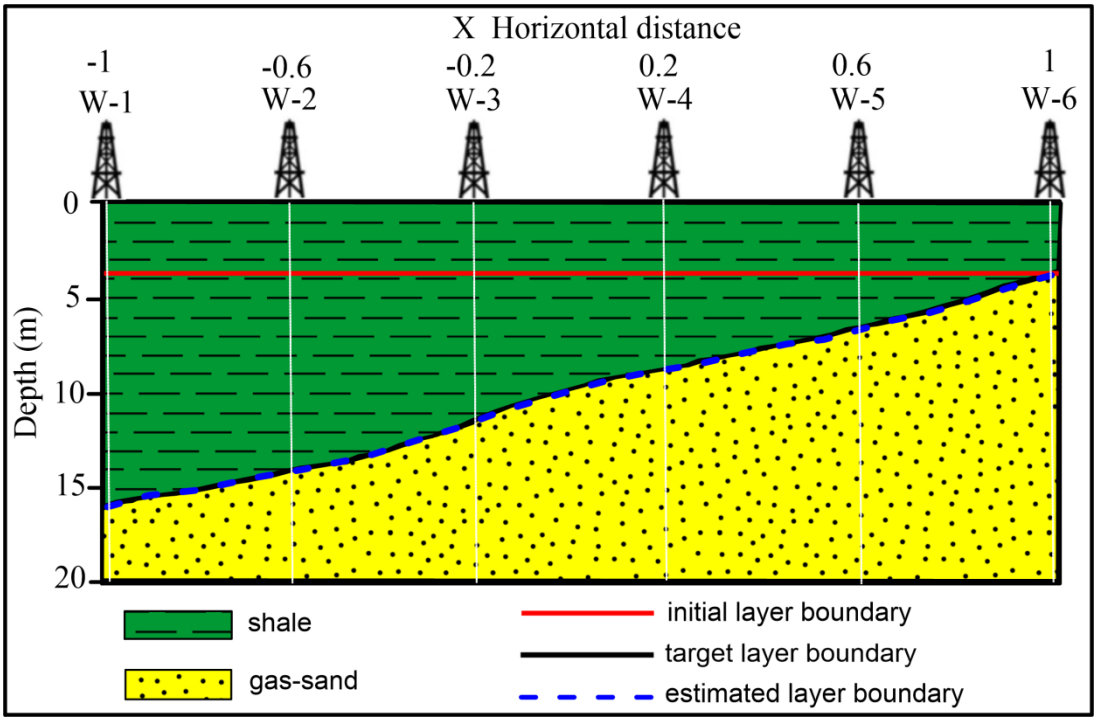

Fig. 54 2D lithological model showing the target, initial and estimated layer thickness function

DOI: 10.14750/ME.2022.027

Table 17 Petrophysical parameters and layer boundary coordinates of Model B estimated by 2D interval inversion (polynomials degree is n= 4)

Layer	Parameter	W-1	W-2	W-3	W-4	W-6	W-5
1	POR	0.102	0.088	0.089	0.090	0.089	0.111
	SX0	0.997	0.995	0.997	0.996	0.994	1.005
	VSH	0.713	0.702	0.716	0.694	0.700	0.739
2	POR	0.234	0.224	0.239	0.245	0.253	0.266
	SX0	0.808	0.816	0.805	0.809	0.827	0.846
	VSH	0.094	0.096	0.101	0.107	0.116	0.128
Boundary	$H_1(x)$	17.07	14.03	13.02	10.02	7.03	4.07

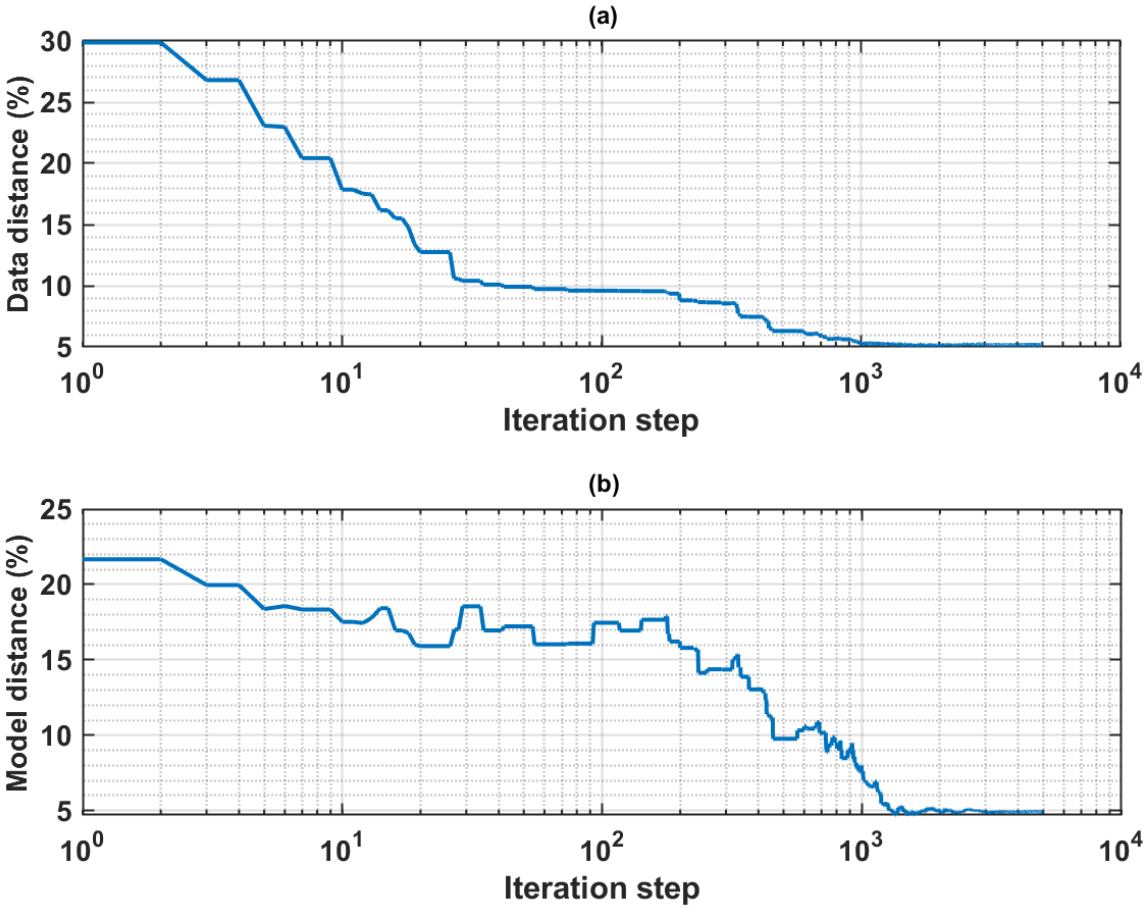

Fig. 55 Development of convergence during 2D interval inversion procedure(polynomials degree is n= 4). a) Data distance vs. iteration step, b) Model distance vs. iteration step

DOI: 10.14750/ME.2022.027

It worth to be noting that describing fine structures and sudden changes require more series coefficients which can be achieved by increasing the polynomials degree in equation (14). In the simulated modeling of Model B by increasing the polynomials degree to 10, the number of unknowns to be estimated are increased up to 77, resulting in decrease of the overdetermined ratio, which may negatively affect the quality of inversion results. However, owing to a large number of inverted data, we could obtain reasonable results as seen in Table 18. The data and model distances are illustrated in Fig. 56, also the 2D cross-section of petrophysical parameters is shown in Fig 57.

Table 18 Petrophysical parameters and layer boundary coordinates of Model B estimated by 2D interval inversion (polynomials degree is n=10)

Layer	Parameter	W-1	W-2	W-3	W-4	W-6	W-5
1	POR	0.092	0.088	0.083	0.093	0.086	0.126
	SX0	1.002	0.998	0.995	1.000	0.997	1.002
	VSH	0.709	0.702	0.717	0.687	0.700	0.758
2	POR	0.225	0.225	0.232	0.237	0.247	0.273
	SX0	0.801	0.823	0.812	0.811	0.824	0.842
	VSH	0.098	0.101	0.106	0.101	0.114	0.134
Boundary	$H_1(x)$	17.17	14.01	13.04	10.04	7.01	4.17

DOI: 10.14750/ME.2022.027

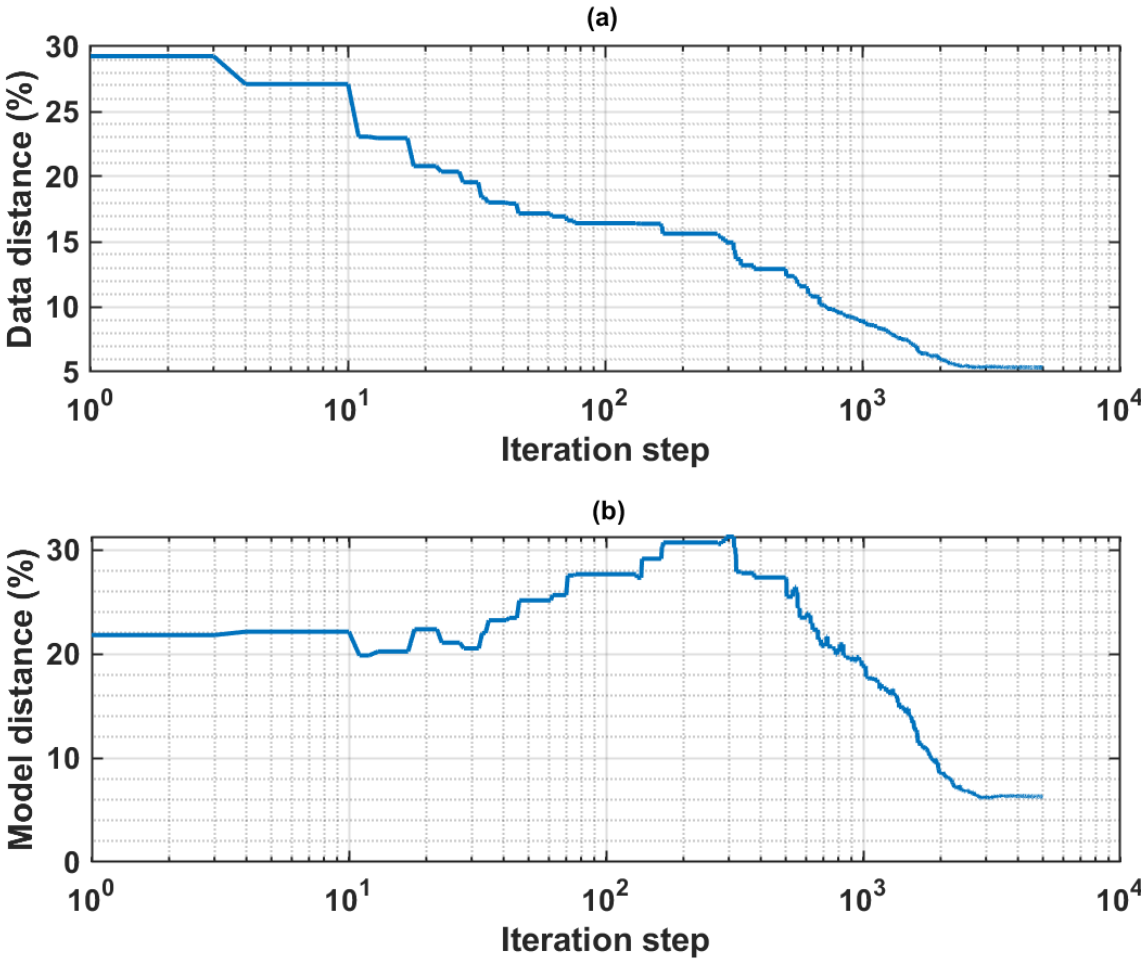

Fig. 56 Development of convergence during 2D interval inversion procedure (polynomials degree is n=10). a) Data distance vs. iteration step, b) Model distance vs. iteration step

DOI: 10.14750/ME.2022.027

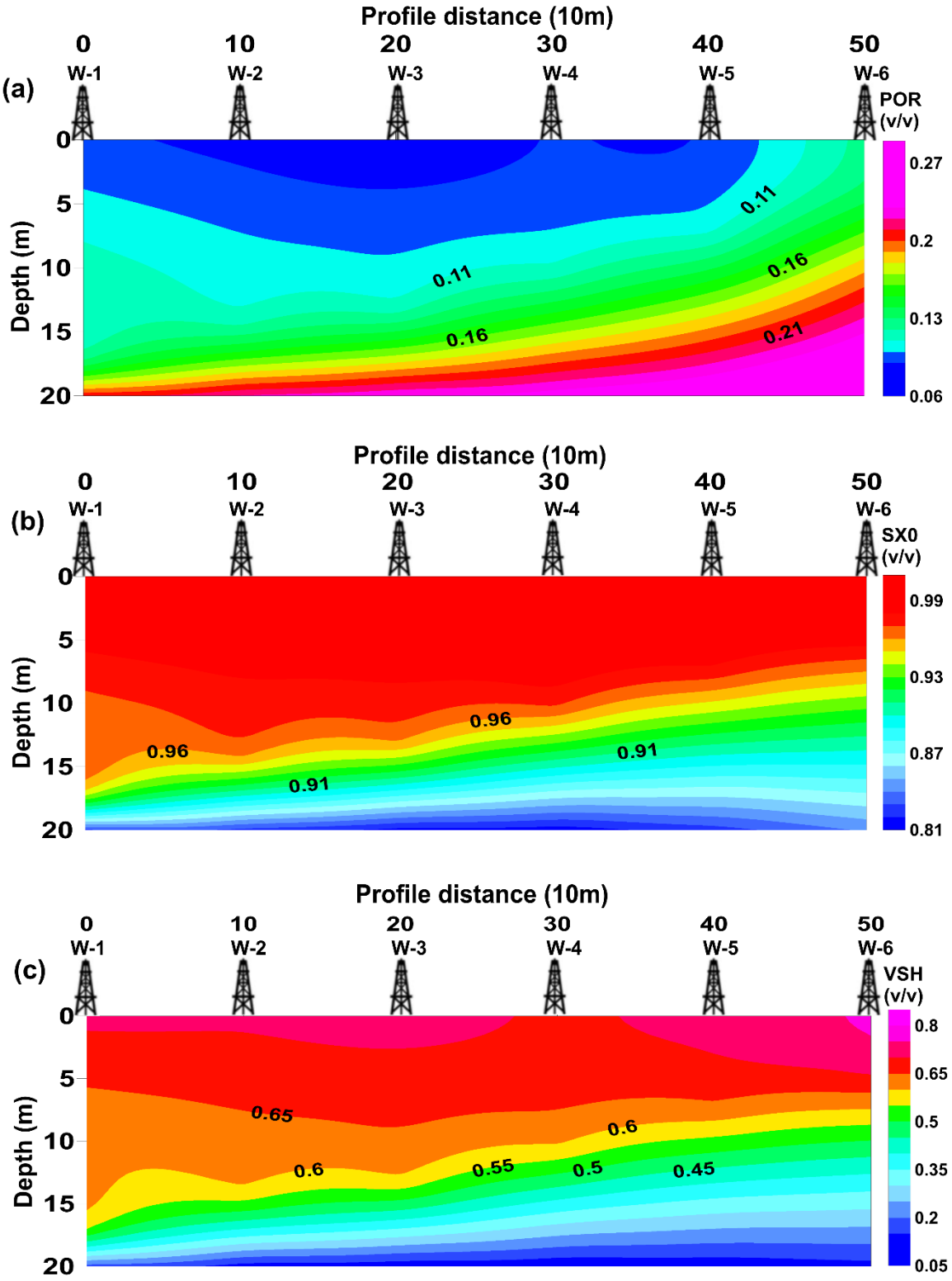

Fig. 57. Results of 2D inversion in drill holes W1-W6 with 10 polynomials degree of Model B : a) porosity b) water saturation c) shale content

DOI: 10.14750/ME.2022.027

5.2 Field test

By using the same measurements of the Egyptian hydrocarbon field, the maximum number of iterations for the global optimization based-inversion operation was 5000. In the first layer, the initial values of the expansion coefficients for porosity, water saturation, and shale content are 0.25, 0.40, and 0.09, respectively. In the second, they are 0.16, 0.1, and 0.7, and in the third, they are 0.23, 0.4, and 0.08. Regarding layer boundaries, $H_1(x)$= 4 m and $H_2(x)$=12 m. The solution was observed at D_d= 6.5 % relative data distance Fig. 58. The estimated model parameters and layer-boundary coordinates are provided in Table 19. Further, 2D models of the results are illustrated in Fig. 59. It can be noticed that the investigated interval revealed two types of lithology, i.e., sand and shale. Two hydrocarbon-bearing zones are well defined, the lower boundary of the first zone is at depth 4m and the upper boundary for the second zone is detected at depth 12m. The interpreted lithological results are well supported by the geological and stratigraphic settings of the investigated area which is a half-graben system filled with thick non-marine sediments deposited during Early Cretaceous (Hauterivian to Barremian) followed by marine deposition during Albian/Cenomanian (argillaceous sandstones and shales) and later shales and marine limestones during Late Cretaceous and early Tertiary (Dolson et al. 1999). Furthermore, the estimated petrophysical parameters utilizing 2D interval inversion showed a close agreement with the results of previous studies by using traditional analysis (Ali 2015; Othman et al. 2015; Senosy et al. 2020). In case of using higher polynomial degree (n=8), considerable estimates of the petrophysical parameters and layer-boundary coordinates are also obtained Table 20. The convergence plot during the inversion procedures is shown in Fig. 60. A glance to the convergence plots of inversion procedures for field measurement, the data distance is slightly higher than for simulated models. This may be attributed to the reservoir conditions and the investigated depths. It worth to noting that the computed sand porosity at 0 shale effective porosity correspondent to the expected porosity according to supposed depth dependent compaction trend. The upper sand-gas shows a higher porosity values. The larger values may be result of a chemical dissolution process during migration of hydrocarbon. There is a strict connection in generation between lower and upper gas sand by migration through shale layer.

DOI: 10.14750/ME.2022.027

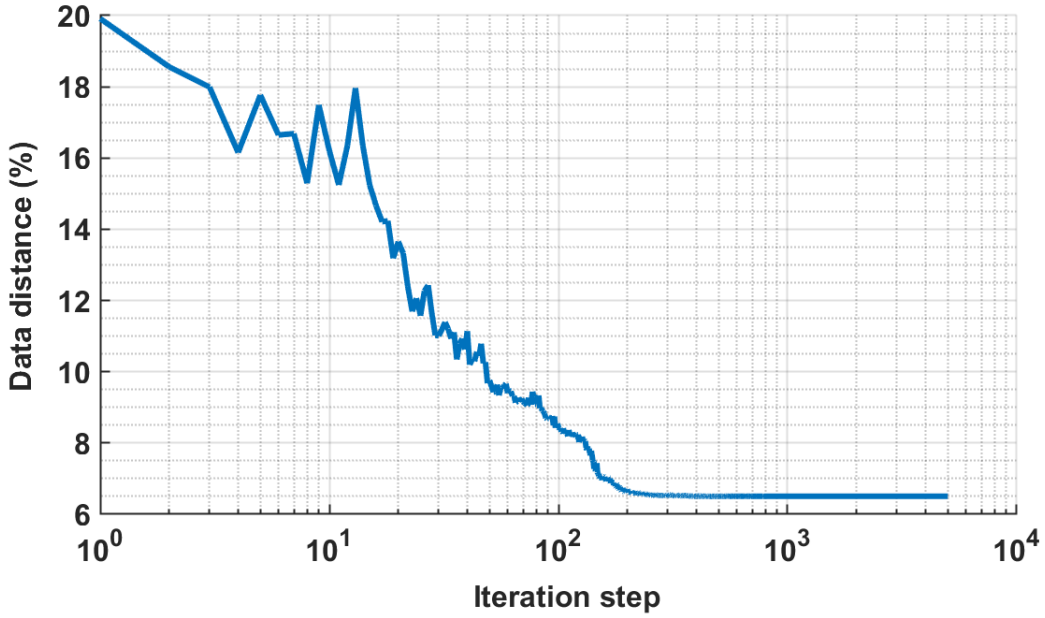

Fig. 58 Convergence plot of the processed Egyptian field data by 2D interval inversion method, the average data distance vs. number of iterations

Table 19 Estimated petrophysical parameters and layer boundary coordinates of Egyptian field data by 2D interval inversion method

Layer	Parameter	W-1	W-2	W-3	W-4
1gas-sand	POR	0.225	0.237	0.248	0.26
	SX0	0.838	0.843	0.850	0.858
	VSH	0.114	0.125	0.136	0.147
2 shale	POR	0.026	0.05	0.082	0.11
	SX0	0.996	0.991	0.987	1.00
	VSH	0.626	0.60	0.617	0.66
3 gas-sand	POR	0.241	0.223	0.229	0.259
	SX0	0.815	0.831	0.852	0.874
	VSH	0.127	0.126	0.138	0.163
Boundary	$H_1(x)$	7.0	8.33	7.33	4.0
	H_2 (x)	12.5	10.5	10.5	12.0

DOI: 10.14750/ME.2022.027

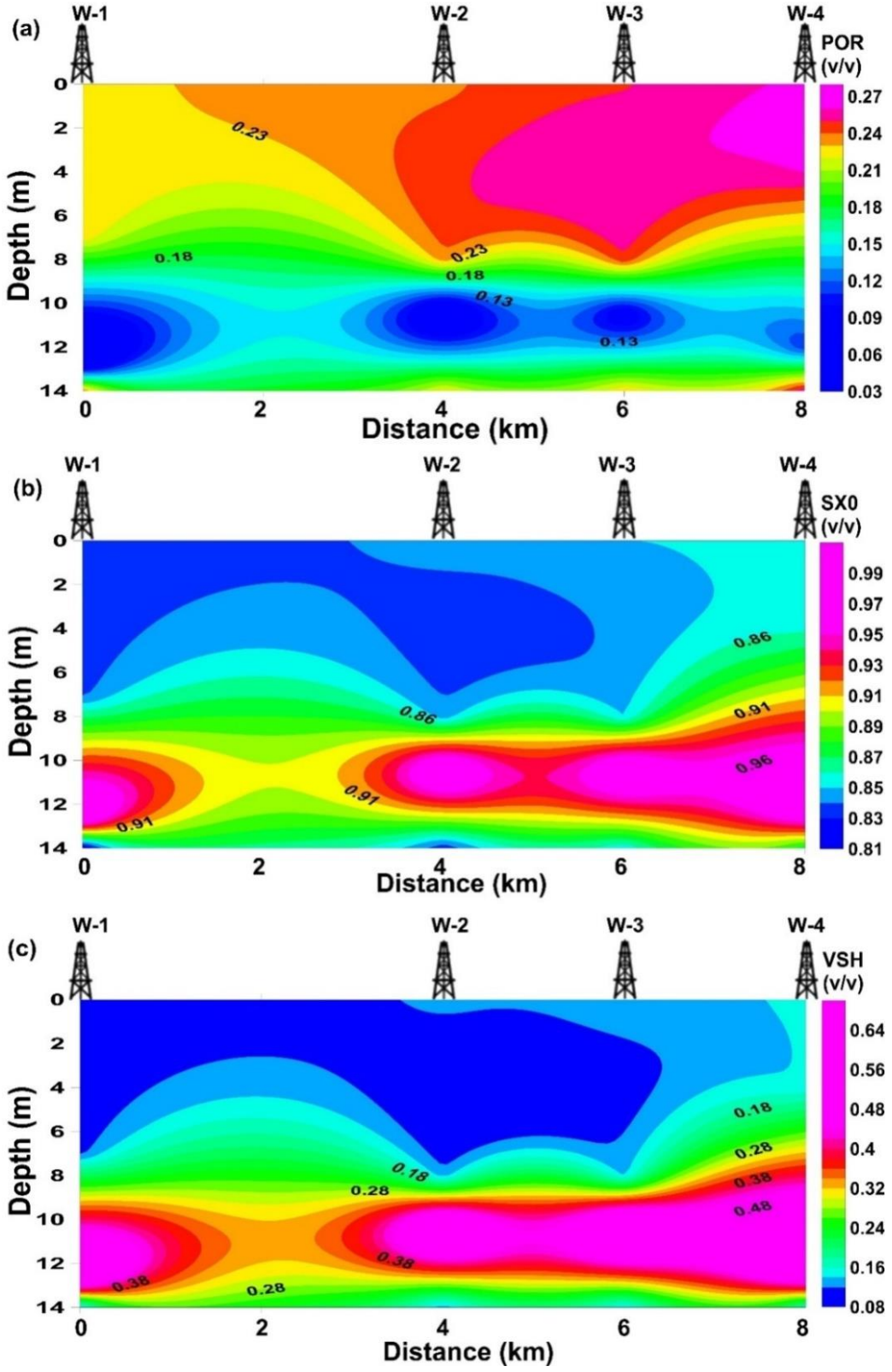

Fig. 59 Results of 2D inversion in drill holes W1-W4: a) porosity b) water saturation c) shale content

DOI: 10.14750/ME.2022.027

Table 20 Estimated petrophysical parameters and layer boundary coordinates of Egyptian field data by 2D interval inversion method (polynomials degree is n=8)

Layer	Parameter	W-1	W-2	W-3	W-4
1gas-sand	POR	0.234	0.227	0.236	0.265
	SX0	0.836	0.819	0.843	0.861
	VSH	0.088	0.125	0.097	0.139
2 shale	POR	0.044	0.073	0.071	0.10
	SX0	0.981	0.982	0.994	1.00
	VSH	0.636	0.62	0.625	0.690
3 gas-sand	POR	0.212	0.220	0.229	0.253
	SX0	0.825	0.831	0.853	0.864
	VSH	0.113	0.137	0.116	0.157
Boundary	$H_1(x)$	7.0	8.34	7.34	4.0
	H_2 (x)	12.51	10.50	10.50	12.01

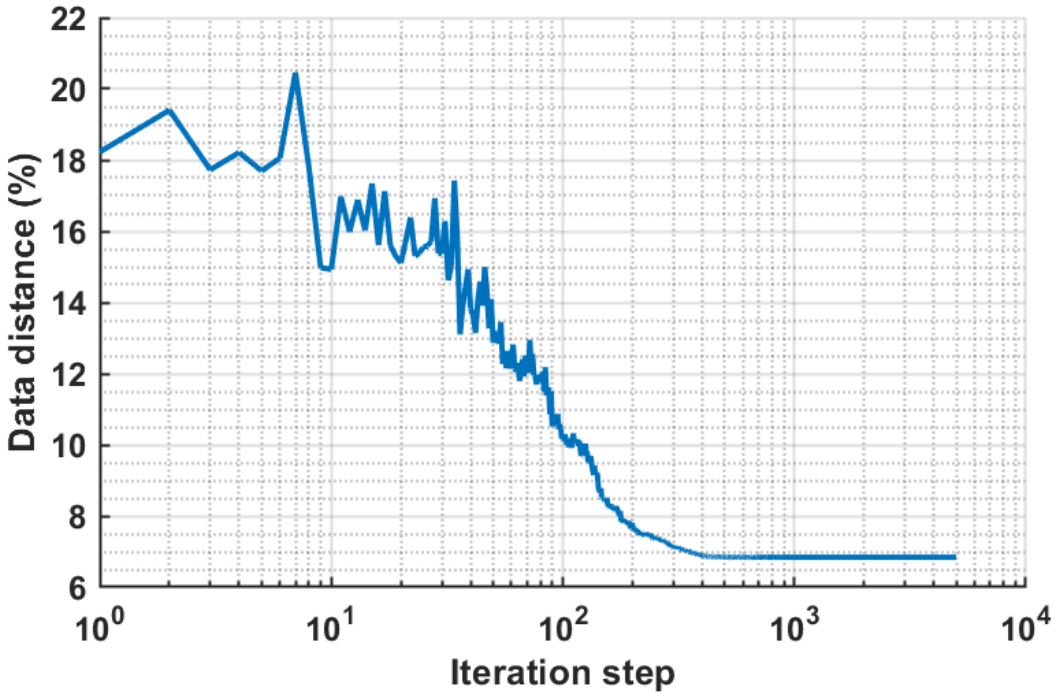

Fig. 60 Convergence plot of the processed Egyptian field data by 2D interval inversion method, the average data distance vs. number of iterations (polynomial degree is n = 8)

DOI: 10.14750/ME.2022.027

5.3 Discussion

In the present chapter, I showed a newly developed 2D interval inversion approach for evaluating 2D petrophysical models. The proposed method allows for the determination of lateral changes of layer boundaries as well as the lateral and vertical variation of the petrophysical parameters along borehole profile in stable and convergent procedures. Accordingly, two-dimensional models were created, the geometry of the geological structures and the morphology of hydrocarbon reservoirs were well defined as well. The feasibility of the modified method was verified on simulated and Egyptian field data related to hydrocarbon bearing formations. With setting a high overdetermination ratio which considered the essential features of the interval inversion method, I successfully estimated the model parameters of synthetic models built up of two-layer structures. Also, reliable results were obtained in case of multi-layers application of Egyptian field data.

Thesis four

I further developed the 2D Legendre polynomials-based interval inversion algorithm which allows the determination of lateral changes of the layer-boundary coordinates together with the vertical and lateral variations of petrophysical parameters along a 2D cross-section of several boreholes. The method is assessed using noisy simulated measurements on petrophysical models made of two-layer structures related to groundwater and hydrocarbon bearing formations. The numerical experiments aided to confirm the stability and convergence of the inversion procedure. To test the accuracy and reliability of the inversion results, the misfit of data and model distance are tested. The feasibility of the 2D interval inversion method is shown by analysing in situ well logging data acquired in four wells situated in Egyptian hydrocarbon field.

DOI: 10.14750/ME.2022.027

6. CHARACTERIZING THE QUALITY OF THE ESTIMATED PARAMETERS

The measurement data are always contaminated by a certain quantity of noise. The measuring errors can be systematic or random. The former can be generally treated well, while the calculation of the latter is of great importance in the practice of geophysical inversion. The general equation

$$\mathbf{m} = \mathbf{G}^{-\mathbf{g}}\mathbf{d}^{(\mathrm{m})} \tag{45}$$

shows the transformation of data to the model space. According to that data noise also will be mapped into the model space. The uncertainty of data causes the appearance of errors in parameter estimation. Several ways can be used to quantify the estimation errors in the inversion procedure. In the last chapters the misfit of data and model distance are tested for this purpose. Here, I implement the discrete inverse theory (Menke 1984) for calculating estimation errors of parameters and correlation coefficients. Detailed explanation can be seen in chapter two (Section 2.1). As a result, after reaching the near vicinity of the optimum via the VFSA algorithm and for quality assurance on inversion results, I switched to the DLSQ for performing linear optimization. At the end of the procedure, the estimation errors and correlation coefficients can be computed, besides estimating the errors of the estimated expansion coefficients by using equation (15), I can ensure the reliability and accuracy of the obtained results. Thus, a detailed flow chart which summarized the full procedures of the hybrid optimization method is shown in Fig. 61.

It must be mentioned that a realistic estimation for the accuracy of inversion results can only be given in the knowledge of the full data covariance matrix (in equation (15)). Since well logging operations lack the repetition of measurements, we do have only approximate information of the error of the observed quantities. Moreover, the unknown modeling error coming from the simplified equations (27)-(36) is also added to the variance of input data. In the industry, generally the data are considered uncorrelated and of the same variance. In the proposed methodology, it is allowed to incorporate the full covariance matrix of well logging parameters (if it is measured) to improve the reliability of error estimation.

6.1 Reliability of synthetic results

In case of Model A, the estimated expansion coefficients and their errors are illustrated in Fig. 62. The standard deviation in case of layer boundary coordinates is smaller than the standard deviation of petrophysical parameters in both models. Very

DOI: 10.14750/ME.2022.027

minimum estimated errors of the petrophysical parameters also of the model can be seen in the 2D error models Fig. 63. For the second Model B the expansion coefficients error and the 2D petrophysical parameter errors can be checked in Figs. 64 and 65. The mean spread value of their correlation coefficients are S = 0.37 and 0.32 for Models A and B respectively, which indicate poorly correlated expansion coefficients and highly reliable inversion results.

6.2 Reliability of Egyptian field results

After quantifying the accuracy of the synthetic examples, it's important to check the estimated results of the Egyptian field measurements. The estimated model parameters and their estimation errors are provided in Table 21; together with the calculated mean spread value which was 0.31 confirm the inversion results dependability.

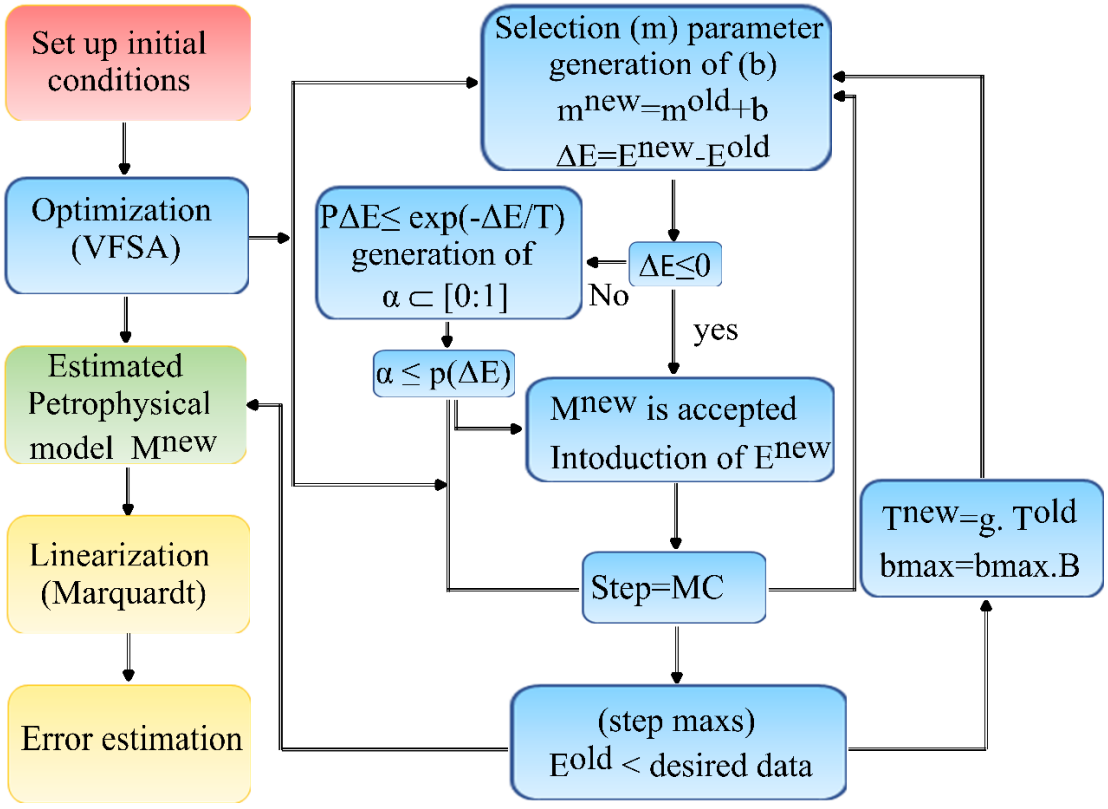

Fig. 61 Flowchart illustrating the interval inversion procedure using a hybrid VFSA+DLSQ optimization

DOI: 10.14750/ME.2022.027

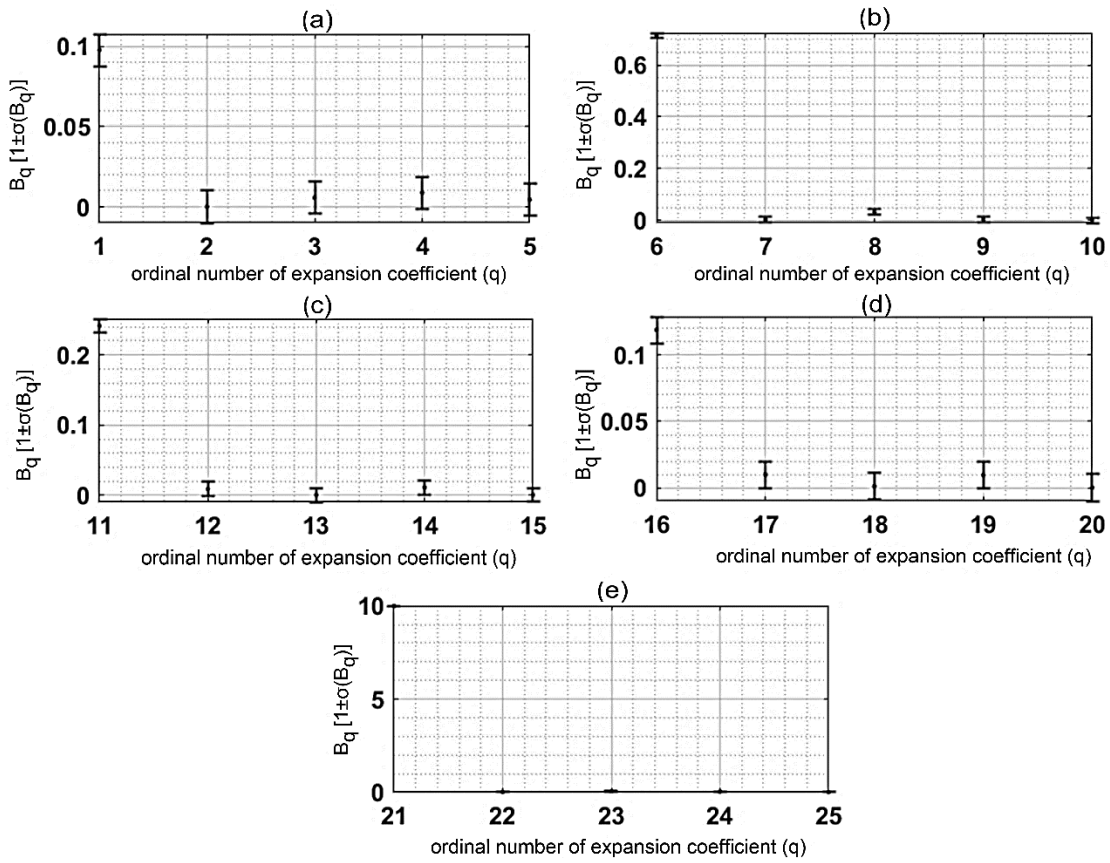

Fig. 62 Results of interval inversion procedure using Legendre polynomials of 4 degrees as basis functions of Model A in well 1-6. Estimated values of expansion coefficients for (a) porosity in layer 1, (b) shale content in layer 1, (c) porosity in layer 2 , (d) shale content in layer 2, (e) layer boundary coordinates

DOI: 10.14750/ME.2022.027

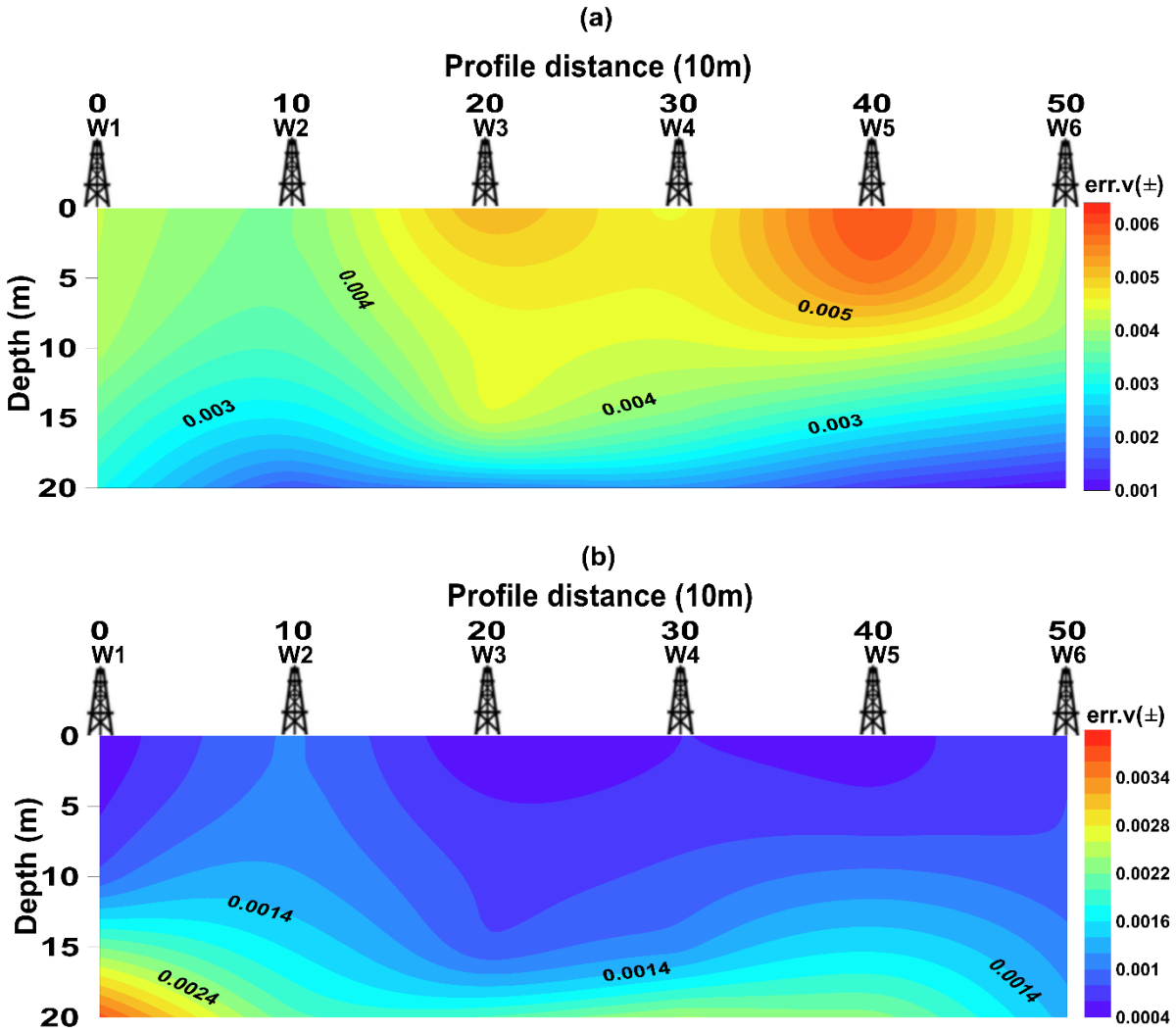

Fig. 63 Results of estimation errors by 2D hybrid VFSA+DLSQ interval inversion in drill holes W1-W6 of Model A for a) porosity, b) shale content

DOI: 10.14750/ME.2022.027

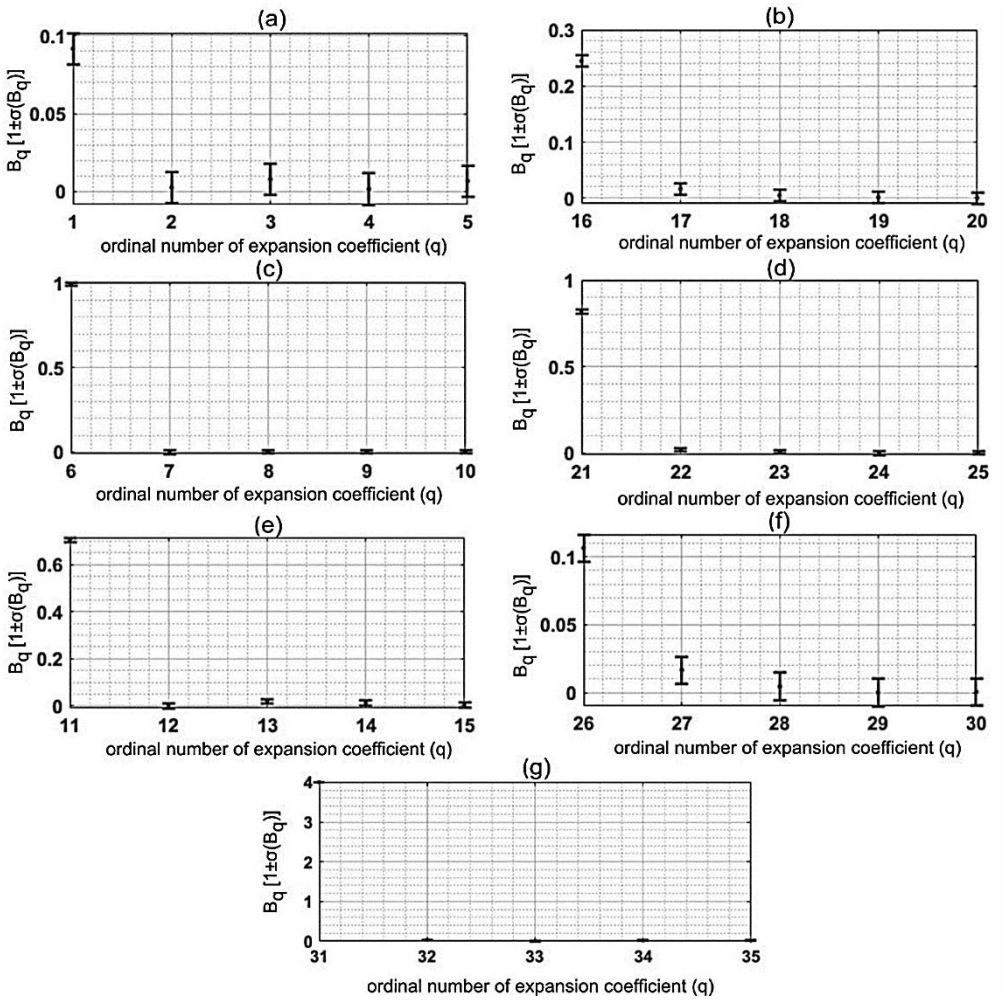

Fig. 64 Results of interval inversion procedure using Legendre polynomials of 4 degrees as basis functions of Model B in well 1-6. Estimated values of expansion coefficients for (a) porosity in layer 1, (b) water saturation of uninvaded zone in layer 1, (c) shale content in layer 1, (d) porosity in layer 2, (e) water saturation of uninvaded zone in layer 2, (f) shale content in layer 2, (g) layer boundary coordinates

DOI: 10.14750/ME.2022.027

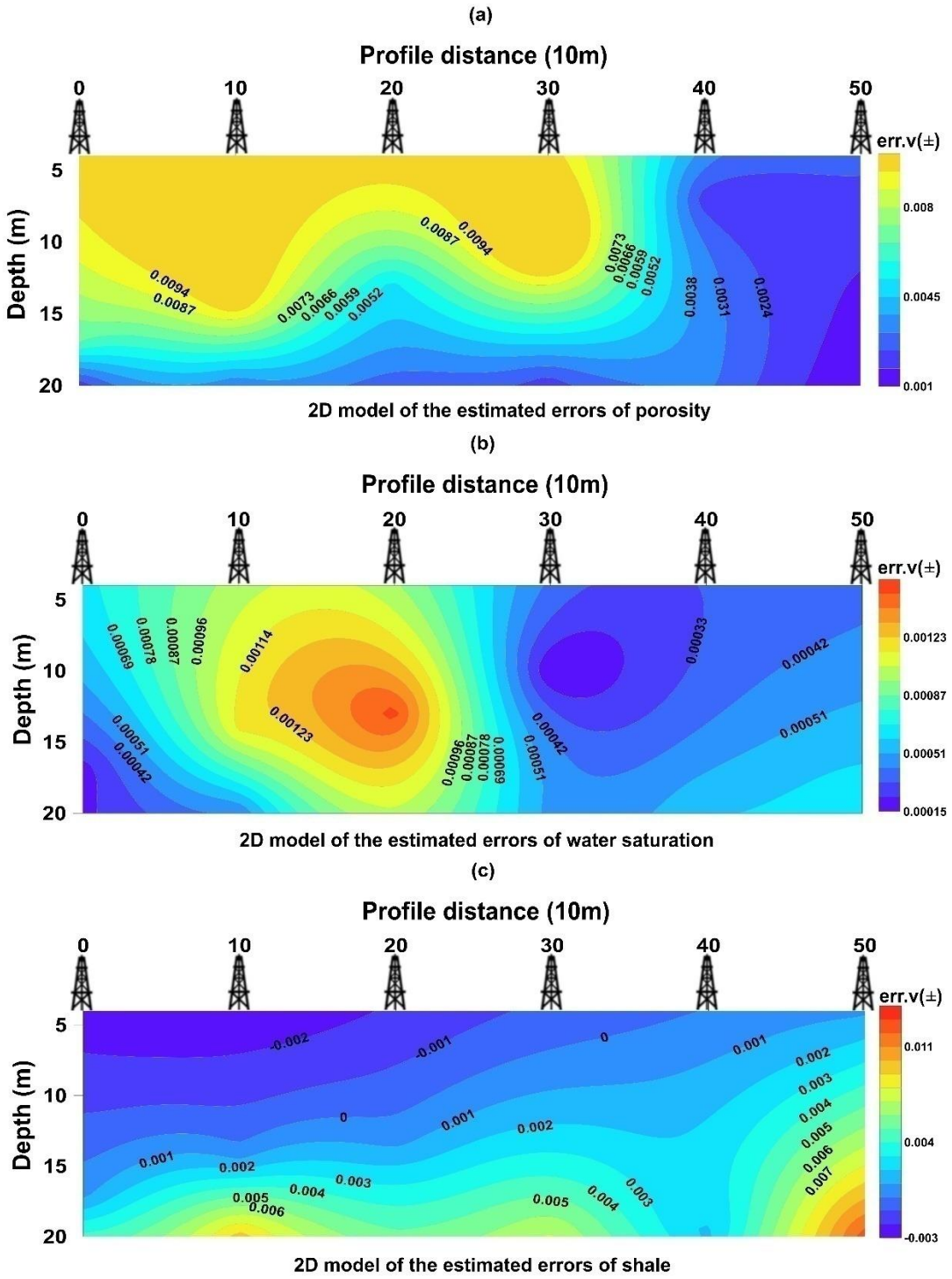

Fig. 65 Results of estimation errors by 2D hybrid VFSA+DLSQ interval inversion in drill holes W1-W6 of Model B for a) porosity, b) water saturation, c) shale content

DOI: 10.14750/ME.2022.027

Table 21 Estimated Parameters of Egyptian field data and their errors by 2D inversion

Layer	Parameter	W-1	W-2	W-3	W-4
1	POR	0.225 (± 0.002)	0.237 (± 0.001)	0.248 (± 0.002)	0.26 (± 0.002)
	SX0	0.838 (± 0.003)	0.843 (± 0.001)	0.850 (± 0.002)	0.858 (± 0.002)
	VSH	0.114 (± 0.006)	0.125 (± 0.008)	0.136 (± 0.005)	0.147 (± 0.001)
1	POR	0.026 (± 0.04)	0.05 (± 0.007)	0.082 (± 0.01)	0.11 (± 0.006)
	SX0	0.996 (± 0.0005)	0.991 (± 0.001)	0.987 (± 0.0007)	1.00 (± 0.002)
	VSH	0.626 (± 0.001)	0.60 (± 0.001)	0.617 (± 0.001)	0.66 (± 0.001)
3	POR	0.241 (± 0.004)	0.223 (± 0.002)	0.229 (± 0.002)	0.259 (± 0.003)
	SX0	0.815 (± 0.001)	0.831 (± 0.002)	0.852 (± 0.001)	0.874 (± 0.002)
	VSH	0.127 (± 0.009)	0.126 (± 0.006)	0.138 (± 0.005)	0.163 (± 0.007)

6.3 Discussion

Several ways can be used for characterizing the accuracy and reliability of the inversion procedures. Besides, misfit of data and model distance which are briefly computed in the last chapters (four and five), the estimation errors and correlation coefficients which are deeply considered in this chapter. To calculate the estimation errors and the correlation coefficients of the petrophysical parameters I switched the program which starts with VFSA to Damped Least Squares (DLSQ) in order to perform linear optimization. I successfully ensure the quality of the results at the end of the procedures.

Thesis five

To measure the accuracy of the inversion results, I further developed the global inversion method. I suggested a hybrid 2D inversion technique VFSA+DLSQ for minimization the inverse problem. At the end of linear inversion phase, I could characterize the estimation error and reliability of estimation by the elements of the model covariance matrix and correlation coefficients, separately. I tested the hybrid inversion method on simulated datasets of the utilized two Models A and B in my study. Furthermore, the feasibility of the method is shown by evaluating Egyptian field data.

DOI: 10.14750/ME.2022.027

7. CONCLUSIONS

This section involved a detailed review about my PhD studies which are related to geophysical inversion developments of well logging datasets. The work was conducted at the Department of Geophysics, Faculty of Earth Science and Engineering, University of Miskolc. The main purposes of my PhD thesis were to develop the interval inversion methods for reliable estimation for one-and two-dimensional petrophysical parameters distributions. The majority of the developments are associated with processing of multi-borehole logging data. All method developments described in the thesis were performed by utilizing MATLAB programming language.

For the 1D case, I have developed the Chebyshev polynomials-based interval inversion approach to characterize the reservoir rock in Komombo basin, Upper Egypt. I used a new alternative basis function (Chebyshev polynomials) for discretizing the model parameters. The modified method shows a consistent estimation of the petrophysical parameters such as porosity, water saturation in invaded and uninvaded zones and volume of shale of Abu Ballas reservoir. I checked the reliability of the results by using a variety of quality techniques that include measuring misfit between the field data and the calculated one, calculating error estimation and correlation coefficients. In addition, I derived the hydrocarbon saturation in the form of irreducible and movable of the investigated reservoir.

The 2D case involves a suit of improved algorithms that help in evaluating the two- dimensional petrophysical models. Initially and considering the estimation of lateral changes of layer boundary coordinates I developed a Legendre polynomials-based interval inversion approach. I solved the inverse problem by applying linear optimization-based Marquardt technique (DLSQ). I utilized simulated measurements of multi-layer structures related to hydrocarbon bearing formations to test the method. The thicknesses are obtained as quadratic values over the interval [-1, 1]. For ensuring the reliability of results, the errors of the estimated expansion coefficients are computed. I proved the feasibility of the suggested method and successfully estimated the lateral variation of layer boundaries of Egyptian hydrocarbon field data acquired along four wells with the help of series expansion-based polynomial coefficients.

After that I was able to improve the 2D inversion method in order to determine vertical and lateral variation of the petrophysical parameters along a 2D cross-section of several boreholes. I used the Metropolis algorithm-based simulated annealing (VFSA) to

DOI: 10.14750/ME.2022.027

estimate the series expansion coefficients which are used to derive the petrophysical parameters. I evaluated the proposed method by using noisy simulated measurements of petrophysical models made of two-layer structures related to groundwater and hydrocarbon bearing formations. The data and model misfits are assessed to ensure the inversion procedures' stability and convergence. A large amount of input data relative to the number of unknowns results in a high overdetermined ratio, therefore more accurate estimates are obtained in stable and convergent procedure than in the conventional local (1D) inversion schemes. The inversion method's feasibility is demonstrated by analyzing in-situ well logging data from four wells in an Egyptian hydrocarbon field.

Successful estimation of both laterally varying petrophysical parameters and formation boundaries separately enabled me to further develop the method for determining both of them in a joint inversion procedure. In this case, the model vector comprises the series expansion coefficients of the petrophysical parameters besides the layer thicknesses which are estimated by using simulated annealing algorithm (VFSA). The feasibility of the modified method was verified on simulated and Egyptian field data related to hydrocarbon bearing formations. Accordingly, two-dimensional models were created, the geometry of the geological structures and the morphology of hydrocarbon reservoirs were well defined as well. After reaching the near vicinity of the optimum via the VFSA algorithm and for quality assurance on inversion results I switched the program to the DLSQ in order to perform linear optimization. I implemented Menke's (1984) discrete inverse theory for calculating estimation errors of parameters and correlation coefficients. With the minimal estimated errors and correlation coefficients in case of the simulated and Egyptian hydrocarbon structure, I effectively proved the efficiency of the hybrid algorithm (VFSA+DLSQ) in processing several neighbouring deep wells.

Finally, in the context of my PhD thesis, I demonstrated a new perspective for interval inversion-based methods relating to single and multi-well data processing applications by using the MATLAB environment. The developed methods could accurately evaluate one- and two- dimensional petrophysical models. The only criterion for making the methods more effective and powerful is to keep the high overdetermined ratio. The application of the developed methods can be extended to include the processing of groundwater and non-conventional reservoirs on both 2D and/or 3D features.

DOI: 10.14750/ME.2022.027

ACKNOWLEDGEMENTS

First and foremost, I must express my inexhaustible gratitude to God, the Ever-magnificent, and the Ever-Thankful.

I would like to express my heartfelt gratitude to Prof. Dr. Norbert Péter Szabó for his guidance and suggestions for the research topics. I would not have been able to complete the work if it hadn't been for his effective contribution, discussions, and assistance in resolving problems at work. In addition, he has done his best to critically revise the manuscript in an attempt for it to be scientifically acceptable.

Many thanks also go to Prof. Dr. Mihaly Dobróka for his great assistance, scientific advice, contribution and suggestions which I've implemented in my research.

I am very grateful also to Dr. Armand Abordán for his encouragement and help.

I would also like to thank all of my colleagues at the department of geophysics for their assistance and advice.

Grateful acknowledgement is to my family, especially my parents, my brothers, my sisters, for their sacrifice and continuous encouragement to carry out this work.

Finally, for the many who the limitation of space cannot allow being named in person, I seize this opportunity to extend my sincere congratulations.

I must thank Ganoub El Wadi Petroleum Holding Company for providing me with the well-logging field data which were used to verify the effectiveness of the improved methods in this work.

Many thanks go also to the Egyptian cultural affairs and missions' sector for their support and great assistance.

The research was carried out within the GINOP-2.3.2-15-2016-00031 "Innovative solutions for sustainable groundwater resource management" project of the Faculty of Earth Science and Engineering of the University of Miskolc in the framework of the Széchenyi 2020 Plan, funded by the European Union, co-financed by the European Structural and Investment Funds.

Mahmoud Abdellatif

DOI: 10.14750/ME.2022.027

REFERENCES

Aguilera, R. (1980). Naturally fractured reservoirs. United States: Petroleum Publishing Company.

Abramowitz, Milton; Stegun, Irene Ann. (1983). Handbook of Mathematical Functions with Formulas, Graphs, and Mathematical Tables. Applied Mathematics Series. Washington D.C.; New York: United States Department of Commerce, National Bureau of Standards; Dover Publications.

Archie G. E. (1942). The electrical resistivity logs as an aid in determining some reservoir characteristics: Transactions of the AIME, 146, 54-62

Alberty, M., Hashmy, K. (1984). Application of ULTRA to log analysis. SPWLA 25th annual logging symposium. New Orleans, Louisiana. Z 1–17

Ali A.S.H. (2015).Geophysical study on Komombo basin, Upper Egypt, Egypt. Unpublished Ph.D. Thesis, Al-Azhar University Cairo, Egypt.pp.1-160

Ali M, Darwish M, Abdelhady A, Essa M (2017). Structural and Lithostratigraphic evolution of Al Baraka Oil field, Komombo Basin, Upper Egypt as deduce from 2D seismic lines and well logging data. J Basic Environ Sci 2:31–51

Akbar, M.N.A. (2021).Naturally Fractured Basement Reservoir Characterization in a Mature Field, Proceedings of SPE Annual Technical Conference and Exhibition held in Dubai - UEA., Sep. 21-23, SPE-206027-MS. https://doi.org/10.2118/206027-MS

Ball, S. M., D. M. Chace, and W. H. Fertl. (1987). The Well Data System (WDS): An advanced formation evaluation concept in a microcomputer environment: Proceedings of the SPE Eastern Regional Meeting, paper 17034, 61–85

Bonter, Dan & Trice, R. (2019). An Integrated Approach for Fractured Basement Characterization: The Lancaster Field, a Case Study in the UK. Petroleum Geoscience. 25. petgeo2018-152. 10.1144/petgeo2018-152

Drahos D. (2005). Inversion of engineering geophysical penetration sounding logs measured along a profile. Acta Geodaetica et Geophysica Hungarica 40, 193-202

Dobróka, M. (1995). Establishment of joint inversion algorithms in well-logging data interpretation. Scientific study, Department of Geophysics, University of Miskolc

REFERENCES

Dolson JC, Shann MV, Hammouda H, Rashed R, Matbouly S. (1999). The petroleum potential of Egypt. AAPG Bull. https :// doi.org/10.1306/E4FD4 6A7-1732-11D7-86450 00102 C1865 D

Dobróka, M., and Szabó, N.P. (2001). The inversion of well log data using Simulated Annealing method, Publs. University of Miskolc. Geoscience and engineering. Series A Mining. Vol .59, pp 115-137

Dobróka M, Szabó N P. (2002). The MSA inversion of open hole well log data. Intellectual Service for Oil & Gas Industry. Ufa State Petroleum Technological University & University of Miskolc. Analysis, Solutions, Perspectives Vol 2. pp. 27-38

Dobróka, M., and Szabó, N.P. (2005). Combined global/linear inversion of well logging data in layer-wise homogeneous and inhomogeneous media, Acta Geod. Geophys. Hung. 40, 2, 203-214, https://doi.org/10.1556/AGeod.40.2005.2.7

Dobróka, M., B. Kiss, Szabó N.P., J. Tóth, and T. Ormos. (2007). Determination of cementation exponent using an interval inversion method. 69th EAGE Conference and Exhibition incorporating SPE EUROPEC, 11-14 June, London, Great Britain, Eur. Assoc. Geoscientists and Engineers, Houten, paper 092, 1-4.https://doi.org/10.3997/2214-4609.201401793

Dobróka M, Szabó N, Ormos T, Kiss B, Tóth J, Szabó I. (2008). Interval inversion of borehole geophysical data for surveying multimineral rocks. 14th European Meeting of Environmental and Engineering Geophysics, Cracow, P11

Dobróka, M., Szabó, N.P., E. Cardarelli, and P. Vass. (2009). 2D inversion of borehole logging data for simultaneous determination of rock interfaces and petrophysical parameters, Acta Geod. Geophys. Hung. 44, 4, 459-479, https://doi.org/10.1556/AGeod.44.2009.4.7

Dobróka, M., Szabó, N.P. (2011). Interval inversion of well-logging data for objective determination of textural parameters. Acta Geophys. **59,** 907. https://doi.org/10.2478/s11600-011-0027-z

Dobróka, M., and Szabó, N.P. (2012). Interval inversion of well-logging data for automatic determination of formation boundaries by using a float-encoded genetic algorithm: Journal of Petroleum Science and Engineering, 86–87, 144–152, https://doi.org/10.1016/j.petrol.2012.03.028

REFERENCES

Dobróka, M., Szabó, N.P. and E. Turai. (2012). Interval inversion of borehole data for petrophysical characterization of complex reservoirs: Acta Geodaetica et Geophysica Hungarica, 47, 172–184, https:// doi.org/ 10.1556/AGeod.47.2012.2.6

Dobróka, M., and Szabó, N.P. (2015). Well Log Analysis by Global Optimization-based Interval Inversion Method. Book Section Artificial Intelligent Approaches in Petroleum Geosciences, P 245-268. https://doi.org/10.1007/978-3-319-16531-8_9

Dobróka, M., Szabó, N.P., Tóth, J., Vass, P. (2016). Interval inversion approach for an improved interpretation of well logs. Geophysics 81, D155–D167. https://doi.org/10.1190/geo2015-0422.1

Drahos D. (2005). Inversion of engineering geophysical penetration sounding logs measured along a profile. Acta Geodaetica et Geophysica Hungarica 40, 193-202.

D. E. Goldberg. (1989).Genetic Algorithms in Search, Optimization and Machine Learning, Addison-Wesley

Geman, S., & Geman, D. (1984). Stochastic relaxation, Gibbs distributions, and the Bayesian restoration of images. IEEE Transactions on pattern analysis and machine intelligence, (6), 721-741

Goswami, J.C., Mydur, R., Wu, P., Heliot, D. (2004). A robust technique for well-log data inversion. IEEE Trans. Antennas Propag. 52, 717–724

Holland J.H. (1975). Adaptation in natural and artificial systems. University of Michigan Press, 232 p

Horváth, Sz, B. (1973). The accuracy of petrophysical parameters as derived by computer processing. Log. Anal. 14, 16–33

Ingber L (1989) Very fast simulated reannealing. Math Comput Model 12(8):967–993

Kennedy, J. and Eberhart, R. C. (1995). Particle swarm optimization. Proc. IEEE int'l conf. on neural networks Vol. IV, pp. 1942-1948. IEEE service center, Piscataway, NJ.

Klitzsch EH, Squyres CH. (1990). Paleozoic and Mesozoic Geological History of Northeastern Africa Based Upon New Interpretation of Nubian Strata. AAPG Bulletin; 74 (8): 1203–1211. https://doi.org/10.1306/0C9B2457-1710-11D7-8645000102C1865D

Kearey, P., Brooks, M., & Hill, I. (2002). An introduction to geophysical exploration (Vol. 4). John Wiley & Sons

REFERENCES

Metropolis N, Rosenbluth A, Rosenbluth M, Teller A, Teller E. (1953). J. Chem. Phys., 21,1087–1092

Marquardt, D. W. (1959). Solution of non-linear chemical engineering models: Chemical Engineering Progress, 55, 65–70

Mayer, C., and A. Sibbit. (1980). GLOBAL, a new approach to computer processed log interpretation: Proceedings of the 55th SPE Annual Fall Technical Conference and Exhibition, paper 9341, 1–14

Menke, W. (1984). Geophysical Data Analysis: Discrete Inverse Theory. Academic Press. https://doi.org/10.1016/B978-0-12-490920-5.X5001-7

Othman, A. A. A., Ewida, H. F., Fathi, M. M. Ali., and Embaby, M. M. A. A. (2015). Prediction of petrophysical parameters applying multi attribute analysis and probabilistic neural network techniques of seismic data for Komombo Basin, Upper Egypt. IJISET - International Journal of Innovative Science, Engineering & Technology, Vol. 2 Issue 9

Pace F., A. Santilano, and A. Godio. (2019). Particle swarm optimization of 2D magnetotelluric data. Geophysics, 84 (3), E125-E141

Serra, O. (1984). Fundamentals of Well-log Interpretation. Series Developments in petroleum science; 15A. Amsterdam; New York: Elsevier; Pau: Elf Aquitaine, ISBN 9780080868691

Schlumberger. (1989). Log Interpretation Principles/Applications. 7th printing. Schlumberger, Houston

S. M. Ball, D. M. Chace, and W. H. Fertl. (1987). The Well Data System (WDS): An Advanced Formation Evaluation Concept in a Microcomputer Environment. Proceedings of SPE Eastern Regional Meeting, Pittsburgh, 1987, pp. 61-85. http://dx.doi.org/10.2118/17034-MS

Szabó N P. (2004). Geophysical Transactions, 44, 313–329

Schlumberger 2017. This is Schlumberger, 90 years of technical innovation.

Szabó N.P., Dobróka M. (2020). Interval inversion as innovative well log interpretation tool for evaluating organic-rich shale formations. Journal of Petroleum Science and Engineering, 186:106696. https://doi.org/10.1016/j.petrol.2019.106696

REFERENCES

Senosy, A.H., Ewida, H.F., Soliman, H.A. (2020). Petrophysical analysis of well logs data for identification and characterization of the main reservoir of Al Baraka Oil Field, Komombo Basin, Upper Egypt. SN Appl. Sci. **2,** 1293. https://doi.org/10.1007/s42452-020-3100-x

Szabó, N. P., Remeczki, F., Jobbik, A., Kiss, K., & Dobróka, M. (2022). Interval inversion based well log analysis assisted by petrophysical laboratory measurements for evaluating tight gas formations in Derecske through, Pannonian basin, east Hungary. Journal of Petroleum Science and Engineering, 208, 109607

Tarantola A. (2005). Inverse problem theory and methods for model parameter estimation. Society of Industrial and Applied Mathematics (SIAM), Philadelphia

Wyllie MRJ, Gregory AR, Gardner LW. (1956). Elastic wave velocities in heterogeneous and porous media. Geophysics 21 (1): 41–70. https://doi.org/10.1190/1.1438217

Wycisk P. (1994). Correlation of the major late Jurassic - early Tertiary low- and high stand cycles of south-west Egypt and north-west Sudan. Geol Rundsch 83, 759–772. https://doi.org/10.1007/BF00251074

Zhou, C., Gao, C., Jin, Z., Wu, X. (1992). A simulated annealing approach to constrained nonlinear optimization of formation parameters in quantitative log evaluation. SPE Annual Technical Conference and Exhibition, Paper, 24723, pp. 1–9